

**Genetic determinants and phenotypic changes of differential
aggregation in *Burkholderia multivorans***

João Miguel de Sines Vilela Figueira Rocha

Thesis to obtain the Master of Science Degree in

Biotechnology

Supervisor: Doctor Leonilde de Fátima Morais Moreira

Examination Committee:

Chairperson: Doctor Arsénio do Carmo Sales Mendes Fialho

Supervisors: Doctor Leonilde de Fátima Morais Moreira

Members of the Committee: Doctor Sílvia Andreia Bento da Silva Sousa Barbosa

November 2019

Preface

The work presented in this thesis was performed at the Institute for Bioengineering and Biosciences (iBB) of Instituto Superior Técnico during the period of September 2018 and September 2019, under the supervision of Dr. Leonilde Moreira and within the frame of the Programa Operacional Regional de Lisboa 2020 (LISBOA-01-0145-FEDER-007317).

Declaration

I declare that this document is an original work of my own authorship and that it fulfills all the requirements of the Code of Conduct and Good Practices of the Universidade de Lisboa.

Acknowledgments

Firstly, a thank you to my supervisor Prof. Leonilde Moreira for the guidance throughout this master thesis and insistence to attempt a better work. A thank you to Sara Gomes and Mirela Ferreira for the teachings and all the time spent. A thank you to João Figueiredo and Teresa Cunha for working with me side by side throughout this year.

Especially I would also like to thank all the family, Ana, and all my friends for the support behind the scenes and for providing the much-needed distractions and encouragement. To the ones who know and listened.

This work was financed by Programa Operacional Regional de Lisboa 2020 (LISBOA-01-0145-FEDER-007317).

Resumo

Muitas bactérias são capazes de alterar a sua estratégia de crescimento, de forma a sobreviver em condições adversas. Uma dessas estratégias consiste na formação de agregados celulares planctónicos, semelhantes a biofilmes, e que ocorrem em infecções respiratórias em doentes com fibrose quística. A espécie *Burkholderia multivorans* é uma das que afectam estes doentes e foi o foco deste trabalho, que tentou estabelecer ligações entre este modo de crescimento e genes ou mecanismos específicos. Assim sendo, usou-se um transposão para obter mutantes de um isolado clínico com capacidade de agregação, *Burkholderia multivorans* P0213-1, e avaliou-se a capacidade de agregação dos mesmos. Após identificação dos genes interrompidos nos mutantes seleccionados, estes foram testados relativamente a outros fenótipos associados à agregação celular, tais como a virulência, motilidade, resistência a antimicrobianos, adesão, crescimento e produção de exopolissacáridos. Confirmou-se que a motilidade tem um papel relevante na formação de agregados celulares planctónicos nesta estirpe, sendo possivelmente necessária para aproximação das células livres de forma a iniciar a formação dos agregados. Mensageiros intracelulares também foram considerados como tendo possivelmente um papel determinante neste fenótipo, embora os mecanismos continuem por elucidar. Outras ligações foram difíceis de estabelecer, contudo alguns possíveis intervenientes foram identificados. Estes incluem reguladores de transcrição, sistemas de dois componentes, metabolismo de lípidos e de uma forma geral, o metabolismo central, que tem repercussões em variadas vias metabólicas, dificultando o estabelecimento de um efeito- causa. A estirpe *Burkholderia contaminans* IST408 e o isolado clínico aqui estudado foram considerados um bom modelo para estudar agregados celulares mistos.

Palavras chaves

Agregados celulares planctónicos, Fibrose quística, *Burkholderia multivorans*, Mutagénesse aleatória, Agregados celulares mistos

Abstract

Some bacteria can accommodate to the surrounding environmental conditions by altering their growth and behavior and thus allowing them to thrive in unfavorable niches. One such survival strategy is the formation of planktonic cellular aggregates, similar to surface attached biofilms, verified in cystic fibrosis (CF) patients. *Burkholderia multivorans*, one of the bacteria that afflicts these patients, was the focus of this work, which attempted to link this mode of growth with specific genes and mechanisms. As such, several mutants created by random mutagenesis of an aggregative clinical isolate, *Burkholderia multivorans* P0213-1, were screened for their distinct aggregation ability. Those selected were assessed for other aggregation-associated phenotypes like virulence, motility, antimicrobial resistance, surface-attached biofilm formation, adhesion, growth and exopolysaccharide production, and the disrupted genes identified in order to relate aggregation ability with specific mechanisms, verifiable by other traits. Motility was confirmed to have a role in planktonic cellular aggregation in this strain, apparently being required for approximation of free cells to initiate aggregate formation. Intracellular messengers might play a determinant role in this phenotype, although the specific mechanisms remain unknown. Other direct links were difficult to establish. However, some possible key players in cellular aggregation were identified. These involve transcriptional regulators, two-component systems, intracellular messengers, lipid metabolism and overall convergence on central metabolism, which has repercussions in numerous pathways, making it difficult to establish cause-effect relationships. *Burkholderia contaminans* IST408 and the clinical isolate used in this study were also found to be a suitable model for studying mixed planktonic cellular aggregates.

Keywords

Planktonic cellular aggregates, Cystic fibrosis, *Burkholderia multivorans*,
Random mutagenesis, Mixed cellular aggregates

Table of contents

Preface	iii
Acknowledgments	v
Resumo	vi
Palavras chaves	vi
Abstract	vii
Keywords	vii
List of figures	xii
List of tables	xiv
List of abbreviations	xv
1. Introduction	1
1.1 Cystic fibrosis	2
1.1.1 Epidemiology	4
1.2 <i>Burkholderia cepacia</i> complex (Bcc)	4
1.2.1 <i>Burkholderia multivorans</i>	6
1.3 Bacterial biofilms within a CF context	6
1.4 Planktonic aggregates	8
1.5 Elements controlling bacterial aggregation	10
1.5.1 Quorum sensing	10
1.5.2 Extracellular DNA (eDNA)	11
1.5.3 Amino acids	12
1.5.4 Exopolysaccharides (EPS)	13
1.5.5 Motility and chemotaxis	13
1.5.6 Cyclic-di-GMP	18
1.5.7 Stresses	19
1.5.7.2 Oxygen and nitrogen	20
1.5.7.3 Pyruvate	22
1.5.7.4 Mannitol	23
1.5.7.5 Temperature	23
1.5.7.6 pH	23
1.5.7.7 Iron	24
1.5.7.8 Magnesium	25

1.5.8 The Immune System.....	25
1.6 <i>Burkholderia multivorans</i> biofilms and cellular aggregates.....	27
1.7 Motivation and thesis outline	29
2 Materials and Methods	30
2.1 Bacterial strains and growth conditions.....	30
2.2 Transposon mutant library construction	31
2.3 Screening of planktonic cellular aggregation ability in transposon library mutants.....	31
2.4 Planktonic cellular aggregation in co-cultures of <i>Burkholderia</i> strains	32
2.4.1 Killing assays.....	32
2.5 Microscopic observations.....	32
2.6 DNA manipulation and cell transformation techniques	32
2.7 Genomic DNA extraction for sequencing.....	33
2.8 Detection of plasposon in the genome of mutants.....	33
2.9 Identification of the genes disrupted by the plasposon	33
2.9.1 Sanger sequencing of flanking regions of the plasposon insertion site and <i>in silico</i> analysis of nucleotide sequences	33
2.9.2 Genome sequencing and assembly	34
2.10 Growth curves and doubling time estimation.....	34
2.11 Quantification of cellular aggregates, free cells and total biomass	34
2.12 Exopolysaccharide production in solid medium.....	35
2.13 Antimicrobial susceptibility.....	35
2.14 Biofilm formation	35
2.15 Motility	35
2.15.1 Swarming motility	35
2.15.2 Swimming motility	36
2.16 Virulence in <i>Galleria mellonella</i>	36
2.17 Adhesion to animal cells.....	36
2.18 Statistical analysis.....	37
3. Results and Discussion	37
3.1 Screening a transposon mutant library for differences in planktonic aggregates formation by <i>B. multivorans</i>	37
3.2 Confirmation of the presence of the plasposon in the mutant's genome.....	40
3.3 Localization of plasposon insertion within the genome of selected mutants	41
3.4 Analysis of disrupted genes and possible role in planktonic cellular aggregation	44

3.5 <i>In vitro</i> growth of selected mutants.....	59
3.6 Quantification of planktonic cellular aggregation and free cells in selected mutants and overall biomass	62
3.7 Surface-attached biofilm formation.....	66
3.8 Swimming and swarming motilities.....	67
3.9 Exopolysaccharide production in static media	69
3.10 Antimicrobial susceptibility.....	70
3.11 Virulence	72
3.12 Adhesion	77
3.13 Co-culturing of <i>Burkholderia</i> strains	78
4. Conclusion and future perspectives	83
5. References	85
6. Supplementary Material	101

List of figures

Figure 1 - Effects of CFTR dysfunction.	3
Figure 2 - Time-dependent formation of a surface-attached biofilm.	6
Figure 3 - Aggregation of <i>S. aureus</i> by different clonal origin cells differentially labelled. Measured between 0.01 and 0.5 OD of culture growth.	9
Figure 4 - Effect of Dnase I on established biofilms of GFP-tagged <i>P. aeruginosa</i> PAO1.	11
Figure 5 - Microcolony formation of <i>P. aeruginosa</i> PAO1C in ASM+ and ASM-.	12
Figure 6 - Model for initiation of <i>E. coli</i> biofilm formation dependent on motility and Type I pili for surface contact and attachment, respectively.	15
Figure 7 - <i>E. coli</i> Che 1 chemotaxis pathway affecting motility.	16
Figure 8 – Relation between iron concentration and cell density (assessed by measurements of OD _{600nm}) and biofilm formation of <i>P. aeruginosa</i> PAO1.	24
Figure 9 - Bacterial count of <i>B. multivorans</i> after lysis of infected (a) murine macrophages, and (b) THP-1 human monocytes after induced differentiation into macrophages.	26
Figure 10 – Screening of the plasposon mutant library of <i>B. multivorans</i> P0213-1 for different abilities to form planktonic cellular aggregates.	38
Figure 11 - Electrophoretic separation in 0.8% agarose gel of the PCR products corresponding to an internal region of the pTnModΩKm plasposon with an estimated size of 1161 bp.	Erro! Marcador não definido.
Figure 12 – Alignment of reads from C48 mutant's genome against P0213-1 wild-type genome using Geneious v.6.1.8.	42
Figure 13 - In F27 mutant the plasposon is inserted in <i>pyrC</i> (Bmul_2520) gene.	45
Figure 14 – <i>De novo</i> Synthesis of Pyrimidine Nucleotides.	45
Figure 15 - In D19 mutant the plasposon is inserted in <i>ppsA</i> (Bmul_1274) gene.	47
Figure 16 - In F69 mutant the plasposon is inserted in <i>tctD_2</i> (Bmul_0075) gene.	47
Figure 17 - In mutant F21 the plasposon is inserted in <i>paaC</i> (Bmul_0230) gene.	48
Figure 18 – Phenylacetate utilization pathway.	48
Figure 19 - In C48 mutant the plasposon is inserted in the upstream region of <i>flhD</i> (Bmul_0160) gene.	Erro! Marcador não definido.
Figure 20 - Overview of FlhDC functioning.	50
Figure 21 - In D3 mutant the plasposon is inserted in <i>hexR_2</i> (Bmul_0558) gene.	52
Figure 22 - In C50 mutant the plasposon is inserted in <i>rsmB_2</i> (Bmul_0786) gene.	53
Figure 23 - In mutant K51 the plasposon is inserted in an unknown gene (Bmul_1477).	54
Figure 24 - In K73 mutant the plasposon is inserted in <i>iscX</i> (Bmul_1150) gene.	55
Figure 25 – Schematic view of FeS cluster biogenesis in the ISC system.	55
Figure 26 - In mutant K50 the plasposon is inserted in <i>xdhA_3</i> (Bmul_4199) gene.	57
Figure 27 – Overview of purine metabolism.	57
Figure 28 - Growth curves of the strains under study.	59
Figure 29 - Doubling time of the strains under study.	60
Figure 30 - Quantification of cellular aggregates and free cells of wild-type (P0213-2) and its derivative mutants.	62
Figure 31 – Overall biomass production in 50 mL of SM medium of P0213-1 and its derivative mutants was determined by summing up the dry weights of both planktonic cellular aggregates and free cells of the quantification assay.	63

Figure 32 - Surface-attached biofilm formation of the P0213-1 and its derivative mutants was determined by absorbance measurement at 590 nm after growth for 48 hours at 37 °C in polystyrene microplates.	66
Figure 33 - Swimming ability of the P0213-1 and its derivative plasposon mutants was measured as the motility zone diameter after growth for 24 hours at 37 °C. -	67
Figure 34 - Swarming motility of the P0213-1 and its derivative strains to antibiotics was measured as the motility zone diameter after growth for 24 hours at 37 °C.	68
Figure 35 - Susceptibility of the P0213-1 and its derivative strains to aztreonam antibiotic was measured as the diameter of cell growth inhibition after growth for 24 hours at 37 °C.....	70
Figure 36 - Susceptibility of the P0213-1 and its derivative strains to piperacillin/tazobactam antibiotics was measured as the diameter of cell growth inhibition after growth for 24 hours at 37 °C.....	71
Figure 37 – Survival of <i>Galleria mellonella</i> larvae inoculated with <i>B. multivorans</i> (wild-type P0213-1 and the selected mutants).....	73
Figure 38 - Percentage of adherence of bacterial cells of each mutant to mammalian cells was determined by counting CFU and dividing adhered cells by total cells, after following described protocol.....	77
Figure 39 - Mixed and independent planktonic cellular aggregates of <i>B. multivorans</i> P0213-1 clinical isolate expressing dsRed and <i>B. contaminans</i> IST 408 expressing GFP.....	79
Figure S40 - Physical map of transposon pTnModΩKm.....	101

List of tables

Table 1 - Strains and plasmids used in this study.....	30
Table 2 - Contigs generated from the assembly of P0213-1 wild-type genome and its corresponding chromosomes of <i>B. multivorans</i> ATCC 17616.....	41
Table 3 - Genes disrupted by the plasposon were identified in the <i>B. multivorans</i> selected mutants	43
Table 4 - Selected mutants were distributed into four groups.	62
Table S5 - Primers used in this work.....	101
Table S6 - Plasposon flanking sequences obtained from the plasmids recovered from the F21 mutant. Sequences A and C were obtained by primer oriR and sequences B and D with primer kmR.	102
Table S7 - Plasposon flanking sequences obtained from the plasmids recovered from the F27 mutant. Sequence A was obtained by primer oriR and sequence B with primer kmR.	103
Table S8 - Plasposon flanking sequences obtained from the plasmids recovered from the D19 mutant. Sequence A was obtained by primer oriR and sequence B with primer kmR.	103
Table S9 - Plasposon flanking sequences obtained from the plasmids recovered from the D3 mutant. Sequences A, B and C were obtained by primer oriR and sequence D with primer kmR.	104

List of abbreviations

ABC – ATP-binding cassette

AHL – Acyl-homoserine lactone

AI-2 – Autoinducer 2

ASL – Airway surface liquid

ASM – Artificial sputum medium

ATP – Adenosine triphosphate

BLAST – Basic Local Alignment Search Tool

Bcc – *Burkholderia cepacia* complex

c-di-GMP – Cyclic dimeric guanosine monophosphate

cAMP – Cyclic adenosine monophosphate

CCR – Carbon catabolite repression

CDS – Coding sequence

CFU – Colony forming units

CoA – Coenzyme A

CF – Cystic fibrosis

CFTR – Cystic fibrosis transmembrane conductance regulator

CTP – Cytidine triphosphate

CRP – cAMP receptor protein

DGC – Diguanylate cyclase

ENac – Epithelial sodium channel

eDNA – Extracellular DNA

EPS – Exopolysaccharide

GFP – Green fluorescent protein

GMP – Guanosine monophosphate

GTP – Guanosine triphosphate

HSL – Homoserine lactone

IL-1 – Interleukin-1

IL-8 – Interleukin-8

IS – Insertion sequence

LB – Lennox-Broth

LTTR – LysR-type transcriptional regulators

KDPG – 2-keto-3-deoxy-6-phosphogluconate

MOI – Multiplicity of infection

MurNAc – N-acetyl-muramic acid

NAD – Nicotinamide adenine dinucleotide

NADH - Nicotinamide adenine dinucleotide phosphate

NCBI – National Center for Biotechnology Information

OD – Optical density

PAA-CoA – Phenylacetyl-CoA

PAA – Phenylacetic acid

PIA – Polysaccharide intercellular adhesion

(p)ppGpp – Guanosine tetraphosphate and guanosine pentaphosphate

PEP - Phosphoenolpyruvate

PDE – Phosphodiesterase

PTS – Phosphotransferase system

QRDR – Quinolone resistance-determining region

QS – Quorum-sensing

ROS – Reactive oxygen species

RT-PCR – Reverse transcription polymerase chain reaction

RR – Response regulator

SAM – S-adenosyl-L-methionine

SCFM – Synthetic Cystic Fibrosis medium

SIS – Sugar isomerase

ST – Sequence types

TCA – Tricarboxylic acid

TCS – Two-component system

Tfp – Type four pili

TNF- α – Tumor necrosis factor alfa

UDP – Uridine diphosphate

UMP – Uridine monophosphate

UTP – Uridine triphosphate

YEM – Yeast Extract Mannitol

XDH – Xanthine dehydrogenase

1. Introduction

In this chapter an overview of different genes, mechanisms and other key factors in the development and maturation of planktonic aggregates of *Burkholderia multivorans* will be presented. Mostly, within the context of cystic fibrosis pathology, a most prominent disease in the Western world and a known niche for the species of interest, which in itself may determine the outcome of afflicting patients.

Since most literature is lacking in these types of aggregates on this species, bibliography will diverge into the similar conventional biofilm mode of growth and associated bacteria, looking for cases closest to *B. multivorans*.

Other than that, some mechanisms and genes deemed important or interesting will be described for explanatory reasons, whilst others will be merely mentioned or explored superficially.

1.1 Cystic fibrosis

Cystic fibrosis (CF) is an autosomal recessive genetic disorder, affecting mostly the Caucasian population. It is caused by gene mutation on chromosome 7, encoding a chloride-conducting transmembrane channel called the cystic fibrosis transmembrane conductance regulator (CFTR), expressed in several organs (Castellani and Assael 2016). This channel is an ATP-binding cassette (ABC) transporter present at the apical membrane of many epithelia, comprised of two ATP-hydrolysis domains and 12 membrane-spanning alpha helices (Li *et al.* 2017). It is responsible for anion transport and mucociliary clearance in the airways (Elborn 2016). The disease is highly variable as the number of possible occurring mutations, with over 2000 identified (Li *et al.* 2017), leads to diverse effects on the CFTR protein. According to the specific CFTR defect, these mutations are attributed to six different classes (Elborn 2016). In a general way however, the resulting malfunction of CFTR leads to mucus retention, chronic infection by bacteria and consequent harmful inflammation in the airway, as well as fat malabsorption at the pancreatic level (Figure 1) (Castellani and Assael 2016).

Epithelial cells are the most affected by this dysfunction, though there is the possibility that immune cells are so, as well (Elborn 2016). Other than the airways of the patient, this disease also affects other body systems such as the pancreas, liver, sweat glands, bone, kidneys and male genitalia (Castellani and Assael 2016). However, the greatest cause of morbidity is owed to bronchiectasis, a condition where the airways expand abnormally, and excessive buildup of mucus occurs; obstruction of the airways; and progressive respiratory impairment (Elborn 2016). Though previously considered lethal during infancy, early diagnosis, progress in the understanding of the disease and development of therapeutic options led to a median of 50 years of life expectancy. Treatment of these patients consists nowadays, among others, of pancreatic enzyme replacement, respiratory physiotherapy, mucolytics, and aggressive antibiotic therapy with tobramycin and others (Castellani and Assael 2016).

Specifically, in the lungs, the malfunction of the channel leads to the CFTR protein upregulating the sodium channel (ENaC) on the apical side of bronchial epithelial cells, resulting in hyper-reabsorption of sodium which in turn reduces hydration of the luminal side by osmosis, increasing density of the mucus to unusual levels, which also displays abnormal carbohydrate and sulfate composition (Staudinger *et al.* 2014). The resulting highly dense and viscous secretions cripple ciliary activity and clearance from the airway normally provided within the airway surface liquid (ASL) that protects epithelial cells. Impairment of this bicarbonate conducting channel also leads to hindered Cl^- and HCO_3^- secretion to the lumen, contributing to ion imbalance and changes in pH of the ASL, on which bacterial killing is highly dependent (Larkin *et al.* 2015).

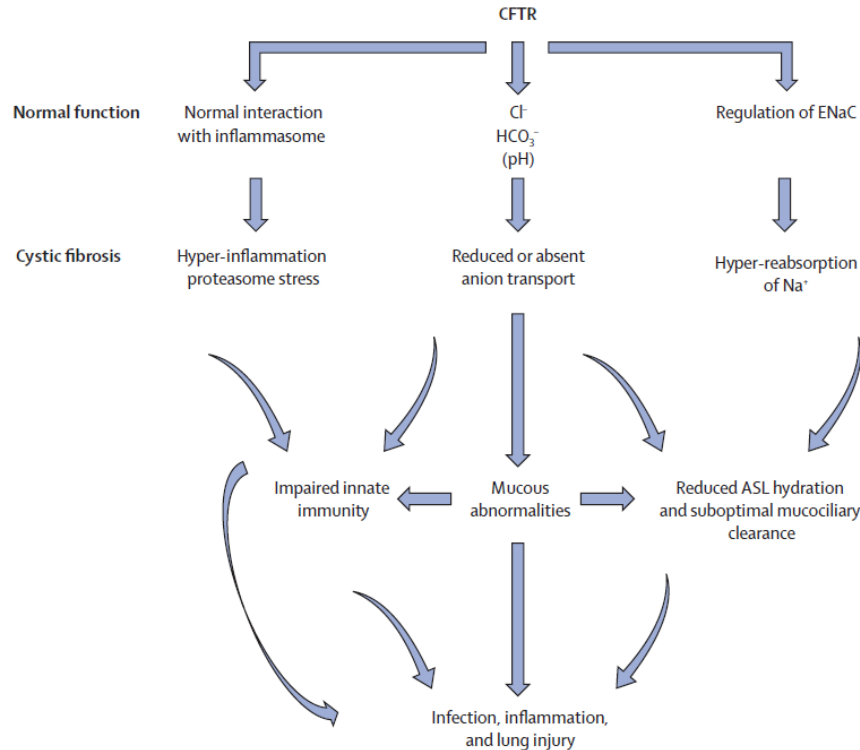


Figure 1 - Effects of CFTR dysfunction. Retrieved from Elborn *et al.* 2016.

Mutated CFTR also leads to increased inflammation and persistent neutrophil accumulation in the airways, derived from the induced host immune response. The airway epithelium is not only a source of interleukin-8 (IL-8), a chemokine which is the main neutrophil chemoattractant in CF lung, but also modulates production of IL-1, TNF- α , and other mediators by recruiting immune cells, including macrophages and neutrophils. Macrophages themselves also produce cytokines that contribute to local inflammatory response in CF airway by mediating neutrophil chemoattraction and degranulation. The secretion of cytokines and chemoattractants promotes neutrophil migration into the airway. On arrival, neutrophils further trigger the release of more proinflammatory mediators and chemoattractants, perpetuating inflammatory response that damages and cripples the lung (Elizur *et al.* 2008). This immune defense response is therefore not advantageous as it leads to accumulation of excessive pro-inflammatory cytokines and neutrophilic infiltration, an environment where bacteria such as *Pseudomonas aeruginosa* can dwell, further intensifying the inflammatory response. Also, CFTR malfunction is associated with reduced activity of the host's natural defenses, motored by the increased levels of neutrophil elastase and other neutrophil-derived proteases like cathepsin S, which impair opsonophagocytosis, degrade several substrates like the structural proteins elastin and fibronectin, and release DNA and oxidases upon death, which increases mucus viscosity and gives rise to oxygen radicals that deteriorate the lung, respectively (Elizur *et al.* 2008). Adding to the fact that some bacteria are even able to survive within macrophages (Brambilla *et al.* 2016; Mesureur *et al.* 2017; Schmerk and Valvano 2013), there is facilitation of the establishment of chronic infections. This, along with the other mentioned effects, may explain the impaired innate immunity, also reducing the function of antimicrobial peptides (Lai, Tremblay, and Déziel 2009) and

increasing vulnerability to bacterial infections, mostly dominated by the opportunistic pathogen *Pseudomonas aeruginosa* and to a lesser extent the *Burkholderia cepacia* complex (Bcc) (Mahenthiralingam and Vandamme 2005).

1.1.1 Epidemiology

Within Bcc infections, *Burkholderia multivorans* and *Burkholderia cenocepacia* were found to be the most prevalent species infecting CF patients (Schmerk and Valvano 2013; Zlosnik *et al.* 2015). Early studies indicated *B. cenocepacia* as the most prevalent CF species in North America and Europe. However, it has been set back to the second one in dominance, most likely due to application of infection control measures, first employed in Canada in 1995, to prevent new acquisition of epidemic strains, mostly belonging to *B. cenocepacia*, and apparently ineffective against other Bcc species in the natural environment. This, aided by the high mortality rate of those infected with *B. cenocepacia*, led to nonclonal *B. multivorans* as the most prevalent species in the U.S., New Zealand and Europe. A worst outcome was found to be associated with infection with *B. cenocepacia* rather than *B. multivorans*, with the highest rates of transmissibility and mortality, and the prognosis being more adverse for females than males. Other than these species, *Burkholderia dolosa* has also been associated with severe outcome in CF disease (Zlosnik *et al.* 2015).

Arguably, the largest CF epidemic was from *B. cenocepacia* ET-12 lineage across Canada and the UK in the late 1980s and throughout the 1990s. This was a hypertransmissible strain, maybe due to its unique combination of cable pili, 22-kDa adhesin, and *B. cepacia* epidemic strain marker (Mahenthiralingam, Urban, and Goldberg 2005).

In developed European countries, the number of adults with cystic fibrosis has been predicted to increase by around 70% by 2025, result of the improvement of life expectancy (Elborn 2016). Regarding the Portuguese paradigm, a study carried out by Cunha *et al.* at the major Portuguese CF center confirmed the prevalence of *B. cenocepacia* (52%). However, a considerable percentage (36%) of the patients at the CF center of Hospital de Santa Maria between 1995 and 2002 were infected or colonized with *Burkholderia cepacia*, contrasting with studies that say otherwise and that support the idea that *Burkholderia cenocepacia* and *Burkholderia multivorans* are predominant in CF Bcc infections. Furthermore, *B. cepacia*, though deemed infrequent in CF, was isolated from 85% of the patients infected with bacteria of the Bcc, which visited this same CF center, between 2003 and 2005 (Cunha *et al.* 2007).

1.2 *Burkholderia cepacia* complex (Bcc)

Bcc bacteria occur naturally in soil and water, having adapted to survive in association with plants and animals, including humans. All its integrating species share a high degree of 16S rDNA sequence similarity, moderate levels of whole-genome DNA-DNA hybridization, cellular lipid and fatty acid composition, and phenotypic characteristics (Mahenthiralingam and Vandamme 2005). Another shared feature is their large genome size, with an average of 8 Mb. *Burkholderia* genomes are also characterized for having on average a high C+G content (62-68 mol %) and consisting of multiple replicons (Ferreira *et al.* 2011; O'Grady and Sokol 2011; Peeters *et al.* 2017).

In the natural environment, Bcc bacteria mostly affect onions, in which infection causes sour skin disease, associated with soft rot of onion tissue. Despite this, most Bcc species are considered highly beneficial, as some isolates can protect commercially useful crops against fungal diseases like root rot and seed-damaging fungal infections.

Moreover, due to their ability to use various complex carbon sources, including groundwater pollutants and chlorinated aromatic substrates found in pesticides and herbicides, they can degrade toxic man-made compounds, potentially having a role in bioremediation (Ferreira *et al.* 2011; Inhülsen *et al.* 2012; Mahenthiralingam *et al.* 2005; Mahenthiralingam and Vandamme 2005).

Bcc bacteria are also some of the bacteria most prominent in chronic infections in the lungs of CF patients. Such infections can develop into “cepacia syndrome”, causing rapid deterioration of lung function, associated with necrotizing pneumonia, bacteremia and sepsis, possibly resulting in death. Infection developed by Bcc pathogens are either acquired in the hospital setting or from the environment, as they are not normally carried as commensal organisms (Jones *et al.* 2004; Mahenthiralingam *et al.* 2005).

B. cenocepacia and *B. multivorans* comprise 85% of all Bcc infections, appearing to be the most abundant and serious forms of disease (Rhodes *et al.* 2016). Infections of this kind are usually difficult to treat with antibiotics, as they present multiple drug resistance due to several mechanisms such as outer membrane penetration barrier, restrictive porin proteins, efflux pumps of the resistance nodulation cell division family, and a modified lipopolysaccharide (LPS) in the outer membrane (Rhodes *et al.* 2016).

Usually, treatment of Bcc infections relies on ceftazidime and other cephalosporins, since the intrinsic resistance of these bacteria make them invulnerable to several other classes of antimicrobials, including aminoglycosides, β -lactams, fluoroquinolones and polymyxins. Intrinsic resistance results from inherent structural or functional characteristics such as differences in cytoplasmic membrane composition and existence of an outer membrane. Specifically, Bcc species from CF patients were found to survive known antibiotics such as chloramphenicol, co-trimoxazole, ciprofloxacin, tetracycline, rifampin, avibactam and co-amoxiclav (Rhodes *et al.* 2016).

It is generally accepted that *P. aeruginosa* bacteria, the other major pathogen, can colocalize Bcc in biofilm-like structures within chronically infected CF lungs. This is supported by *in vitro* studies demonstrating mixed biofilms (Bragonzi *et al.* 2012; Nielsen, Tolker-nielsen, and Barken 2000; Riedel *et al.* 2001). *P. aeruginosa* can however, in some instances, produce growth inhibitory substances to protect their biofilms against invasion by Bcc bacteria (Al-Bakri, Gilbert, and Allison 2004). On the opposite spectrum there is evidence that both bacteria do not coexist in biofilm-like structures, since *P. aeruginosa* has been shown to grow in a sessile manner within biofilm matrix, but Bcc species in biofilm-like structures have not yet been identified within the intraluminal CF mucus inhabited by *P. aeruginosa* *in vivo* (Costerton, Stewart, and Greenberg 1999; Fung *et al.* 2010; Ghani and Soothill 1997; Lam *et al.* 1980; Miller *et al.* 2014; Sriramulu *et al.* 2005; Worlitzsch *et al.* 2002). It may be that either *in vitro* systems are not able to properly mimic the CF lung environment, that Bcc have been missed *in vivo*, or that they occupy different niches within the CF airway, the Bcc bacteria being found within pulmonary macrophages and respiratory epithelial cells (Butler *et al.* 1994; Leelarasamee 1998). Nonetheless, *B. multivorans* has been found as small aggregates within the mucus layer (Schwab *et al.* 2014).

Other than CF, Bcc pathogens can also establish themselves in patients with other diseases such as chronic granulomatous disease and meningitis, and in general, in immunocompromised patients (O’Grady and Sokol 2011; Peralta *et al.* 2018).

1.2.1 *Burkholderia multivorans*

B. multivorans is an aerobic, glucose non-fermenting Gram-negative bacillus belonging to the Bcc (Peralta *et al.* 2018). It was first deemed an environmental pseudomonad with high metabolic versatility, integrating the *Pseudomonas* genus, after taxonomic studies in the 1970s. However, this genus was dissected, and its taxonomic heterogeneity led to the transfer of this species to the then new genus *Burkholderia*. It is an opportunistic pathogen able to install itself in the airways of CF patients, establishing antimicrobial resistant chronic infections in their lungs (Mahenthiralingam and Vandamme 2005).

A study has confirmed the genomic structure of this species to be highly conserved. Distinct multilocus sequence types (ST), which compare DNA sequence variations of housekeeping genes among strains and characterize each strain according to their unique profile, were shown to define specific genomic lineages and thus predict both phylogeny and gene content. This has been proven by analyzing several isolates of the species, which confirmed: conservation of a high content of ortholog genes which may clue in on species-specific lifestyle; location of each coding sequence (CDS), as it may influence the evolutionary course and different chromosomes are associated with different gene copy numbers, mutation rates and expression levels; and over- or underrepresented biological functions from isolates. Each of these STs also displayed unique orthologs. Furthermore, the analyzed isolates from this work originated from different geographic locations, sources (CF sputum and soil) and were years apart, further supporting the verified genomic conservation (Peeters *et al.* 2017).

1.3 Bacterial biofilms within a CF context

Once established, whether within a niche in the environment or in a CF patient's lung, many species of bacteria can grow in one of two ways: either as dispersed and free single cells, or as a biofilm. The latter consists of a structured community of densely packed sessile cells enclosed within a self-produced extracellular polymeric matrix adherent to an inert or living surface (Costerton *et al.* 1999) .

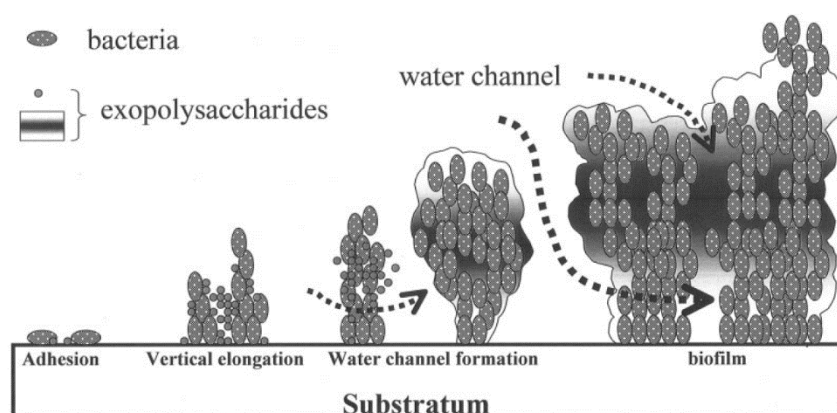


Figure 2 - Time-dependent formation of a surface-attached biofilm. Retrieved from Maeyama *et al.* (2004).

Generally, biofilm development takes place in multiple stages (Figure 2). First an initial attachment of the bacteria to the surface occurs. The planktonic cells form a single layer of surface-adherent cells, during which flagella and pili are involved. Once established, this attachment becomes irreversible as the formation of microcolonies takes place. These then mature until highly porous mushroom-shaped structures are formed by the extracellular polymeric matrix. Finally, detachment of some cells occurs, returning to their planktonic and mobile form, so as to begin the process elsewhere. The porosity of biofilms allows the liquid in the environment to pass through and deliver the required nutrients for survival through channels (Kim and Lee 2016).

This growth mode is also deemed a virulence mechanism that grants the bacteria protection against host immune response or antibiotic treatment as well as environmental stresses such as desiccation, nutrient limitation and predation (Gambino and Cappitelli 2016; Tseng *et al.* 2016). Biofilms are also generally accepted to have reduced metabolic activity, which associated with specific genetic components and the physical barrier that the biofilm itself constitutes, results in a decrease of their susceptibility to a range of antibiotics. Slow-growing or nongrowing cells are not very susceptible to many antimicrobial agents (Costerton *et al.* 1999; Haaber *et al.* 2012). Biofilms are yet still vulnerable, especially at an early stage, to dispersion by DNase, for instance, shown to restore antibiotic sensitivity (Nemoto *et al.* 2003).

Planktonic single cells on the opposite spectrum, have much more freedom of movement within the environment, mostly attributed to the presence of flagellum. Despite this, bacteria in biofilms display increased antibiotic tolerance when compared to planktonic microbes, supporting the suggestion that for bacteria to be able to form biofilms, planktonic single cells are merely a transition state at the most, needed for the seeding of biofilms and subsequent release and dispersion from these. However, how aggregates impact biofilm initiation and development, is not well known (Diggle *et al.* 2016).

Though the biofilm form of growth, as mentioned, can be advantageous for bacteria for several different reasons, it is not always so. The arrangement of bacteria within biofilms limits the access of nutrients to its interior and therefore to the overall bacterial community, presenting a disadvantage when in comparison to single cells. However, when competition is high, propelled by nutrient limitation and presence of other bacteria or density of single cells, aggregated bacteria display a higher fitness when comparing to single cells, because they can protrude above the biofilm surface and cells at the top of it have better access to the resources. Even though such conclusion takes only into account competition as the sole pressure on cells, it suggests that adaptations like motility loss, often occurring in CF patients, could be selected for, since they enhance aggregate growth. The same is verified between more spread aggregates or more concise ones, as those that extend for a wider area perform better when competition is low since they have more access to nutrients, but those that are tighter and less dispersed perform better when competition is high (Diggle *et al.* 2016; Melaugh *et al.* 2016).

Bcc bacteria appear to have the ability to form biofilms *in vitro* regardless of species, mostly associated with quorum-sensing (Schwab *et al.* 2014). Several genes have been identified as required for biofilm maturation in Bcc, encoding surface proteins, genes involved in biogenesis and maintenance of outer membrane, and genes encoding regulatory factors that affect acyl-homoserine lactone (AHL) production. A meaningful number of CF pathogens can also grow planktonic cellular aggregates, as well as single cells, a trait shared by several Bcc strains (Silva *et al.* 2017).

The extracellular polymeric matrix that holds the bacterial community of a biofilm together is usually composed by several components such as extracellular DNA (eDNA), exopolysaccharides (EPS), proteins and lipid vesicles. The process by which these biofilms are formed is species-specific (Tseng *et al.* 2016). It is generally accepted that biofilms are seeded from preformed aggregates or single planktonic cells, providing bacteria with a mode of colonization of new niches in a hostile environment. The biofilm structure is also influenced by factors such as microbial mobility, adhesion, initial attachment frequency and bacteria re-attachment to the biofilm (Jayatilake *et al.* 2017), with specific molecules also known to be crucial in its development, which will be marginally explained here, as well as some mechanisms.

1.4 Planktonic aggregates

Under a conventional biofilm growth mode, bacteria are trapped in a sessile community, with limited mobility. However, another considered form of biofilm consists in a mode where bacteria still aggregate, but in a surface-independent way. These free-floating suspended biofilms are, in several instances, called planktonic aggregates, which is also used to denominate tight bacterial microcolonies and mobile biofilms (Pönisch *et al.* 2018). It is speculated that aggregates provide bacteria with the benefits of a biofilm while maintaining mobility, and that this combination may contribute to the difficulties of eradicating infections (Haaber *et al.* 2012). Other similar modes of growth are the so-called clumping, a cellular behavior in which cells transiently interact by adhering to one another at their non-flagellated poles before swimming apart (Bible *et al.* 2008). One hypothesis of how cells adhere at their non-flagellated poles is that adhesins present in the polar region of the cells or secreted at this location stabilize cell-cell contacts in clumps and flocculation (Alexandre 2015). Flocculation is yet another mode growth which is preceded by clumping and is an irreversible process by which vibroid motile cells transition to nonmotile round cells encased in an extracellular polymeric matrix and in a surface-independent way (Bible *et al.* 2015). Flocculated and biofilm-bound cells are functionally similar (Alexandre 2015).

With this, rises the hypothesis that bacteria do not need to be attached to surfaces in order to establish chronic infections. Non-attached aggregates from stationary-phase cultures have comparable growth rates to surface attached biofilms as stated by experiments measuring the rRNA of both through RT-PCR, since number of ribosomes is linear with growth rate. Internal structures of the aggregates matrix components and capacity to survive antibiotics and phagocytes also appear to be very similar. More so, these types of aggregates were already verified in CF lungs (Alhede *et al.* 2011).

Planktonic aggregation has been observed in quite a few bacterial species. *Campylobacter jejuni*, a food borne pathogen, is regularly verified to auto-aggregate. *Streptococcus pyogenes*, a human pathogen, forms planktonic aggregates in liquid culture, granting resistance to phagocytosis and virulence (Haaber *et al.* 2012). *Staphylococcus aureus* is known to also grow in small clusters up to a macroscopically visible size (Figure 3). Furthermore, its aggregates started to appear in the early exponential growth phase, proceeding until post-exponential phase, where more than 90% of the population was part of the aggregate community (Haaber *et al.* 2012).

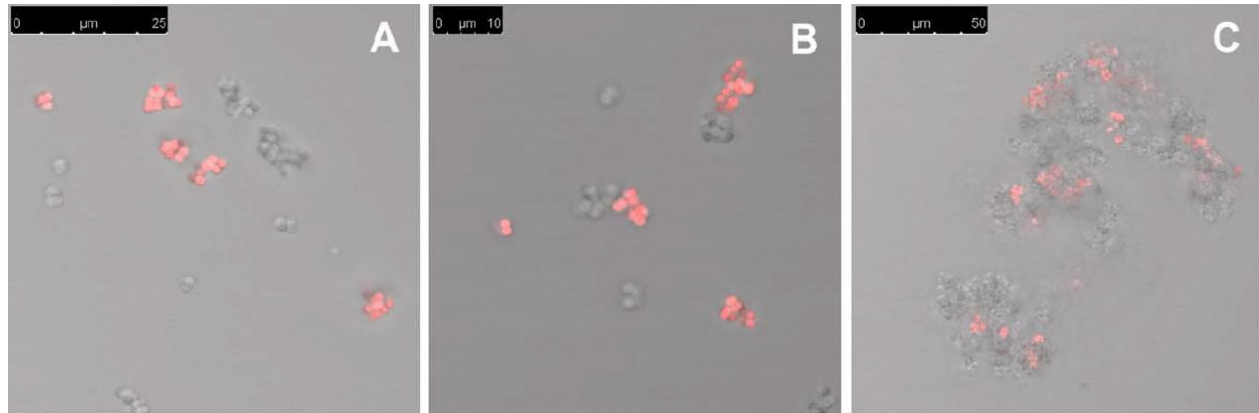


Figure 3 - Aggregation of *S. aureus* by different clonal origin cells differentially labelled. Measured between 0.01 and 0.5 OD of culture growth. Retrieved from Haaber *et al.* (2012).

P. aeruginosa has possibly used this growth mode, attaining large aggregates of packed viable cells, to circumvent the limited mobility characteristic of a conventional biofilm (Haaber *et al.* 2012). Furthermore, it has been verified in lungs of CF patients, near the epithelial cell surface, as non-surface-attached microcolonies, but *in vitro* it disperses into single cells upon nutrient starvation (Schleheck *et al.* 2009). An interesting note is that in planktonic cultures of this species, the production or absence of EPS had no effect on antibiotic tolerance, as the minimal inhibitory concentration values were comparable for both (Goltermann and Tolker-Nielsen 2017).

Several Bcc species and strains can produce this type of cellular aggregates in a salts-based medium with mannitol, namely *B. multivorans*, *Burkholderia ambifaria* and *Burkholderia contaminans*. Moreover, these types of aggregates were found in both mucoid and non-mucoid isolates of *B. multivorans*, suggesting the possibility that perhaps *cepacia* exopolysaccharide is not required for the formation of such structures. They also displayed increase in size over time, under stress conditions, as opposed to what was verified in *P. aeruginosa* PAO1 (Silva *et al.* 2017). A specific LysR-type transcription regulator (LTTR) encoded by the highly conserved gene *ldhR* (Bmul-2557) has been shown to have a significant, but not exclusive, influence on cellular aggregates and attached biofilm formation through the direct regulation of *ldhA* gene encoding D-lactate dehydrogenase. This LdhA enzyme is therefore also implicated in the formation of these planktonic cellular aggregates and biofilms in *B. multivorans* (Silva *et al.* 2017).

The process of inflammation may also have a role in the formation of these aggregates. When it is induced by bacterial infection in CF patients, the result is a sputum enriched in neutrophil derived products such as DNA and F-actin (Caceres *et al.* 2014). These are then polymerized and used as a scaffold instead of a surface, to form biofilm. Therefore, surface independent biofilm formation is accelerated when dying neutrophil count is abundant, altering bacteria survival and greatly increasing biofilm mass in the first 24 to 48 hours, at which time the planktonic bacteria

are generally more vulnerable. This can also explain why *P. aeruginosa* typically occurs in the setting of intense preexisting inflammation in the CF airway and the verified occurrence of this kind of aggregates in CF lungs (Caceres *et al.* 2014).

This type of aggregates may not be regulated by the same genes that control conventional biofilm formation since in gel growth environments *P. aeruginosa* displayed cell aggregation even when possessing biofilm inhibiting mutations (Staudinger *et al.* 2014).

In a comparative point of view, in *S. aureus* both aggregates and biofilms were found to have increased antibiotic resistance, as well as an increased rate of mutations, when compared to planktonic single cells, supporting the idea that external stresses have a role in inducing these modes of growth and present advantages needed for survival under certain conditions. Furthermore, aggregated cells display a higher metabolic activity than both planktonic cells and cells in a biofilm, possibly being another strategy of survival that differs from conventional biofilms (Haaber *et al.* 2012).

1.5 Elements controlling bacterial aggregation

1.5.1 Quorum sensing

Quorum sensing is a cell-density dependent process, through which bacteria communicate and control the expression of various genes, many associated with virulence. Small signaling molecules or autoinducers, AHL, are produced and when they reach critical concentration they interact with specific bacterial receptor proteins, which in turn switch genes on or off. This mechanism was first reported to regulate bioluminescence in the marine bacterium *Vibrio fischeri*. Two proteins were the basis of this system: an AHL synthase called LuxI and a transcriptional activator, LuxR, which turns on the expression of the bioluminescence genes (Cámara *et al.* 2002).

P. aeruginosa uses three interconnected quorum-sensing systems *las*, *rhl* and *pqs*, all of which take part in the development and stabilization of its biofilms, also controlling a wide array of virulence factors (Yang *et al.* 2007). The LasR-LasI system controls the expression of a group of extracellular virulence factors, and it also controls the system RhlR-RhlI, which in turn controls genes for the production of a number of secondary metabolites. Wild-type strain, *lasI* mutant and *rhlI* mutant can colonize a glass surface and form microcolonies. However, while the *rhlI* and wild-type form thick, biocide-resistant biofilms, the *lasI* forms thin, undifferentiated and dispersion-sensitive biofilms. Thus, this specific QS may be required for biofilm differentiation and maturation (Costerton *et al.* 1999).

In *B. cenocepacia* a quorum sensing system was first identified by Lewenza *et al.* and consisted of LuxIR homologs, designated CepI and CepR, the latter being the putatively ancestral regulator found in all Bcc bacteria (Lewenza *et al.* 1999). Subsequently it has been shown to regulate expression of pathogenic traits like motility and biofilm production; secretion of extracellular enzymes; virulence during infection and general host toxicity; as well as siderophore synthesis, protease production and a type III secretion system (Mahenthiralingam and Vandamme 2005). *cepR* and *cepI* mutants were also shown to be able to attach to surfaces but could not differentiate and develop into a mature biofilm, suggesting that the CepIR QS system is not required for adhesion but is crucial for biofilm development. Furthermore, the gene downstream of *cepI*, *Bcam1871*, co-transcribed with *cepI* and directly regulated

by CepR positively regulates the LTTR ShvR, which in turn negatively regulates *cepIR* and *ccilR* transcription, having a toll on the effect these QS systems have on biofilm formation. Nonetheless, this ShvR has also been found to positively regulate biofilm formation, independent of the CepIR and CcilR QS systems (Fazli *et al.* 2014).

In the case of *Burkholderia multivorans*' ability to form biofilms, it is thought that quorum-sensing does not take part in regulation of the *ldhR* gene, identified to be implicated in aggregate and biofilm formation, since it lacks the presence of a *lux box* in its upstream region (Silva *et al.* 2017).

1.5.2 Extracellular DNA (eDNA)

eDNA is DNA thought to be released from dead cells by controlled cell lysis or of lysis of DNA containing vesicles (Haaber *et al.* 2012). It is a component thought to be important in the early establishment of biofilms, having a role in cell-to-cell interconnecting (Alhede *et al.* 2011). It was even verified to be the most abundant polymer of the extracellular matrix produced in *P. aeruginosa* PAO1 biofilms, being crucial for its development and maturation (Shircliff *et al.* 2002). Whitchurch *et al.* (2002) experimented on these bacteria incubated in media with or without extracellular DNase I. Its presence in the medium prevented biofilm formation, whereas its absence led to an extensively colonized environment. DNase I was also found to be able to dissolve biofilms at an early stage, namely 12, 36 and 60 hours after their formation (Figure 4). However, they almost did not affect biofilms 84 hours old. This suggests that at this point the matrix may already produce other substances that provide it with resistance, or that it may produce enough proteolytic enzymes to inactivate the DNase I. Either way eDNA is proven to be required for biofilm development and maturation (Whitchurch 2002).

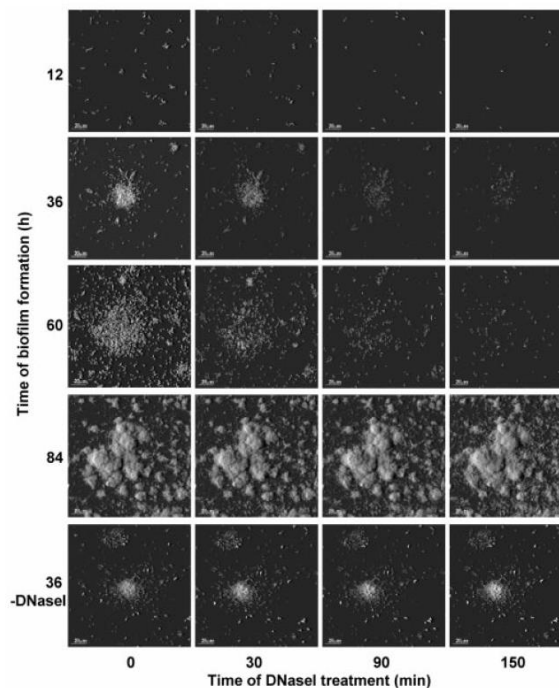


Figure 4 - Effect of Dnase I on established biofilms of GFP-tagged *P. aeruginosa* PAO1. Retrieved from Whitchurch *et al.* 2002

In some bacteria this DNA release may be regulated by quorum-sensing, as verified for *P. aeruginosa*, presumably involved in the aforementioned lysis of a subpopulation of cells or vesicles (Kim and Lee 2016).

1.5.3 Amino acids

Amino acids may also have a role in biofilm development and morphology. *P. aeruginosa* has been shown to adapt to amino acid starvation through the so-called stringent response, described as a global regulation mechanism. This response starts with accumulation of uncharged cognate tRNA. When the ratio of charged/uncharged tRNA falls below a certain level, the ribosomal A site in the mRNA codon is occupied by the uncharged cognate tRNA, stalling peptide chain elongation. Another aspect of this response is that the synthesis of the pseudomonal nucleotide (p)ppGpp (guanosine pentaphosphate) from GTP and ATP is induced, and as demonstrated in *E. coli*, it inhibits RNA polymerase, causing downregulation of a wide range of energetically demanding cellular processes, stimulating certain amino acid synthesis pathways and inducing stationary phase-specific genes through this phase's specific sigma factor, RpoS, thus adjusting metabolism according to the lesser availability of amino acids, and which corresponds to the slower metabolism of biofilms (Shircliff *et al.* 2002). Sigma factors are constituents of transcription regulation in bacteria. They have the role of recruiting the core RNA polymerase to recognize promoters with specific DNA sequences (Tripathi *et al.* 2014). RpoS, specifically, is a factor implicated, in *E. coli*, in the response to osmotic stress, acid shock, heat shock, oxidative DNA damage and transition to stationary phase, in addition to the amino acid starvation. Its transcriptional regulation is under positive control of (p)ppGpp and negative control by the cAMP receptor protein. As it has been shown in *P. aeruginosa* that *rpoS* mutant led to thicker biofilm structures, it is possible that under stress, this factor may be either induced or repressed in order to control biofilm size and allow more or less access to nutrients, respectively (Shircliff *et al.* 2002).

Sriramulu *et al.* also verified that when amino acids were not available in ASM medium (ASM-), which normally contains components such as mucin, DNA, surfactant, salt ions, iron and amino acids to emulate patient's lung environment, visible *P. aeruginosa* microcolony appeared smaller, when in comparison to growth in ASM+, able to form macroscopically visible clumps (Figure 5). They also verified a proportional correlation between tight microcolony formation and amino acid content (Sriramulu *et al.* 2005).

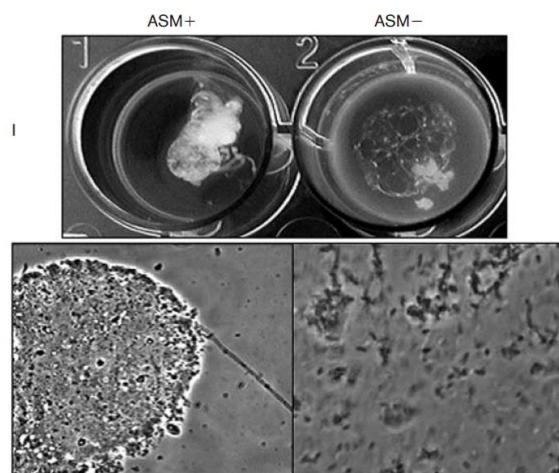


Figure 5 - Microcolony formation of *P. aeruginosa* PAO1C in ASM+ and ASM-. Retrieved from Sriramulu *et al.* 2005

This is not true for all amino acids. Several tested L-amino acids like arginine, ornithine, isoleucine, leucine, valine, phenylalanine and tyrosine were found to promote biofilm production in *P. aeruginosa*. On the other hand, some D-amino acids can cause biofilm disassembly, without however inhibiting planktonic growth (Kim and Lee 2016).

1.5.4 Exopolysaccharides (EPS)

EPS are high-molecular weight sugar-based polymers synthesized and secreted by many microorganisms. It is often suggested as being the major component of biofilm mature structures (Ferreira *et al.* 2011). EPS mediated adhesion is known to be important for bacterial biofilm development, as it affects both the initial attachment to surfaces and the subsequent resistance to shear flows by providing mechanical integrity and resistance against attack from foreign entities (Jayatilake *et al.* 2017). When *B. multivorans* EPS is produced, virulence of the respective isolate appears to be enhanced when in comparison to their isogenic non-producing mutants, as well as increasing antibiotic resistance (Ferreira *et al.* 2013). However, its absence does not eliminate the possibility of causing a severe infection (Drevinek and Mahenthiralingam 2010).

Some Bcc species produce a single exopolysaccharide, while others produce mixtures. However, the most common EPS produced by *Burkholderia* genus is *cepacia*. Yet again, it is another factor that can be switched on and off according to the needs of the bacteria to survive in host environments, since Bcc isolates from CF patients *in vitro* have shown that transition between mucoid and non-mucoid mutants is relatively frequent and can be induced by exposing cells to stresses such as high concentrations of antibiotic. Furthermore, the type of EPS produced depends on growth conditions, therefore its expression is regulated according to the different external conditions, crucial in bacterial colonization and adaptation to different environments and hosts (Ferreira *et al.* 2011). Naturally these transitions are accompanied by mutations and genomic rearrangements that also impact motility, chemotaxis, biofilm formation, bacterial survival rate under nutrient starvation and virulence.

While clinical *B. cenocepacia* isolates are frequently non-mucoid as a result of mutations in EPS biosynthetic or regulatory pathways, early clinical isolates of *B. multivorans* have the capacity for EPS production while late isolates lose this trait (Denman and Brown 2013).

1.5.5 Motility and chemotaxis

There are 4 main ways of movement in bacteria: swimming and swarming, for those possessing flagella; twitching for those possessing pili; and gliding for other movement mechanisms that occur in the absence of such appendages (Alexandre 2015).

Motile bacteria can react to stress conditions via negative chemotaxis, swimming away from the stressful environment and into a more favorable niche (Rossi *et al.* 2018). *Helicobacter pylori* achieves its specific orientation in the stomach by sensing a pH gradient that guides it away from the lumen and towards the epithelium, allowing it to colonize a specific region where it can achieve high local cell density and establish chronic infections. Stresses can also lead to an adaptation to such environment, transpired through the loss of motility and transition from single

planktonic cells to biofilms. Even negative chemotaxis can be in itself a trigger for biofilm formation, characteristically accompanied by loss of motility (Rossi *et al.* 2018).

The production of components required for biofilm production and flagella are, however, not mutually exclusive, since the flagella, at least in an initial stage may help the colonization and invasion within the host, where the biofilms will establish themselves. The quorum-sensing-related signal autoinducer 2 (AI-2) in *E. coli* for instance, can activate both biofilm-related and flagellar and chemotaxis genes, although the mechanisms are not well-known (Rossi *et al.* 2018).

When aggregating still in the planktonic phase, the spreading of the aggregate in its initial shape, determined partially by the motility of the cells, may determine the fate of biofilm development, as mentioned earlier. More spread aggregates perform better when competition with surrounding unaggregated bacterial cells is low, since it has a larger surface over which it can absorb nutrients, presenting an initial growth advantage. Initially rounded aggregates, or tighter ones, perform better when competition with surrounding unaggregated cells is high (Melaugh *et al.* 2016).

Formation of cell aggregates as a result of chemotaxis signaling is deemed by some authors to be a transient behavior in which the cells are not yet committed to permanent adhesion (Alexandre 2015).

Successful aggregation depends on physical forces like attractive van der Waals and biological mechanisms like the bridging of protein adhesins and saccharide receptors between opposing cell walls. However, for this to happen cells must approach each other, either through swimming motility or through Brownian motion (Dienerowitz *et al.* 2014). They can undergo this type of motion since they are small enough to be deflected by the force of impact from individual liquid molecules (Conrad 2012). In a study performed in *Bacillus subtilis* it was shown that the strongest repulsive forces between bacteria were verified under nutrient-rich conditions, and weaker forces or the absence of them were verified in systems (deionized water or NaCl solution) where planktonic aggregation was more prominent, leading to the suggestion that under nutrient-starved systems there is a switch in the repulsive forces in order to facilitate aggregation. These repulsive forces are attributed to cell motility rather than electrostatic repulsion since the latter are very limited beyond the cell surface, thus they cannot explain the repulsion under nutrient-rich conditions (Dienerowitz *et al.* 2014).

Motility in *E. coli* has been shown to be critical for the initiation of biofilm formation as mutants lacking flagella ($\Delta fliC$) or those with paralyzed flagella ($\Delta motA$, $\Delta motB$, $\Delta motAB$) were severely defective in biofilm formation. At the same time, chemotaxis was deemed dispensable since Δche mutants showed almost no difference to the wild-type strain in regard to biofilm formation. Thus, it is suggested that motility may be required to overcome repulsive forces at the cell and surface or may allow the initial spread of a biofilm by facilitating movement of growing cells along the surface. Though flagella are also regarded as important in adherence, they do not appear to be the main factors since the absence of type I pili in these mutants resulted in no cells attached to the surface. Based on these results it appears that motility is important for cells to come into contact with an abiotic surface by overcoming surface repulsion (Figure 6). Once attached, type I pili is required to achieve a stable cell-to-surface attachment. Non-specific adhesins are then used to promote adherence and finally motility may then facilitate development of a mature biofilm, by promoting movement along a surface and spreading the biofilm. Another study reports that *P. aeruginosa* lacking type IV pili are able to form a monolayer on the surface, but do not develop past this stage, being unable to form a multilayered biofilm.

This type IV pili is associated with twitching motility, which facilitates movement along a surface. This movement, in the case of *E. coli* type I pili, does not happen, but both appendages appear to contribute to biofilm formation and development evidencing different approaches for bacteria to initiate biofilm formation (Pratt and Kolter 1998).

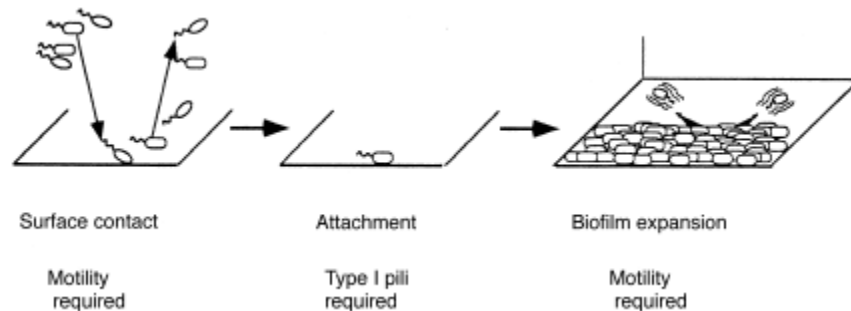


Figure 6 - Model for initiation of *E. coli* biofilm formation dependent on motility and Type I pili for surface contact and attachment, respectively. Retrieved from Pratt and Kolter (1998).

Mutations abolishing flagellar motility negatively affect pathogenesis by *Burkholderia pseudomallei* and *B. cepacia*, suggesting the flagellum is a virulence factor in these bacteria (Rossi *et al.* 2018).

A model chemotaxis pathway is most well described in *E. coli*, the Che1 pathway (Figure 7). According to its description, these bacteria sense external stimuli, received by membrane bound chemoreceptors. This leads to a conformational change and signaling activity of the chemoreceptors which bind to the cytoplasmic histidine kinase CheA via CheW and regulate its activity. CheA which once activated autophosphorylates, subsequently causes phosphorylation of the response regulator CheY, which will bind to effectors and induce alterations in genetic expression. The chemoreceptors activity is controlled by methyltransferase CheR and methylesterase CheB, allowing sensory adaptation. CheR constitutively adds methyl groups to the glutamate residues on the C-terminal of the receptors increasing the ability of the chemoreceptors to activate CheA autophosphorylation and CheB depends on phosphorylated CheA and is phosphorylated by it. Once activated, it demethylates specific methylated glutamate residues within the chemoreceptors, producing a second conformational change that counters the initial change induced by ligand binding (Bible *et al.* 2008). In *Azospirillum brasilense*, an alphaproteobacterium isolated from various soils and the rhizosphere, the Che1 chemotaxis-like pathway contributes to chemotaxis and aerotaxis. It has also been demonstrated to contribute to cell surface adhesive properties that affect clumping and flocculation. It has been shown to clump in transient cell-cell contacts under conditions of elevated aeration, thus reducing surface to volume ratio and limiting diffusion. This clumping appears to be controlled by chemotaxis signaling since mutations in genes encoding proteins of the chemotaxis signaling pathway, caused a defect in chemotaxis and in clumping and flocculation (Bible *et al.* 2008). It is also thought to control changes in adhesive properties, likely in EPS structure or composition. A similar process is also found in *H. pylori*. Once CheY is phosphorylated, it interacts with FlhM, a protein of the flagellar motor switch, causing clockwise rotation. This response is terminated by CheZ which accelerates decay of

phosphorylated CheY. CheY and CheAY2 have been shown to be necessary for flagellum-regulated movement and chemotaxis towards mucin (Foyne *et al.* 2000).

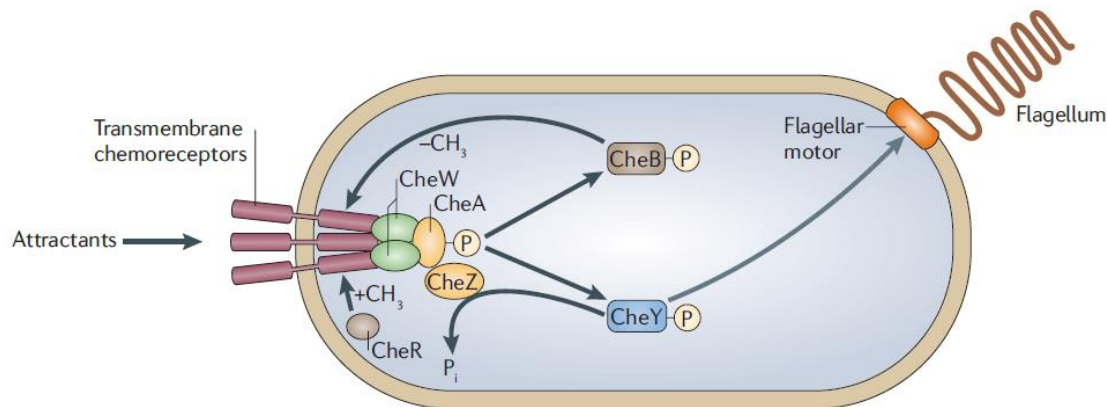


Figure 7 - *E. coli* Che 1 chemotaxis pathway affecting motility. Retrieved from Porter *et al.* (2011).

By controlling the activity of the motility apparatus, chemotaxis can actively promote the initiation of cell-cell contacts during aggregation and as a result regulate transient cell aggregation prior to irreversible adhesion. Thus, it promotes the transient accumulation of cells within a certain region, increasing probability of cell-cell interaction, including transient attachment. Chemotaxis signal transduction links environmental sensing to changes in the motility pattern and directs movement toward attractants or away from repellants. It controls flagellar motility by regulating the frequency at which the flagellar motor changes its direction of rotation or the speed at which the flagellar motor rotates (Porter *et al.* 2011). This is a mode of control conserved across flagellated bacteria, regardless of flagellar arrangement or number (Alexandre 2015).

M. xanthus, a predatory bacterium in soil is also shown to depend on twitching and gliding motility to produce aggregates. This is controlled by the Frz chemotaxis pathway, which in turn is regulated by sensory input provided by the FrzCD receptor when cells are brought into contact (Porter *et al.* 2011). This further supports that chemotaxis is required for transient aggregation, by changing motility and orienting cells into aggregates. These changes of motility through chemotaxis are specifically associated with unfavorable conditions for the growth of each species, usually corresponding to physicochemical conditions related to energy metabolism, sensed by their respective receptors.

According to Laganenka *et al.*, *E. coli* aggregation could be divided into three phases: initial formation of “seeding” aggregates by random collisions of motile cells, which do not require chemotaxis (small aggregates are formed for *cheY* mutant but not for *fliC* or *motA* mutants). When bacteria reach a physiological cell density, they secrete considerable levels of AI-2 to mediate gradient formation and chemotactic attraction of individual cells to the aggregates. This increases growth rate by increasing local cell density. As the aggregates reach an equilibrium with free-swimming cells and a gradual increase of background AI-2 occurs, chemotaxis is disrupted since cells are no longer able to follow gradients of AI-2 above high background, thus aggregate dispersal occurs (Laganenka *et al.* 2016).

P. aeruginosa uses two motility appendages to move near surfaces: a single polar flagellum that acts as the helical propeller, encoded by *fliM*, and various type IV pili (TfP), acting as linear actuators, encoded by *pilA*. Both of them can also work as adhesins to stick bacteria to surfaces and to one another. The distal tip of TfP bears an adhesin that

can stick to several materials, pioneering the initial attachment to surfaces (Conrad, 2012). This is followed by block of flagellar rotation and production of proteinaceous adhesins type IV pili, which secure bacteria to the surface and allow cells to spread over the surrounding area (Rossi *et al.* 2018). This suggests that motility and adhesion are related, as supported by a study showing that mutants lacking the motility appendages adhere to surfaces at a much slower rate than the wild-type strain. Near solid surfaces, hydrodynamic interactions with the surface modify the physics of flagellated swimming. They can reorient bacteria and allow them to swim against the direction of flow, and thus bacteria can rapidly spread on surfaces against adverse flow and form biofilm (Conrad, 2012).

TfP is constituted of semiflexible polymers that can polymerize and depolymerize through the cell wall, giving it the unique ability to extend or retract. This is useful as it allows the bacteria to “crawl” when adhered to a surface, and therefore spread or displace itself from the surface (Conrad, 2012).

In a study, *P. aeruginosa* mutants defective in the initial steps of biofilm formation were described. There were two classes of these mutants, called the *sad* (surface attachment defective). One class constituted flagella and motility mutants and were unable to adhere to the plastic surface used. The other class was defective in the biogenesis of the hair-like appendages, type IV pili, which were only able to form a monolayer, but not microcolonies, like the wild-type (Costerton *et al.* 1999).

In *P. aeruginosa*, aggregation has been found to be caused by GGDEF domain-containing WspR, linked to the regulation of *cup* genes, which encode a putative fimbrial adhesin required in wild-type cells for biofilm formation. Thus, WspR can control biofilm formation through facilitation of adhesion to surfaces (D’Argenio *et al.* 2002).

Furthermore, insertion mutants made in *P. aeruginosa* PAO1 led to the discovery of a strain which grew wrinkled colonies, mostly vertically, and did not spread by twitching, swarming or swimming motility. It was denominated the *wspF10*. The aggregates formed were so tight they could be grabbed with forceps. Sure enough, this gene lied within a gene cluster predicted to encode a chemotaxis-like cascade and was found to be homologous to the *wsp* cluster from *P. fluorescens* also involved in aggregation and wrinkled morphology. WspF is 30% identical to CheB of *E. coli*. Assuming a similar function in *P. aeruginosa*, inactivation of WspF would result in hypermethylation of the methyl-accepting chemotaxis protein, WspA. This would cause constitutive activation of the Wsp chemosensory pathway and ultimately of the response regulator WspR. Since WspR controls the structural components necessary for the wrinkled-colony morphology, this would mimic the effect of expressing the heterologous constitutively active WspR. Thus, it is possible that WspR controls aggregation in *P. aeruginosa*, as further supported by the loss of wrinkled colony formation in *wspR* mutant (D’Argenio *et al.* 2002).

All Bcc species possess the trait of motility, expressing flagella and moving through liquids. The number of flagella appears to be strain dependent and a key virulence factor. The flagellum also serves as an adhesin and enables pathogens to invade host cells.

The relatively high density found within CF may also restrict motility and thus localize bacteria into groups, promoting aggregation. Despite association of pilus with bacterial adhesion, its role however is rather ambiguous. Studies on *B. cenocepacia* revealed that disruption of the gene responsible for pilus expression, *cblA*, led to cells maintaining their ability to adhere to respiratory epithelial cells and mucin. It did however greatly increase the ability

of bacteria to self-aggregate. This suggests that cable pilus expression in *B. cenocepacia* is important to mediate cell-cell interactions, and that it may contribute, though not solely, to adherence to surfaces (Tomich and Mohr 2003).

1.5.6 Cyclic-di-GMP

It is an intracellular messenger molecule for signal transduction. Widely implicated in biofilm formation, dispersion, motility, virulence and more. The intracellular level of cyclic-di-GMP (c-di-GMP) determines the life mode between planktonic and biofilm. Its increase facilitates biofilm formation while its decrease results in increased dispersal or switch into a planktonic mode of growth. It is synthesized from two GTPs by diguanylate cyclase activity (DGC), and it is degraded into pGpG (5'-phosphoguanylyl-(3',5')-guanosine) or into two GMPs by phosphodiesterase activity (PDE). The level of c-di-GMP is therefore balanced between these two reciprocal enzymatic activities. The proteins with diguanylate cyclase activity have conserved GGDEF domains and the proteins with PDE activity have EAL or HD-GYP domains. These are often fused with periplasmic or membrane-embedded ligand-binding sensory domains, indicating that they may have the ability to modulate their enzymatic activity according to sensed environmental stresses. The c-di-GMP molecule binds to effectors in one of three ways: associating with proteins through c-di-GMP binding motifs; associating with proteins that do not have such motives and whose mechanism is unknown; or associating with RNA molecule. Either way they modulate gene expression upon binding, directly influencing phenotype of cells, namely the capacity to aggregate. One such example is the binding of c-di-GMP to a PilZ binding motif, which modulates twitching motility in *P. aeruginosa*, as the proteins that contain these domains are known to interact with the flagellar motor switch proteins, FliG and FliM (Kim and Lee 2016).

High internal levels of c-di-GMP induce the production of adhesins and extracellular matrix components, as well as inhibit flagellar motility, enabling the formation of biofilm. If its levels are low, the opposite happens, and planktonic mode of growth takes place (Fazli *et al.* 2014).

One of the best-known DGCs is the RR WspR, part of the Wsp chemotaxis-like regulatory system in *P. aeruginosa*. The chemoreceptor WspA is activated in response to growth on surfaces, inducing phosphorylation of WspR, which is stimulated to synthesize c-di-GMP. The c-di-GMP can then have different effectors such as Alg44 for the production of alginate; FimX for twitching motility; FleQ, the master regulator for the biosynthesis of flagellum and PelD for production of Pel polysaccharide. All of these are thought to contribute to biofilm formation (Fazli *et al.* 2014).

A matter that is rather ambiguous concerning the role of c-di-GMP is related to the tyrosine kinase protein BceF of *B. cenocepacia* IST408. This was shown to regulate expression of genes related to stress response, motility, c-di-GMP signaling, cell adhesion and biofilm formation. However, its gene inactivation led to a decrease in biofilm formation and non-concurrent induced production of intracellular c-di-GMP. This antithetical relation is not yet understood, however other mechanisms or processes in which *bceF* is involved may supplant the identified role of c-di-GMP in biofilm formation (Ferreira *et al.* 2013).

The alternative sigma factor RpoN (σ 54) was shown to regulate phenotypes in *B. cenocepacia* such as motility, biofilm formation and survival in infected macrophages (Fazli *et al.* 2014). This work showed that the enhancer-binding protein BerB binds to c-di-GMP and activates RpoN-dependent transcription of the *berA* gene encoding a c-

di-GMP responsive transcriptional regulator. In response, BerA protein production increases and induces production of Bep exopolysaccharide that stabilizes biofilms. In the same work, *rpoN* mutants were created by plasmid insertion. Although they did not affect initial surface attachment, they greatly impaired biofilm formation. This was confirmed by creation of a specific deletion mutant of *rpoN*. As expected, biofilm formation remained impaired and was restored when a complementation assay was performed. The same was verified for a *berB* mutant. It was stipulated, according to the discriminated association of these components to c-di-GMP, that this decrease of biofilm formation was due to an effect of these mutations on the intracellular c-di-GMP concentration. However, when c-di-GMP levels were measured in these mutants and compared to wild-type strain in *B. cenocepacia* and they showed no significant differences were found, suggesting they may act upon other components required for biofilm formation. RpoN was originally identified as a sigma factor required for transcription of genes involved in nitrogen assimilation. However, it is known to be implicated in other biological activities in bacteria, like utilization of alternative carbon sources. It also displayed the ability to control flagellum-related motility in *B. cenocepacia*, essential for biofilm formation. Its mutant however was not absent of flagellum, meaning it is not involved in its biosynthesis. RpoN also positively regulates expression of genes involved in biosynthesis of *cepacia* under nitrogen-limiting conditions (Fazli *et al.* 2017).

1.5.7 Stresses

Both aggregated growth and biofilm produce gradients of oxygen, nutrients and metabolic products, inducing bacterial stress responses. To support the idea that planktonic aggregates are formed in response to stressful agents through gene modulation, it has been shown that contact of *P. aeruginosa* with CF sputum led to formation of aggregates more resistant to stressful agents like hypochlorous acid, human neutrophils and hydrogen peroxide. The sputum of CF patients itself is a complex mixture of compounds that closely emulates the CF lung environment, being a close approximation to the combination of stresses experienced within the organ. *In vitro* it leads to the formation of aggregates of *P. aeruginosa*, even in low density environments, suggesting that stresses exerted by CF sputum promote aggregate formation (Staudinger *et al.* 2014).

An established chronic infection has the ability to undergo genetic evolution moved by combinations of stresses found within CF patient's lungs, becoming an adaptation with the aim of survival. In a biofilm of supposedly genetically identical clones, the constituent cells develop differentiated patterns of gene expression and growth. Thus, evolution may not be linear and is often linked to the positioning of the cells in the biofilm structure, which leads to different stresses and stress intensity throughout the biofilm, as the spatial location affects resource availability and intercellular contact (Melaugh *et al.* 2016). Examples of key mutations are the ones that altered topoisomerase DNA gyrase and dihydrofolate reductase targets, associated to topological transitions of DNA and purine and thymidylate synthesis, which result in fluoroquinolone and trimethoprim resistance, respectively (Rhodes *et al.* 2016).

Studies have shown that multiple insertion sequences (IS) families were present in the Bcc and that they could be involved in both genome plasticity and expression. In fact, in *B. cenocepacia*, genomic islands comprised of almost 10% of total genome. These were not only verified to have a role in virulence, but also display the potential for mutations to occur in the face of stressful pressure (Mahenthiralingam *et al.* 2005).

Traverse et. al performed a long-term selection for *B. cenocepacia* in order to identify permanent mutations acquired over the course of several generations in a biofilm mode of growth in minimum medium, using plastic beads as surface. Among the many mutations it is of note the acquired mutations verified both in biofilm selection and in chronic infection isolates, also analyzed. These affected TCA cycle, iron metabolism and RNA polymerase. This suggests that altered central metabolism may be favored by evolution in biofilms (Traverse *et al.* 2012).

Such evolutions have been shown to progress non-linearly and in a non-specific rate in *B. multivorans*. These mutations were often found in genes related with lipid metabolism and accompanied by phenotypic changes, possibly desired for the survival in the airway stressful environment, such as antimicrobial resistance, biofilm regulation and presentation of O-antigen repeats. Namely, some acquired mutations trace back to genes involved in c-di-GMP that lead to lower motility and increased biofilm formation and adhesion to epithelial cells, important for bacterial survival and resistance (Silva *et al.* 2016).

1.5.7.1 Antimicrobial compounds

Aggregation of *S. aureus* is shown to, in a similar way to biofilms, be influenced by sub-inhibitory concentrations of antibiotics, possibly inducing mutations or differential genetic expression that causes phenotype alteration and thus grants resistance to such compounds. Moreover, the aggregate's structural component, polysaccharide intercellular adhesion (PIA), was found to have a correlating production with the level of aggregation, possibly altered due to such external factors and consequent genetic alterations (Haaber *et al.* 2012).

Resistance to antibiotics is not however a linear advantage acquired by bacteria when forming biofilms. In *P. aeruginosa*, aggregates formed showed relative sensitiveness to ciprofloxacin when in comparison with dispersed cells (Staudinger *et al.* 2014).

1.5.7.2 Oxygen and nitrogen

When biofilms are formed, they themselves form gradients due to the structure they constitute. However, in specific environments, the lack or excess of specific physical or chemical factors is already present and may induce the switch from a motile to a sessile form of growth, accompanied by the required genetic and phenotypic alterations.

Azospirillum brasilense, though having a dynamic oxidative metabolism, the maximum energy obtained is under environments with limited oxygen, or microaerophilic conditions. As mentioned before, they are able to move through oxygen gradients by aerotaxis, in search of low oxygen environments that can support metabolism. When exposed to high levels of oxygen, motile *A. brasilense* implements an alternative response to aerotaxis and form transient clumps by cell-to-cell interactions, a behavior suggested to protect motile cells from transiently elevated levels of aeration. Mathematical modeling predicts that cell-to-cell clumping limits surface area-to-volume ratio, reducing oxygen diffusion through cells, attaining the desired microaerophilic environment. This process is reversible, according to the evolution of oxygen concentrations in the environment. Also, in this species, it was shown that the subsequent stage of clumping, flocculation, was only induced under nitrogen limitation. Therefore, both these processes are thought to be induced by metabolic alterations that result from unfavorable conditions (Bible *et al.* 2012).

Initial clumping of *A. brasilense* is caused by impaired function of the Che1 chemotaxis-like signaling pathway, that controls the swimming speed during chemotaxis. Both clumping and flocculation require the regulation of this pathway as a response to oxygen gradient. A mutant strain AB104 (*ΔcheY1*), unable to synthesize the chemotaxis RR, CheY1, was shown to clump much more as it was unable to increase its swimming speed in search of low concentrations of oxygen. Instead it simulated that environment itself, by clumping far more than the wild-type strain. On the opposite spectrum, the created mutant strain BS106 (*ΔcheB1 ΔcheR1*), lacking the adaptation proteins CheB1 and CheR1, swims much faster in search of a favorable environment, impairing clump formation when compared to wild-type control. A shotgun proteomic analysis revealed that the up- or downregulation patterns of genes from both mutant strains were severely different, therefore, there isn't a lot of common genes differently expressed in both, to which the converse ability to clump can be attributed to. Each mutant strain responds differently to those clumping conditions. Thus, differently expressed identified genes may not be directly related to clumping. The most important identified set of genes were those exclusively upregulated in the hyper clumping strain, AB104, since they were specific to clumping cells and undetected in non-clumping cells of BS106. These corresponded to amino acid metabolism, metabolism of cofactors and vitamins, motility and signal transduction, protein turnover and protein secretion. Of distinction, key enzymes in amino acid biosynthesis were overexpressed, and a putative urease and aspartokinase were downregulated. Amino acid production coincides with the idea that in clumping cells, metabolism aims to conserve amino acids. Proteins associated with carbon storage materials, like acetyl CoA, also increased, as enzymes from glycolysis and the pentose phosphate pathway decreased. Decreased enzyme of the oxidative electron transport chain and superoxide dismutase, as well as several transporters was also verified. A type VI secretion system protein was upregulated, which can be connected to the increased cell-to-cell contacts and cell envelope remodeling associated with clumping (Bible *et al.* 2015).

As far as nitrogen goes in this work, mutant strains lacking genes involved in nitrogen sensing and metabolism (*amtB*, *ntrC*, *glnB* and *glnZ*) were grown in media with elevated aeration and limiting nitrogen. *amtB* and *ntrC* showed little clumping and flocculation phenotype, while *glnB* and *glnZ* displayed reduced clumping, but mostly, severely affected flocculation. This suggests that nitrogen is indeed required in this species for flocculation, since after removing the ability of bacteria to sense low nitrogen concentration and metabolize it, flocculation was reduced severely compared to wild-type strain. To further confirm this, nitrogen was then supplemented under the form of ammonium chloride or glutamate, both of which restored flocculation phenotype. Since no other source, like nitrate did the same, it's hypothesized that flocculation is induced by fixed nitrogen starvation, and that these structures represent a nitrogen scavenging strategy accompanied by a loss of motility and increased EPS production, among other changes (Bible *et al.* 2015).

One such similar case of oxygen stress response is of the gram-negative microaerophilic pathogen, *Campylobacter jejuni*. Under oxygen rich conditions it has also been reported to have increased biofilm formation. However, this appeared to follow a different path of adaptation. By being exposed to oxygen, the formation of ROS within organisms is a naturally occurring phenomenon. However, their accumulation may become hazardous, and therefore a balance of these compounds needs to be performed by a set of genes involved in oxidative stress resistance. By comparing growth in microaerobic and aerobic conditions, Oh *et. al* observed that indeed in the latter conditions an increased production

of both ROS and biofilms was verified. Especially in aerobic conditions, the antioxidant genes *ahpC*, *sodB* and *kata*, encoding for alkyl hydroperoxide reductase, superoxide dismutase and catalase, respectively, were found to have increased transcription levels, namely *ahpC*, suggesting that this may have a critical role in the development of biofilms (Oh *et al.* 2016). Thus, we can see that bacteria, though they may respond in similar ways to a specific stress, they may employ different mechanisms.

P. aeruginosa also displayed more robust biofilms under anaerobic conditions, suggesting markedly more adaptive behavior when in response to low oxygen stress (Kim and Lee, 2016). One important stress response protein, OxyR, senses H₂O₂ and activates the transcription of several genes involved in antioxidative defense. It is also involved in biofilm formation since *oxyR* mutants of various bacterial species, display increased auto-aggregation and ability to form biofilms in minimal medium. *B. pseudomallei* and *Pseudomonas chlororaphis* are such cases. In *P. aeruginosa* more specifically, OxyR promotes the biofilm lifestyle to reduce metabolism and ROS production. The oxidized form of OxyR binds to both the promoter region of the bacteriophage Pf4 operon, deemed essential for biofilm formation. The opposite effect has also been verified in other species like *Serratia marcescens*, *Neisseria gonorrhoeae* and *Tannarella forsythia*, which displayed impaired formation of biofilms (Gambino and Cappitelli, 2016).

RpoS is yet another important protein, involved in general stress response. It has been shown to be activated in *E. coli* under oxidative stress, synergizing with OxyR and SoxRS to induce genes involved in protection from oxidative damage, like *dspA*, *katE* and *sodC*. This RpoS when activated also controls the expression of several genes involved in biofilm growth. For instance, in *Klebsiella pneumonia*, RpoS and SoxR trigger the expression of the protein YjcC, which regulates oxidative stress response and biofilm production by modulating levels of second messenger c-di-GMP (Gambino and Cappitelli 2016).

1.5.7.3 Pyruvate

In *P. aeruginosa*, microcolony formation is dependent on the two-component regulator MifR. *mifR* mutants have been shown to form biofilms with an overall thin structure lacking microcolonies, that can be reversed to the wild-type phenotype by complementation of the gene, which restored the microcolony forming phenotype and its overexpression led to hyper-microcolony formation. Petrova *et al.* have shown, through transcriptomic and proteomic analysis, that microcolony formation is associated to stressful, oxygen-limiting but electron-rich conditions, since under this type of stress, anaerobic and fermentative processes are activated, and which have effects on microcolony formation. Specifically, inactivation of *uspK*, *acnA* and *ldhA*, all encoding proteins involved in pyruvate utilization, led to abrogation of microcolony formation, with effects like those of *mifR* mutants. Depletion of pyruvate from the medium also impaired microcolony formation, and its addition boosted it. Therefore, pyruvate utilization and consequent fermentation may be a microcolony-forming specific adaptation for this facultative anaerobic microorganism to survive biofilm environment. Also, it was verified that *P. aeruginosa* PA14 was able to release pyruvate under oxygen limitation, and subsequently use it during stationary phase. The boost of microcolony formation by addition of pyruvate to the medium confirms that other than intracellular, extracellular pyruvate also promotes biofilm microcolony formation. Measurements of the NADH/NAD⁺ ratios on the *ldhA* mutant also showed an increase in NADH/NAD⁺ ratios when compared to wild-type and decreased available NADH when *ldhA* was overexpressed. This leads to the

suggestion that pyruvate utilization under oxygen limiting conditions has a role in redox balancing, a means to establish microcolonies (Petrova *et al.* 2012).

1.5.7.4 Mannitol

This compound promotes EPS production by Bcc. It has been shown to promote adherence of two representative *B. multivorans* strains. In these however, the adherence was EPS-dependent in an environmental isolate, but EPS-independent within a CF outbreak strain, suggesting strain-to-strain variation in adhesins. Genome sequencing of the latter strain enabled the identification of two distinct loci encoding putative fimbrial and afimbrial adhesins, the first being widely distributed among environmental and clinical isolates, but the second one restricted to clinical isolates. Both loci were found to have an expression promoted by mannitol and both contributed to biofilm formation and mucin adherence (Denman and Brown 2013).

Mannitol has also been used in CF therapy as an inhalant and displayed enhanced lung function in CF patients. However, the potential impact over the course of the *Burkholderia* infection within CF lung is unknown (Denman and Brown 2013).

1.5.7.5 Temperature

Heat has been shown to reduce bacterial biofilm population with reductions of up to six orders of magnitude when subjected to temperatures between 70 to 80 °C. In *P. aeruginosa* PAO1 biofilms, increases in temperature displayed a synergistic effect with ciprofloxacin, tobramycin and erythromycin, enhancing their ability to kill bacteria and reduce cell aggregation. As temperatures only ranged between control temperature (37 °C) and 80 °C, it is suggested that this synergistic effect is likely due to an induced metabolism acceleration by the bacteria, usually low under biofilm growth, facilitating the killing action of the antibiotics (Ricker and Nuxoll, 2016). Also, it may be that higher temperatures reduce viscosity of extracellular polymeric matrix, resulting in improved transport and access of antibiotics.

D'Argenio showed that the insertion mutant *wspF10* grown in LB cultures formed a pellicle at 23°C and presented diffuse turbidity at 42°C, indicating that auto aggregation was suppressed by higher growth temperatures (D'Argenio *et al.* 2002).

1.5.7.6 pH

Within a CF lung epithelial surface an acidic pH is usually found. Bacterial cells have mostly negative charges at physiologic pH. At an acidic pH however, the negative ionized groups can be neutralized by protonation, reducing the strength of the repulsive forces between bacteria and leading to aggregation. This idea is further supported by experiments in which the wild-type strain Cd and mutant strain FAJ0204 (defective in production of flagella) of *A. brasilense* showed increased ability of reaggregation at low pH levels. Nonetheless at neutral and alkaline pH aggregates remained stable and intact (Burdman *et al.* 1998).

Still within the realm of charged groups, the Cd strain of *A. brasilense* displayed floccs visible to the naked eye after 24 hours in a medium with high ratio of C/N, using fructose as carbon source and ammonium chloride as nitrogen source. No such aggregates were found in media with low ratios of C/N. What is interesting is that the aggregated cells

in the first case displayed a cell envelope containing a well-defined electron-dense layer outside the outer membrane, which may be susceptible to the aforementioned protonation and therefore be more susceptible to bacteria interaction (Burdman *et al.* 1998).

1.5.7.7 Iron

It is already known that in *P. aeruginosa* high levels of iron suppress the expression of the *pvdD* gene, which encodes pyoverdine, one of the systems used by bacteria to uptake iron. Further influence of iron concentrations on the cellular aggregation of *P. aeruginosa* PAO1 was tested by Yang *et al.* What was found was that the level of iron in the microtiter trays where the bacteria are cultivated, was inversely proportional with the cell density attained and consequent ability to form biofilms (Figure 8). With the lowest concentration of 5 μM not limiting growth extensively and the highest concentration of 100 μM not inhibiting it. Thus, as previously reported, high concentrations of iron salts inhibit *P. aeruginosa* biofilm formation. Presumably this stress acts upon the ability of the bacteria to release eDNA. By using a medium with propidium iodide, which fluoresces when bound to DNA and does not penetrate live bacteria, this eDNA was able to be quantified and showed to be inversely proportional to the concentration of iron used. Furthermore, it was previously determined that the release of eDNA was regulated by the PQS QS system. Different PQS mutants were tested in the same way, in order to identify the gene most responsible for the process. It was found that a *pqsL* mutant released more eDNA than the wild-type strain, through a pathway suppressed by high iron concentrations, resulting in the overproduction of PQS and hyper-autolysis that releases DNA. Not only does this confirm the role of iron in modulating gene expression but it also states the importance of eDNA in biofilm formation (Yang *et al.* 2007).

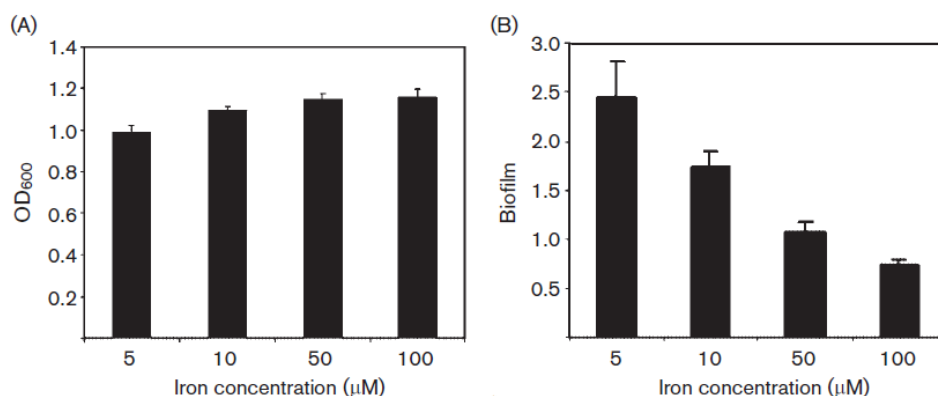


Figure 8 – Relation between iron concentration and cell density (assessed by measurements of OD_{600nm}) and biofilm formation of *P. aeruginosa* PAO1. Retrieved from Yang *et al.* 2007

In *P. aeruginosa* eDNA release was also assessed in *lasIrhII*, *pqsA*, *pqsL* and *fliMpiA* mutants. What was found was that eDNA generation was dependent on AHL and PQS, but also on flagella and type IV pili. All mutants except *pqsL* contained less eDNA than wild-type and its biofilms were more susceptible to rupture by sodium dodecyl sulphate, further confirming the importance of eDNA in the formation and stability of biofilms. Also, great release of eDNA was found to occur at the late-log phase, suggesting it was a quorum-sensing related process. Sure enough, in

the *laslrhl* mutant, such sudden eDNA increase was not found, substantiating the role of quorum sensing in DNA release (Allesen-Holm *et al.* 2006).

It was demonstrated that the mammalian iron chelator lactoferrin restricts development of *P. aeruginosa* biofilms. In its absence however, thicker biofilms were formed. This indicates iron is an environmental signal for the bacteria to develop biofilm. Then, this study concluded that even at low external iron concentrations, *P. aeruginosa* can acquire iron and develop biofilms with mushroom-like structures. Therefore, enough iron concentration is attained for biofilm development, as long as there is means of transporting it to the intracellular environment, like the siderophores pyoverdine or pyochelin. It can also use specific iron-responsive ECF sigma factor systems to acquire ferric citrate or ferrioxamine for that purpose. Otherwise, passive diffusion of iron does not amass iron in enough quantity for biofilm development (Banin *et al.* 2011).

1.5.7.8 Magnesium

RetS is one of the sensors responsible for the switch from planktonic to biofilm growth in *P. aeruginosa*. When extracellular concentration of Mg^{2+} is limited within the environment, it leads to a reduced expression of known biofilm repressor *retS*, which in turn results in increased aggregation, EPS production and biofilm formation. This repression of *retS* in low Mg^{2+} is directly controlled by the two-component system PhoPQ which therefore senses the decreased ion concentration and downregulates the gene. The same mechanism has been shown to be activated when greater quantities of eDNA are present, since they are proven to function as a cation chelator. Therefore, by sequestering the ion, reduced quantities of magnesium are sensed and the PhoPQ system is triggered, promoting biofilm formation (Mulcahy and Lewenza, 2011).

1.5.8 The Immune System

In a way, the innate immunity response may represent a stress for bacteria as they work to clear them within the host. However, in some cases they may work the other way around, inadvertently fomenting bacterial establishment.

Both *B. multivorans* environmental and clinical isolates have been proven to be able to replicate and survive within murine macrophages, in a manner similar to also previously verified in *B. cenocepacia* strain K56-2 (Figure 9). These very same strains, however, were able to survive but not replicate within human THP-1 macrophages. The uptake into the macrophages of these *B. multivorans* strains were different among all three tested strains, mostly due to differences at the O-antigen production. While the environmental strain had the highest uptake rate, coinciding with an absence of O-antigen, the clinical isolates had lower uptake rates, the lowest being the strain with the longest O-antigen chains, apparently presenting an obstacle to phagocytosis, which taking into account the results in murine macrophages, may be an advantage (Schmerk and Valvano 2013).

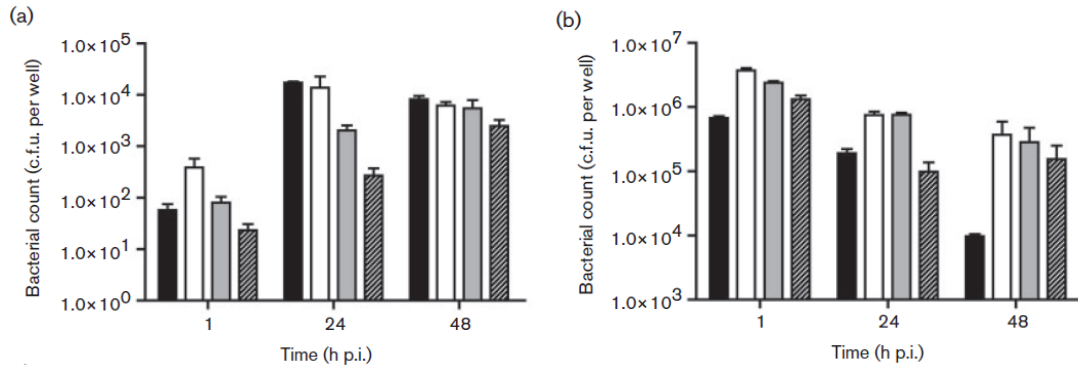


Figure 9 - Bacterial count of *B. multivorans* after lysis of infected (a) murine macrophages, and (b) THP-1 human monocytes after induced differentiation into macrophages. Strains: black bars, MH1K; white bars, ATCC 17616; grey bars, C5568 Gm^S; striped bars, C0514 Gm^S. Retrieved from Schmerk and Valvano, 2012.

Injection of bacteria into zebrafish embryos, which have a similar immune system to that of humans, has also been shown to result in phagocytosis of the epidemic strains *B. cenocepacia* K56-2, J2315 or *B. cepacia* CEP509 into macrophages. Depletion of macrophages from the embryos through chemical ablation or knockdown of pu.1, the transcription factor involved in early myeloid progenitor formation, and subsequent infection with the same strains has shown a significant decrease in host mortality, attributed to lower bacterial count, confirmed by intravital imaging. This leads to the conclusion that macrophages are critical for bacteria replication within the host (Mesureur *et al.* 2017).

Under an aggregation perspective, *Mycobacterium abscessus*, a human pathogen that established chronic pulmonary infections in patients and able to form aggregates, has been tested to understand interaction of macrophages with bacterial clumps. To that end macrophages were infected with both isolated bacilli and clumps of this bacteria. Both were successfully taken in by the macrophages in approximate proportions. Yet, those aggregated as a clump were observed to grow within the phagocytic vesicles, resulting in damage to macrophages and ultimately leading to their disruption and propagation of the bacteria (Brambilla *et al.* 2016). This supports the idea that macrophages aid replication of bacteria, acting as a mediator for infection when they should otherwise have the opposite role. Furthermore, this advantage of aggregates in comparison to single cells indicates an increase in phenotypic alterations in this mode of growth that enhances virulence.

In *Mycobacterium tuberculosis* rough morphotypes, associated with the most severe illnesses in humans, grew in a manner that left no spaces among them, forming large aggregates or clumps. These were used to infect J774 macrophages and were verified to grow within their phagocytic vesicles, killing all macrophages within 72 hours. Furthermore, this was only verified in the rough morphotype, while the smooth morphotype induced no changes in the macrophages (Brambilla *et al.* 2016).

1.6 *Burkholderia multivorans* biofilms and cellular aggregates

Literature on planktonic aggregates formed by Bcc bacteria is scarce, being one of the few examples the work of Silva *et al.* which have shown that both environmental and clinical isolates of various Bcc species can aggregate in salts media with different carbon sources like fructose, glucose or mannitol. Specifically, for *Burkholderia multivorans* ATCC 17616, it was shown that the transcriptional regulator LdhR which regulates lactate dehydrogenase expression, when absent, decreases the ability to aggregate, and thus has an important role in this species' ability to perform these structures. It is likely then, that pyruvate metabolism is essential in this mode of growth, where created gradients limit oxygen, nutrients and energy and thus pyruvate fermentation into lactate may circumvent these limitations (Silva *et al.* 2017).

More recently, work has been done regarding the link between *B. multivorans* ability to form aggregates and specific genes, mechanisms or stress inducers. On this subject, (Ferreira, 2018) selected a few mutants from a gene library created through random insertional mutagenesis, originating from a clinical isolate of this species. The disrupted genes were identified, and several different phenotypes thought to be important for biofilm formation were assessed with the aim of trying to establish a link between said phenotypes and respective mutations. Overall it was difficult to establish a link between the mutations and the ability to form aggregates. However, specific cases are of note.

A specific mutant, named G38, had a *gltB* disrupted gene, resulting in a non-functional glutamate synthase which might cause accumulation of glutamine and subsequent inactivation of the NtrBC signaling system. This mutant displayed decreased swarming motility, exopolysaccharide production, and growth rate in SCFM, as well as reduced ability to produce macroscopic aggregates when compared to its ancestor. This may be due to impairment of the regulation controlled by the NtrBC system. This system is, for instance, known to regulate swarming motility. Also, its inability to produce glutamate may lead to imbalance of its levels and consequently of other components that integrate it.

Another mutant of interest in these phenotypic studies was B63, with a *xdhA_3* disrupted gene, which encodes a xanthine dehydrogenase molybdenum-binding subunit XdhA. This is an enzyme required for purine salvage pathways, and therefore for the synthesis of purine integrating components such as DNA, RNA, cofactors, signaling molecules and carriers of energy. It is an essential pathway for energy and GMP/GTP maintenance, and subsequently, c-di-GMP. It is therefore also related to (p)ppGpp which also regulates GTP concentration. It was shown to have decreased virulence and capacity to produce surface-attached biofilms and produced large aggregates.

Other prominent mutations were found in E70 and B74 mutants, with disrupted *ppsA* and *rpsI* genes, respectively. The first encodes a phosphoenolpyruvate synthase that converts pyruvate into phosphoenolpyruvate, thus pyruvate conversion is blocked, possibly leading to increase of pyruvate, acetyl-CoA and lipid metabolic reactions. It was also found to be involved in forming AHL in *B. cenocepacia*. The second encoding a ribosomal protein, S9, involved in 30S subunit assembly and thus in association of the other ribosome subunits and finally translation. Both displayed medium to low ability to form aggregates, respectively.

The LdhA enzyme, also previously deemed important in *B. multivorans* ATCC 17616 aggregation, was tested to confirm its role in aggregation of *B. multivorans* P0213-1. A *ldhA* mutant showed decrease in aggregation, compared to WT, and LdhA overexpression a strong increase. Thus, it is confirmed that LdhA activity contributes to cellular

aggregate formation. This is most likely due to the need of pyruvate fermentation to maintain redox balancing since in biofilms there is lack of oxygen and energy and thus bacteria need to resort to alternative means of getting energy.

Considering these results, Ferreira (2018) suggested (p)ppGpp and c-di-GMP to possibly be key in mechanisms that act upon the different formation of the two types of biofilms. Furthermore, ribosomal proteins, quorum-sensing control and cell membrane constitution may contribute for aggregate formation, as well as proteins involved in nitrogen and lipid metabolism.

In another work, Gomes (2018) tested clinical isolates for susceptibility to different stresses and how that impacted the aggregation phenotype. Of note, stressful media appeared to induce aggregative behavior, with SCFM and SM causing overall more aggregation than the richer medium, LB. Osmotic stress and nitrogen excess also appeared to have impact, but to be strain-specific. The most prominent stress was ciprofloxacin, found to greatly increase aggregate biomass percentage and induce aggregation in isolates that previously did not display this ability.

B. multivorans P0213-1 was also subject to an evolution assay in which cellular aggregation was assessed over a period of 30 days in SM. Samples were also taken every two days and analyzed. The isolate did form aggregates and one colony was obtained from the last time-point. Its genome was sequenced, and the acquired mutations were analyzed. Of remark, there were mutations in the genes *amiC*, *nlpD*, and *flp*. The first encodes a peptidoglycan hydrolase involved in peptidoglycan degradation which has a role in septum cleaving during cell division, possibly preventing that process to keep an aggregated phenotype. The second encodes for a lipoprotein, NlpD, which anchors to the membrane and interacts with the peptidoglycan, also influencing cell division by modulating AmiC. And the third one is related to the expression of adhesive Flp pili, possibly leading to alteration of pili production and higher cell adhesion in this mutant since there was an aggregation phenotype. Overall, it appears that cell division and adhesion play key roles in planktonic aggregation of *B. multivorans*.

1.7 Motivation and thesis outline

Infections by the *Burkholderia cepacia* complex and overall bacterial infections in the airways are usually associated with biofilm formation or planktonic cellular aggregation. Treatment with antibiotics is a viable and frequent therapeutic option, especially to prevent transition into this mode of growth as it provides bacterial communities with greater resistance. However, its structure physiology and the progressive genetic adaptation of these communities renders most treatments useless or temporary. As previously reported in other works, it would appear that transition into planktonic cellular aggregation is triggered by specific mutations and/or changes at gene expression level that allow establishment of chronic infections in the host as a response to the aggressive environment it provides constituted by various stresses like oxidative stress, osmotic stress, nutrient starvation, microbial competition and immune response. Therefore, a plausible path to seek weaknesses in this transitioning process are these key genes that spark planktonic cellular aggregation. If properly identified and its mechanisms understood, they can become therapeutic targets, prone to disruption to prevent chronic infections.

For this work, random mutagenesis of a *Burkholderia multivorans* clinical isolate known to aggregate was made and differential ability to form cellular aggregates evaluated. Genes disrupted were identified and a relationship with initial evaluation was attempted, in terms of function and mechanism. Other phenotypes such as motility, antimicrobial resistance, virulence, adhesion, growth, exopolysaccharide production and surface-attached biofilm formation, widely associated with aggregation were also assessed and compared to the wild-type strain, seeking to understand if genes involved also have an impact on these and further establishing a link between gene and bacterial susceptibility.

Due to the complex composition of bacterial communities within CF lung, we also attempted to understand the disposition or impact that different *Burkholderia* strains able to aggregate would have on the structure of planktonic cellular aggregates by performing co-cultures and observing them.

2 Materials and Methods

2.1 Bacterial strains and growth conditions

Bacterial strains and plasmids used in this study are listed in Table 1. *E. coli* used was grown at 37 °C in Lennox Broth (LB) with agar supplemented with Km₅₀ (kanamycin 50 µg/mL), for plating under selective pressure and afterwards in liquid LB for use in assays. *B. multivorans* P0213-1 was grown in solid LB plates while its mutant strains were grown at 37 °C in plates of LB medium supplemented with Km₅₀₀ (kanamycin 500 µg/mL) to maintain selective pressure of inserted transposon. Both wild-type and its derivatives were also grown in either liquid LB or liquid SM medium (12.5 g/L Na₂HPO₄·2H₂O, 3 g/L KH₂PO₄, 1 g/L K₂SO₄, 1 g/L NaCl, 0.2 g/L MgSO₄·7H₂O, 0.01 g/L CaCl₂·2H₂O, 0.001 g/L FeSO₄·7H₂O, 1 g/L yeast extract, 1 g/L casamino acids, pH 7.2), supplemented with 20 g/L of D-mannitol, at 37°C, and at 180 or 250 rpm orbital agitation, according to the assay performed.

Table 1 - Strains and plasmids used in this study

Strain/Plasmid	Description	Source
<i>Burkholderia multivorans</i> Bacterial strains		
<i>Burkholderia multivorans</i> P0213-1	Cystic fibrosis isolate, Canada Date of isolation 12-02-1996 ID: VC7495	D.P. Speert University of British Columbia
F21	P0213-1 derivative with the plasposon pTnModΩKm, inserted in <i>paaC</i> gene, Km ^r	This study
F27	P0213-1 derivative with the plasposon pTnModΩKm, inserted in <i>pyrC_2</i> gene, Km ^r	This study
F69	P0213-1 derivative with the plasposon pTnModΩKm, inserted in <i>tctD_2</i> gene, Km ^r	This study
D19	P0213-1 derivative with the plasposon pTnModΩKm, inserted in <i>ppsA</i> gene, Km ^r	This study
D3	P0213-1 derivative with the plasposon pTnModΩKm, inserted in <i>hexR_2</i> gene, Km ^r	This study
C48	P0213-1 derivative with the plasposon pTnModΩKm, inserted upstream of <i>flhD</i> gene, Km ^r	This study
C50	P0213-1 derivative with the plasposon pTnModΩKm, inserted in <i>rsmB_2</i> gene, Km ^r	This study
K28	P0213-1 derivative with the plasposon pTnModΩKm, inserted in a 23S rRNA encoding gene, Km ^r	This study
K50	P0213-1 derivative with the plasposon pTnModΩKm, inserted in <i>xdhA_3</i> gene, Km ^r	This study
K51	P0213-1 derivative with the plasposon pTnModΩKm, inserted in a hypothetical protein encoding gene, Km ^r	This study
K73	P0213-1 derivative with the plasposon pTnModΩKm, inserted in a hypothetical protein encoding gene, Km ^r	This study

Table 1 (continuation) – Strains and plasmids used in this study.

P0213-1/dsRed	P0213-1 containing the monomer red fluorescent protein expressing pIN 29 plasmid	This study
<i>Burkholderia contaminans</i> IST 408/GFP	<i>Burkholderia contaminans</i> IST 408 containing the green fluorescent protein expressing pIN 25 plasmid	This study
<i>Escherichia coli</i> Bacterial strains		
DH5-α	DH5 α <i>recA1</i> $\Delta(lacZYA-argF)U169 \phi80dlacZAM15$	Gibco BRL
pTnModΩKm	Carrying a Km ^r Plasmid with pMB1oriR	(Dennis <i>et al.</i> 1998)
pRK600	ColE1 oriV; RP4tra ⁺ RP4oriT; Cm ^r ; helper in triparental mating	(Kessler <i>et al.</i> 1992)
pIN 25	Plasmid containing GFP; Cm ^r	This study
pIN 29	Plasmid containing dsRed; Cm ^r	This study

Abbreviations: Cm^r, chloramphenicol resistance; Km^r, kanamycin resistance.

2.2 Transposon mutant library construction

A new transposon mutant library of the clinical isolate *B. multivorans* P0213-1 was prepared by triparental mating with *E. coli* cells carrying either the helper plasmid, pRK600, or the donor plasmid, pTnMod Ω Km (Fig. S6). The donor strain was inoculated in 3 mL of LB+Km₅₀, the helper in 3 mL with chloramphenicol (25 μ g/mL) and the recipient strain in 3 mL of LB. All three cultures were incubated for 5 hours at 37 °C, 250 rpm orbital agitation. Afterwards, 1 mL of the recipient strain was mixed with 1 mL of both helper and donor. This final mixture was transferred to a LB plate, incubated for 24 hours at 30 °C. After incubation, the mixture was resuspended and 100 μ L were plated onto each of 10 LB+Km₅₀₀ plates, further supplemented with 40 μ g/mL of gentamicin. These plates were incubated for 48 hours at 37 °C. Colonies obtained were inoculated into each well of 96-well plates and frozen at -80 °C with 30% glycerol. Mutant colonies were numbered, for instance, K28 (mutant of cystic fibrosis isolate P0213-1 from well 28 of plate K).

2.3 Screening of planktonic cellular aggregation ability in transposon library mutants

A pre-inoculum was performed for each bacterial mutant, left growing overnight at 37 °C and 250 rpm orbital agitation in 3 mL of SM medium. Suspensions with OD_{640nm} = 0.1 were prepared in fresh medium in the morning and left to grow at 37 °C with 180 rpm orbital agitation for 48 hours. After this, each mutant was observed macroscopically and microscopically for the presence of aggregates when compared with the wild-type strain, *B. multivorans* P0213-1.

2.4 Planktonic cellular aggregation in co-cultures of *Burkholderia* strains

Three *Burkholderia* strains were made fluorescent with GFP and dsRed. Other already fluorescent strains were also used in this assay, namely *B. multivorans* D2214 with GFP, and *B. contaminans* IST408 with either dsRed or GFP.

The same procedure as the screening assay was performed, except in this case two strains were introduced in the flask, both with an initial $OD_{640nm} = 0.1$. After growing for 48 hours in the described conditions, they were observed at the naked eye and microscopically, both with and without appropriate fluorescence filters and lamp. All possible GFP + dsRed were tested. Due to lack of success in obtaining fluorescence producing cells in some strains, as well as due to a selection of the best yielding pair, only two co-cultured strains were further observed: *B. contaminans* IST 408 with GFP and P0213-1 with dsRed. It is worth mentioning that microscopic observation was hampered by the aggregate structure itself and that different mechanical methods to break it were attempted, to no avail. Three washes with NaCl 0.9 % were also made, previous to observation, to remove background and enhance fluorescence contrast.

2.4.1 Killing assays

To verify that the strains paired in this assay did not have negative impact on each other, other than possible competition, both were grown in solid medium simultaneously. Briefly, each strain was first grown overnight in liquid LB medium, at 37 °C and 250 rpm. After that, inoculums were made, for an initial $OD_{640nm} = 0.1$ in liquid LB. These were grown until exponential phase. Each culture was then centrifuged for roughly 5 minutes at 13200 rpm. The supernatant was collected and set to an $OD_{640nm} = 0.1$. This final solution was plated onto solid LB plates. 15-20 μ L of the supernatant of a different strain were then placed in a sterilized piece of paper at the center of the plate. The plates were stored at 37 °C until growth of the bacteria, upon which they were observed.

2.5 Microscopic observations

Microscopical observation of *B. multivorans* strains grown in SM medium for 48 hours was performed using a Zeiss Axioplan microscope, equipped with an Axiocam 503 color Zeiss camera controlled with Zen software, and using a 10x0.3 NA objective. For microscopic observations pertaining fluorescent strains, the same equipment was used, complemented by appropriate fluorescence filters for GFP and dsRed observation. 100x0.3 NA objective was also used in this case when attempting to observe free cells.

2.6 DNA manipulation and cell transformation techniques

Plasmid DNA extraction and isolation, DNA restriction, agarose gel electrophoresis, DNA amplification by PCR were performed using standard procedures (Russel 2001). Plasmid DNA extraction was performed with ZR Plasmid Miniprep™. Primers used in PCR are discriminated in Table S5. Genomic DNA of *B. multivorans* strains to be used in electroporation was extracted using a previously described protocol (Meade *et al.* 1982).

E. coli and *Burkholderia* electrocompetent cells were also obtained by standard procedures. These were transformed by electroporation using a Bio-Rad Gene Pulser system (*E. coli* - 400 Ω , 25 μ F, 2.5 kV; *Burkholderia* – 200 Ω , 25 μ F, 2.5 kV). *E. coli* cells were then grown for 1 hour in LB before plating onto LB+Km₅₀, while *Burkholderia*

strains were grown for 4 hours before plating onto plates of LB + Cm₅₀₀ (chloramphenicol 500 µg/mL). In a similar fashion, fluorescent proteins were also introduced in specific *Burkholderia* strains for co-culture assays. Thus, plasmid DNA with each fluorescent marker was extracted and electroporated into electrocompetent *Burkholderia* cells. Specifically, plasmid pIN 25, producing green fluorescent protein (GFP), and plasmid pIN 29, producing red fluorescent protein (dsRed), were independently introduced into three *Burkholderia* strains previously known to form considerable aggregates.

2.7 Genomic DNA extraction for sequencing

To obtain highly pure and concentrated DNA needed for genome sequencing, a different method was used. A small mass of cells grown in solid medium was resuspended in 1 mL of solution K (10 mM Tris, pH= 7.8; 5 mM EDTA, pH = 8; SDS 0.5%; proteinase K at 50 µg/mL) and incubated for 3 hours at 40 °C. 600 µL of potassium acetate 3M, pH = 5.5 was then added and mixed. This preparation was then centrifuged at 13000 rpm for 10 minutes. The supernatant was collected onto a new tube and 0.7 volumes of cold isopropanol added and mixed. A new centrifugation was performed in the same conditions. The supernatant was then discarded with a syringe and the pellet washed with 200 µL of ethanol 70 %. This was followed by another centrifugation at 13000 rpm for 5 minutes. The supernatant was discarded with the syringe and the pellet was dried in the Speed Vacuum for 15 minutes at 45 °C in V-AL mode. 50 µL of sterile water was added and the solution was incubated for at least 1 hour at 55 °C to dissolve.

2.8 Detection of plasposon in the genome of mutants

To confirm insertion of plasposon into the genome of each analyzed mutant, DNA amplification was performed by PCR, followed by agarose gel electrophoresis. Genomic DNA was used as template for 50 µL PCR reactions with 2 µL primers pTnModΩKm-fw and pTnModΩKm-rev each. PCR setup was as follows: denaturation at 94 °C for 1:30 minutes; 30 cycles of 30 seconds at 94 °C, 1 minute at 59 °C, and 1:30 minutes at 72 °C; final extension at 72 °C for 7 minutes; end of reaction cooling until 4 °C.

2.9 Identification of the genes disrupted by the plasposon

2.9.1 Sanger sequencing of flanking regions of the plasposon insertion site and *in silico* analysis of nucleotide sequences

Genes disrupted by plasposon insertion were identified by digestion of selected mutants' genomic DNA with EcoRI, which does not cut within the plasposon, followed by self-ligation of resulting fragment. Ligated product was electroporated into electrocompetent *E. coli* cells, following the procedures previously stated. From obtained colonies, plasmid DNA was extracted, and the obtained DNA was run in agarose gel against its EcoRI digested counterparts for confirmation of plasmid presence. Once confirmed, plasmid DNA was sequenced using primers kmR and oriR (Table S5), through a Sanger sequencing system at Instituto Gulbenkian de Ciência (IGC) (Portugal).

BLAST algorithm (Altschul *et al.* 1997) was used to compare disrupted gene sequences obtained by Sanger sequencing to database sequences available at the National Center for Biotechnology Information (NCBI). A

nucleotide BLAST search was also conducted against the genome of *Burkholderia multivorans* ATCC 17616 using the *Burkholderia* Genome Database. Furthermore, these sequences were also compared with the ones of the wild-type clinical isolate *B. multivorans* P0213-1, available in our laboratory, but not yet deposited in any repository.

2.9.2 Genome sequencing and assembly

Genomic DNA of selected mutants was extracted, as previously described and DNA was sent for sequencing by Illumina short reads technology at IGC.

All reads received refer to both strands of the genome. These *fastq* files were concatenated, joining the data. Statistics were run with the FastQC software (Andrews 2010), returning, among other data, the number of base pairs. However, these still include the primer adapters and low-quality sequences. As such, they were trimmed with software Sickle (Joshi and Fass 2011), going through a new statistical analysis, returning different results with less base pairs, translated into higher quality sequences. These are the reads used to perform the reference assembly. These were then aligned using Burrows-Wheeler Aligner (Li and Durbin 2010) and used to perform a reference assembly, with P0213-1 genome as the reference. Visual representation of both genomes side-to-side is obtained with Geneious software (Kearse *et al.* 2012), which also allows to see the base pairs, their location and BLAST sequences such as the plasposon region for confirmation of insertion or the corresponding reference gene disrupted in the mutant in search of homologs.

2.10 Growth curves and doubling time estimation

A pre-inoculum for each bacterial mutant of interest and P0213-1 as control was performed and left growing at 37 °C and 250 rpm orbital agitation in 3 mL of LB medium. Suspensions were made for $OD_{640nm} = 0.1$ in fresh medium and left to grow at 37 °C with 180 rpm orbital agitation for 24 hours. OD_{640nm} readings were taken over time for a period of 8 hours and then at 23 and 24 hours. Growth rates were calculated from the exponential phase of growth from at least two independent experiments. Doubling time was calculated from the growth rate of the exponential growth phase.

2.11 Quantification of cellular aggregates, free cells and total biomass

Quantification of cellular aggregates and free cells was performed according to a previously described protocol (Haaber *et al.* 2012), with a few adjustments. After growing mutant cultures as previously described in section 2.3, the content of each Erlenmeyer was transferred to a 50 mL Falcon tube, which was then centrifuged at 4000 rpm, 25 °C for 30 seconds. Supernatant obtained was transferred to a second 50 mL Falcon tube and the loose pellet was transferred to a 2 mL Eppendorf tube, previously weighed. This was subject to short-spin centrifugations and the resulting pellet, corresponding to cellular aggregates, was obtained. The Falcon tube with the free cells supernatant was centrifuged for 10 minutes at 4000 rpm, 25 °C. Resulting supernatant was discarded until around 5 mL were left, used to resuspend the pellet. Resuspended cells were transferred to a 2 mL Eppendorf tube, also previously weighed, and centrifuged at 13400 rpm for 2 minutes. Supernatant was discarded, and a pellet, corresponding to free cells, was obtained. Both the Eppendorf tubes of cellular aggregates and free cells were left to dry at 60 °C for 72 hours, until they were dried, and a brown color was displayed. At this time, each Eppendorf tube was weighed again.

2.12 Exopolysaccharide production in solid medium

YEM (yeast extract mannitol medium) plates containing 4 g/L mannitol, 0.5 g/L yeast extract and 15 g/L agar were used to evaluate exopolysaccharide production (Zlosnik *et al.* 2008) of studied mutants. After inoculation of respective cultures onto these plates, these were incubated for 48 h at 37 °C. Exopolysaccharide production was assessed by visual observation of colonies with mucoid morphotype.

2.13 Antimicrobial susceptibility

Antimicrobial susceptibility was assessed following the agar disc diffusion method (Bauer *et al.* 1966). Overnight cultures of selected mutants and wild-type strain were performed in LB at 37 °C and 250 rpm. For each isolate, the volume required for an OD_{640nm} of 0.1 was transferred to an Eppendorf tube, which was then centrifuged for 5 minutes at 8000 rpm. The resulting supernatant was discarded, and the pellet was resuspended in 1 mL of 0.9% NaCl. From these suspensions, 100 µL were plated onto Müller-Hinton agar (Sigma-Aldrich). Paper discs (BD BBL Sensi-Disc) containing aztreonam (30 µg), piperacillin (75 µg) plus tazobactam (10 µg) were placed upon the surface of the inoculated plates. These plates were incubated for 24h at 37 °C, after which the diameter of the growth inhibition region was measured. Results pertain to at least four replicates of three independent experiments.

2.14 Biofilm formation

Mutant isolates and wild-type strain were grown in liquid LB medium at 37 °C and 250 rpm overnight. These cultures were then diluted in the same medium to attain an OD_{640nm} of 0.05. 200 µL samples of the cell suspensions were used to inoculate 96-well polystyrene microtiter plates. 200 µL of LB medium were used to inoculate the first and last rows and columns of each plate, to function as blanks. These plates were statically incubated for 48h at 37 °C. Afterwards, the wells were washed three times with 0.9% NaCl. The biofilms in each well were stained with 200 µL of a 1% (wt/vol) crystal violet solution for 20 minutes at room temperature (Ferreira *et al.* 2007), followed by another three washes with 200 µL of 0.9% (wt/vol) NaCl. The dye was then solubilized with 200 µL of 96% ethanol and the absorbance of the solution in each well was measured at 590 nm in a microplate reader (Spectostar nano, BMG LabTech), thereby quantifying biofilm formation. Results pertain to at least fifteen replicates of two independent experiments.

2.15 Motility

2.15.1 Swarming motility

Overnight cultures of selected mutants and wild-type strain in liquid LB were performed. For each isolate, the volume required for an OD_{640nm} of 1 was transferred to an Eppendorf, which was then centrifuged for 5 minutes at 8000 rpm. The resulting supernatant was discarded, and the pellet was resuspended in 100 µL of 0.9% NaCl. 5 µL of these suspensions were then inoculated in swarming agar plates, containing 0.04% (wt/vol) tryptone, 0.01% (wt/vol) yeast extract, 0.0067% (wt/vol) CaCl₂, 0.6% (wt/vol) bacto agar (Difco) (Silva *et al.* 2016). After inoculation, the

swarming plates were incubated for 48h at 37 °C, after which the diameter of the swarming region was measured. Results obtained pertain to at least four replicates of three independent experiments.

2.15.2 Swimming motility

This procedure followed the same steps as the swarming motility assessment, except for the facts that swimming agar plates were used, containing 1% (wt/vol) tryptone, 0.5% (wt/vol) NaCl, 0.3% (wt/vol) noble agar (Difco) (Silva *et al.* 2016), and that these were incubated for 24h after inoculation instead. After this, diameter of swimming region was measured. Results obtained pertain to at least four replicates of three independent experiments.

2.16 Virulence in *Galleria mellonella*

Virulence ability of mutants and wild-type was tested through killing assays previously described (Seed and Dennis 2008) in *Galleria mellonella* virulence model. Larvae of *Galleria mellonella* were injected with cell suspensions containing a total CFU of approximately 1×10^6 in 10 mM MgSO₄ with 1.2 mg/mL ampicillin and incubated at 37 °C. Survival rates were assessed by counting dead larvae at 24, 48 and 72 hours. A solution of 10 mM MgSO₄ with 1.2 mg/mL ampicillin was used as a negative control. For each mutant isolate, ten larvae were used, in at least three independent experiments.

2.17 Adhesion to animal cells

B. multivorans isolates under study were analyzed for adhesion to the bronchial epithelial cell line CFBE41o₂, derived from a patient homozygous for the CFTR F508del mutation (Goncz *et al.* 1999). Host cell attachment was performed as described by (Ferreira *et al.* 2015). Briefly, epithelial cells have to be previously grown in a coated T-flask containing 9 mL of minimal essential medium (MEM) supplemented with 10% (vol/vol) fetal bovine serum (FBS) and 1% (vol/vol) PSG (Penicillin streptomycin glutamine) at 37 °C, 5% CO₂, until confluence. Afterwards, the medium from the T-flask containing the cells is discarded and washed three times with phosphate buffered-saline solution (PBS). 3 mL of trypsin is then added to release cells adhered to the wall of the T-flask, and it is incubated for roughly 15 min, until cells are free. Then, coating solution is added to 24-well plates and left to dry at room temperature. Cells from the T-flask are then taken out and centrifuged for 5 minutes at 1200 rpm. The resulting supernatant is discarded, and 25 mL of MEM is added and used to resuspend the cells. Then, 10 µL of this solution is placed in a Neubauer chamber, which is seen at the microscope and the cells are counted for each of the four squares and a median is calculated. This number is used to calculate the volume of cell solution required according to a designated MOI (here 50). Once calculated, this volume is placed into each of the wells and completed with MEM until 1 mL, seeding the cells. The plate is incubated for 24 hours at 37 °C.

Optical density of each overnight bacterial culture was measured, and a calculated volume is transferred to a 2 mL Eppendorf tube assuming a final volume of 1 mL and a specific OD previously calculated according to growth characteristics of each strain. These Eppendorf are centrifuged for 5 minutes at 13200 rpm and the resulting supernatant is discarded. The pellet is resuspended in 1 mL of MEM. These are the Eppendorf tubes containing bacterial cell solutions. For each strain another three 2 mL Eppendorf are prepared with 990 µL of MEM each. To each of them 10

μL of the respective bacterial culture is added and mixed. One of the Eppendorf is used to perform serial dilutions with 0.9% NaCl in a 96-well plate, then plating 100 μL of dilutions 10^{-4} through 10^{-6} in solid LB. Therefore, two Eppendorf tubes containing bacterial cells out of these three remain. Meanwhile, the medium from the 24-well plate prepared in the previous day is discarded and each well is washed three times with PBS. Afterwards, 1 mL of each of the two remaining 2 mL Eppendorf tubes containing bacterial cells is added to a respective well. The 24-well plate is centrifuged for 5 minutes at 700 RCF and then incubated for 30 minutes at 37 °C and 5% CO₂ atmosphere. After that, all liquid within the wells is discarded and they are washed three times with PBS. 1 mL of lysis buffer (0.01 M PBS, 10 mM EDTA, 0.25% [vol/vol] Triton-X-100; pH 7.4) is then added to each well, and the plate was left to incubate for 20 minutes at 4 °C. The lysis buffer is then well resuspended within each well and used to make dilutions with 0.9% NaCl in a 96-well plate, plating dilutions 10^{-3} through 10^{-5} in LB plates. Every plate is then incubated for 48 hours at 37 °C, after which CFU counting is made and percentage of adhered cells is calculated.

2.18 Statistical analysis

Error bars and statistical significance of the data obtained was determined using one-way analysis of variance (ANOVA), followed by Dunnett's multiple comparison test. These analyses were performed using GraphPad Prism 8 software for Windows (GraphPad Software, Sand Diego California USA, www.graphpad.com). Kaplan-Meier survival curves were also performed with GraphPad Prism software v.5.04. Differences were determined to be statistically significant for *P-values* lower than 0.0332.

3. Results and Discussion

3.1 Screening a transposon mutant library for differences in planktonic aggregates formation by *B. multivorans*

A *B. multivorans* clinical isolate, P0213-1, used as a wild-type strain in this study, is known to form planktonic cellular aggregates (Fig. 10), in addition to free cells, when grown in the stressful environment that is liquid SM medium due to its high carbon to nitrogen ratio. After 48 hours in this medium, robust and ramified aggregates become macroscopically visible.

With the aim of identifying relevant genes and mechanisms involved in the formation of these structures, a plasposon mutant library was created from P0213-1 by random mutagenesis with the transposon pTnMod Ω Km (Fig. S6). From this library, roughly 300 colonies were stored and screened to assess different abilities to form planktonic cellular aggregates when comparing to the wild-type strain. Another approximately 100 mutants from a previously constructed transposon library were also assessed. This evaluation was made by growing them in stressful medium for 48 hours in the conditions previously described, followed by macroscopic and microscopic observation, while

performing the same with the wild-type strain. Out of the screened mutants, 11 were selected due to their markedly different phenotype (Fig.10) and their growth in the same conditions was repeated in order to confirm the assessment.

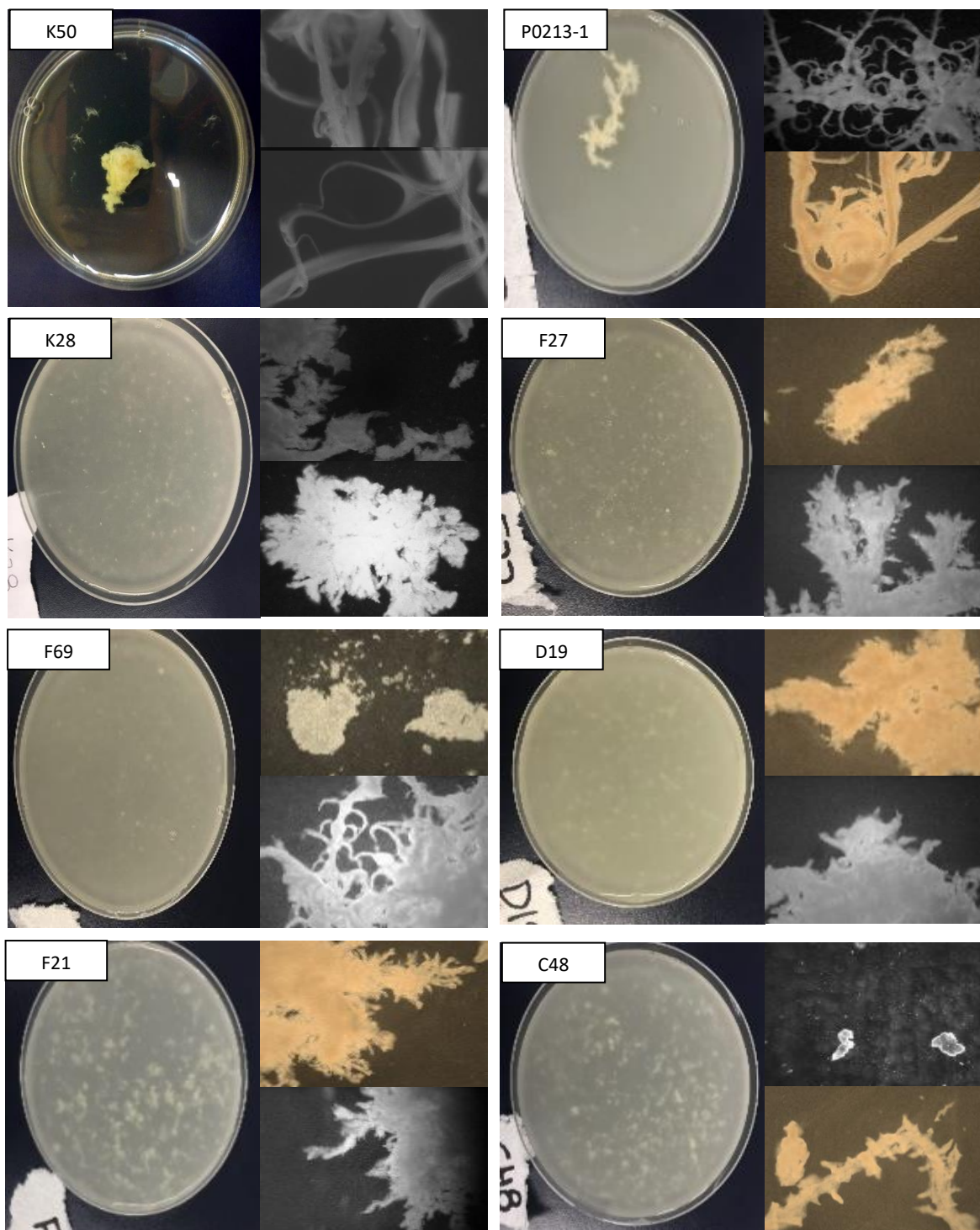


Figure 10 – Screening of the plasposon mutant library of *B. multivorans* P0213-1 for different abilities to form planktonic cellular aggregates. For each strain a macroscopic image is shown (left) as well as two other microscopic images (right). Each culture was grown in SM medium at 37 °C, 180 rpm of orbital agitation, for 48 hours. A magnification of 10x was used.

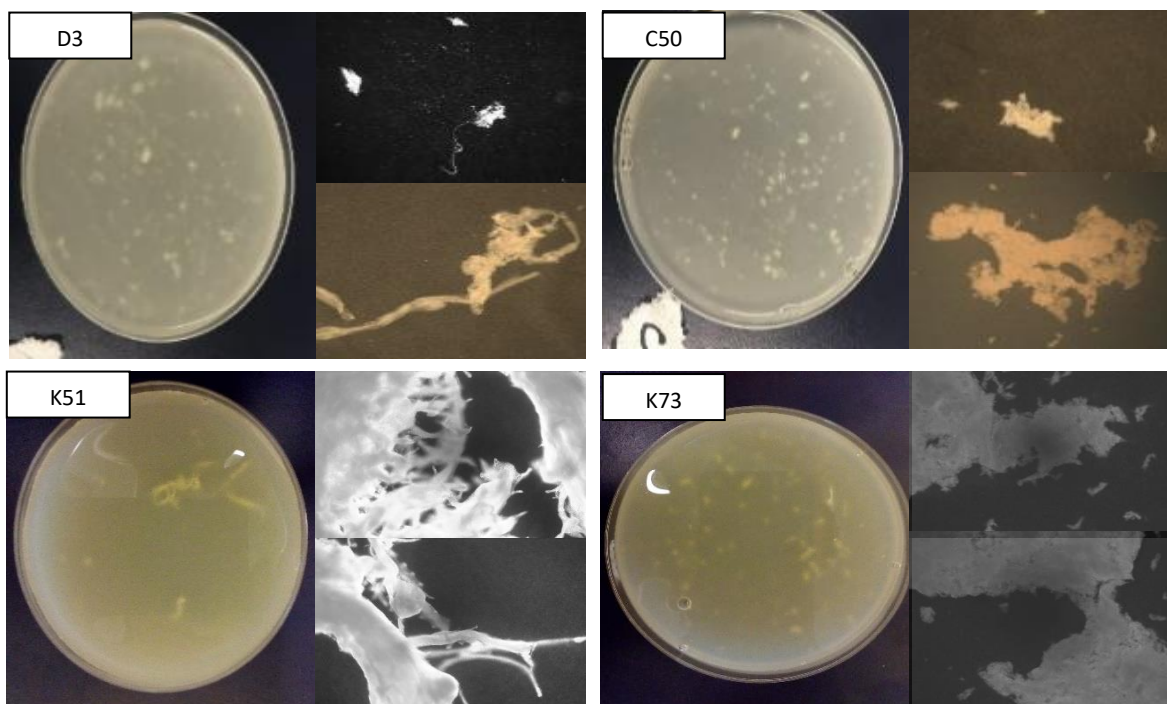


Figure 10 (continuation) - Screening of the plasposon mutant library of *B. multivorans* P0213-1 for different abilities to form planktonic cellular aggregates. For each strain a macroscopic image is shown (left) as well as two other microscopic images (right). Each culture was grown in SM medium at 37 °C, 180 rpm of orbital agitation, for 48 hours. A magnification of 10x was used.

As seen in Fig. 10, in the macroscopic images, P0213-1 produces relatively large aggregates in these conditions. The group of mutants comprised by F27, D19, F69 and K28 appear to have notably less aggregates macroscopically visible than the wild-type and the remaining mutants. The following group composed by F21, C48, D3, C50, K51 and K73, on the other hand, appears to produce more noticeable aggregates, either due to bigger size or to a greater quantity of small aggregates, falling within a category of intermediate aggregates. Except for K50, both groups produce less aggregates than the P0213-1. The last mutant, K50, presents a much denser and more compact cellular aggregate than the wild-type strain, as evidenced by the nearly transparent medium, apparently with very few free cells.

At the microscopic level, with a magnification of 10x, the P0213-1 control produces very ramified and branched aggregates. Similar structures are more evidently verified in F69 and K51. Possibly in D3, C48, F21, D19 and F27 as well, though not as prominent and defined and without the characteristic curly like structure. C50, K28 and K73 appear to have a compact cloud like appearance with a few protrusions at the edges. They appear smoother and less ramified, distinctively different than P0213-1. K50 appears to be more distinct than all remaining ones as it presents very long and ramified structures of the aggregates, however in a very different manner than the wild-type, as they don't have the curly protrusions, thus appearing much less branched and much smoother.

3.2 Confirmation of the presence of the plasposon in the mutant's genome

To confirm that the verified phenotypes are derived from the plasposon insertion and not due to spontaneous resistant colonies to the used antibiotic, an internal fragment of the plasposon was amplified. This was done by extracting the genomic DNA of each mutant, performing a PCR with appropriate primers and visualization of the amplicons by agarose gel electrophoresis was run.

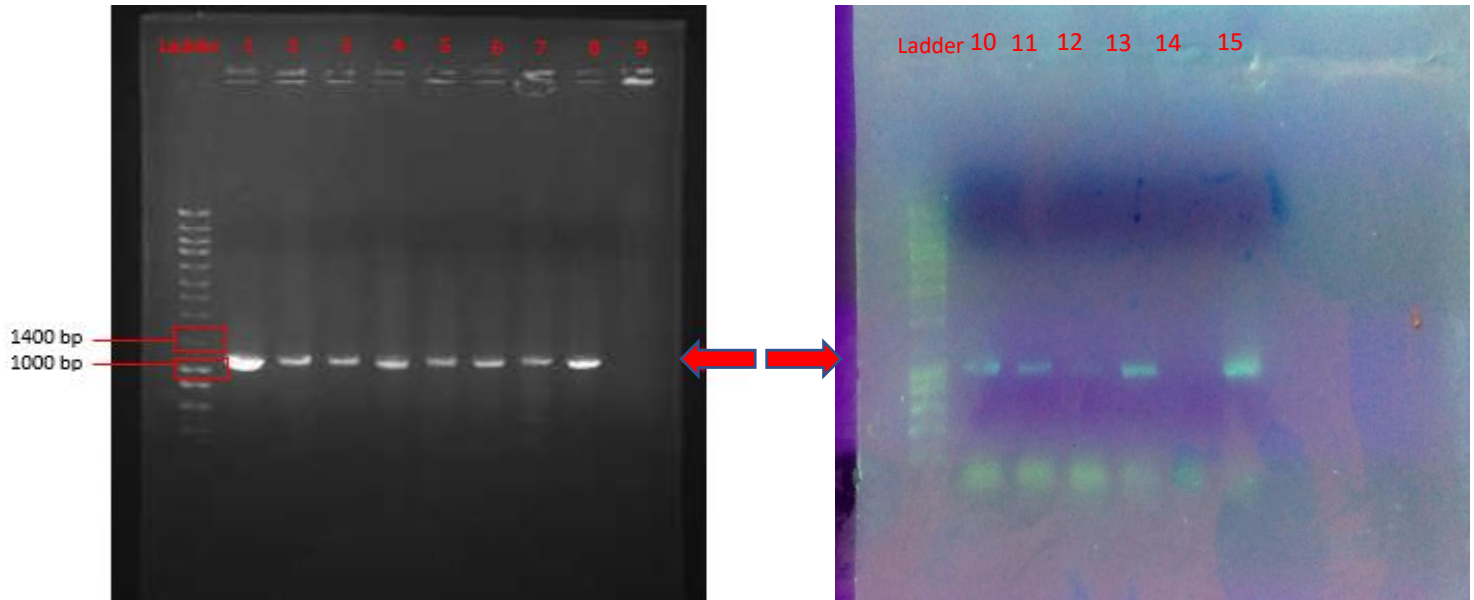


Figure 11 - Electrophoretic separation in 0.8% agarose gel of the PCR products corresponding to an internal region of the pTnModΩKm plasposon with an estimated size of 1161 bp. DNA marker is NZYDNA Ladder III. 1, 15 – Plasposon; 2 – D3; 3 – D19; 4 – C48; 5 – C50; 6 – F27; 7 – F69; 8 – F21; 10 – K28; 11 – K50; 12 – K51; 13 – K73; 9, 14 – P0213-1

As seen in Fig. 11, all selected mutants possessed a band with a size between 1000 bp and 1400 bp, corresponding to the expected 1161 bp of the plasposon. Thus, in every selected mutant, the observed phenotypes are likely caused by the disruption of a gene where the transposon got itself inserted. As expected, P0213-1 did not present any band since it possessed no plasposon.

3.3 Localization of plasposon insertion within the genome of selected mutants

After plasposon presence was confirmed in each selected mutant, its localization within the genome had to be determined. For mutants F21, F27, D19 and D3, this was done so by sequencing the flanking regions of the plasposon's place of insertion, by Sanger sequencing. For mutants F69, C50, C48, K28, K50, K51 and K73, their whole genome was sequenced by Illumina short reads technology.

Regardless of the approach, the wild-type genome, previously sequenced and assembled (Pessoa, 2017), was used as reference. The assembly of this genome generated 5 contigs with lengths between 813 and 3298492 bp. Using BLAST, it was possible to identify which contig corresponded to each *B. multivorans* ATCC 17616 chromosome. Contigs 1, 2 and 3 correspond to chromosomes 1, 3 and 2, respectively, and contig 4 also aligned to chromosome 1. Contig 5 did not map onto the reference genome of *B. multivorans* ATCC 17616 and is likely a plasmid.

Table 2 - Contigs generated from the assembly of P0213-1 wild-type genome and its corresponding chromosomes of *B. multivorans* ATCC 17616

P0213-1 contigs	Contig length (bp)	<i>B. multivorans</i> ATCC 17616 chromosome	<i>B. multivorans</i> 17616 chromosome length (bp)
1	3 298 492	1	3 448 421
2	706 259	3	919 805
3	2 464 683	2	2 473 162
4	813	1	-
5	28 489	-	-

In the first approach, the genomic DNA of the mutants was extracted and digested by a restriction endonuclease that does not cut within the plasposon, in this case EcoRI. This was followed by self-ligation and introduction of these fragments into electrocompetent *E. coli* cells by electroporation. From the resulting colonies, plasmid DNA was extracted and sent for Sanger sequencing. The returned flanking sequences (Tables S6-S9) allowed identification of the gene by performing a BLAST of the sequences with both *B. multivorans* ATCC 17616 and P0213-1 as reference.

As for the second approach, the genome was sequenced by Illumina short reads technology, returning reads that are then trimmed and assessed for quality. After that, the sequences are aligned against the reference genome (P0213-1) and uploaded onto the software Geneious, which allows visual comparison of sequences, from gene to base pair level. As such, plasposon insertion in the mutant and its localization and disrupted gene can be confirmed through the localization of a high coverage of unaligned reads in both strands of the genome.

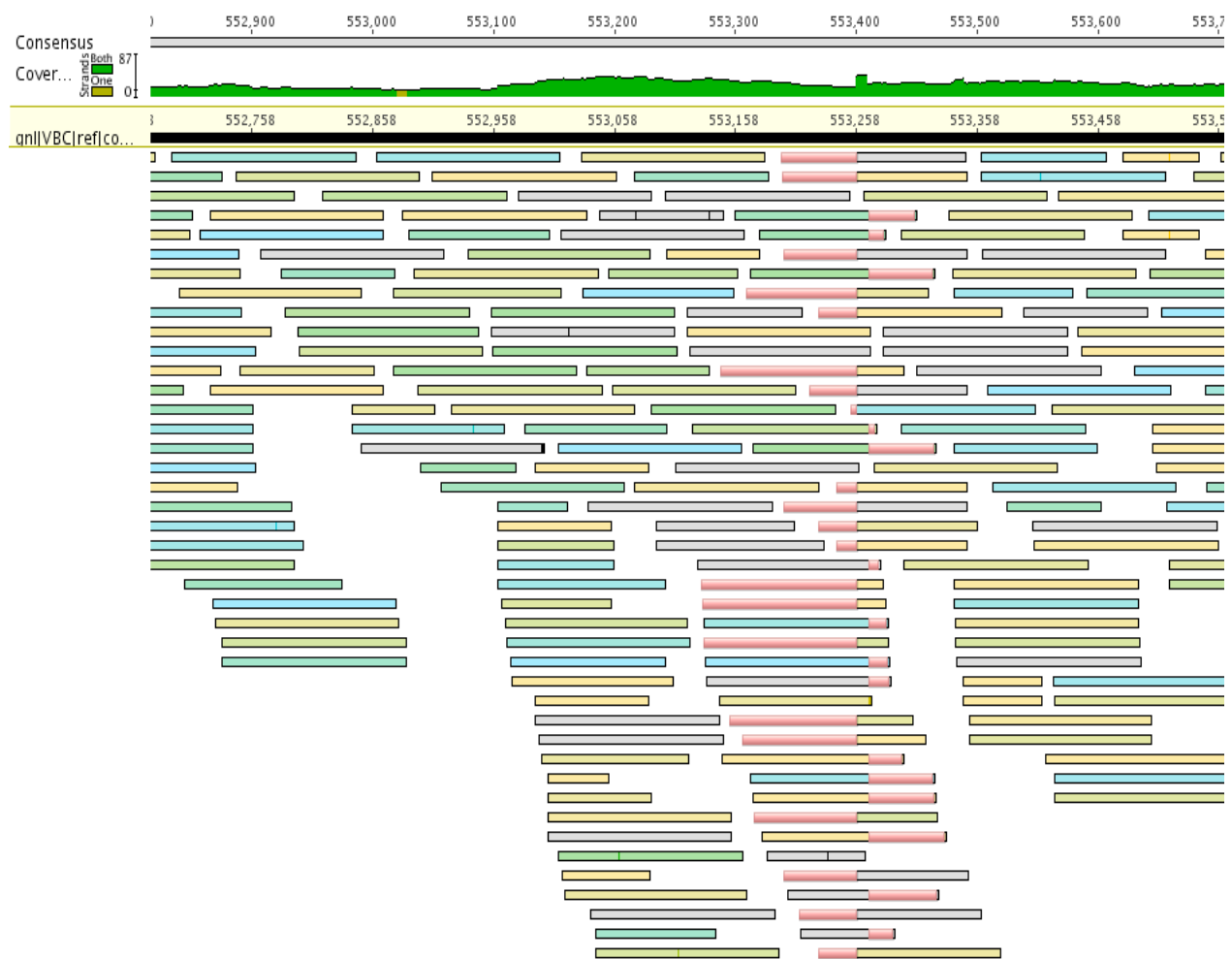


Figure 12 – Alignment of reads from C48 mutant’s genome against P0213-1 wild-type genome using Geneious v.6.1.8. In red are represented the reads unable to align with the reference genome.

As seen in Fig. 12, there is a highly covered region of unaligned reads (red reads) in both strands, with a small aligned interval between them corresponding to the natural complementary polymerization of the sticky ends formed after opening of the genome for transposon insertion, which does not produce sticky ends. By using those reads to get a BLAST hit result correspondent to the transposon, we can confirm that the unaligned region is the transposon. Thus, with the software, we know the exact position of the transposon and by the reference genome coordinates, we can identify the disrupted gene, as well as perform a BLAST search for homologs, namely in *B. multivorans* ATCC 17616. The results from the identification of disrupted genes using either strategy is represented in Table 3.

Table 3 - Genes disrupted by the plasposon were identified in the *B. multivorans* selected mutants

<i>B. multivorans</i> mutant	Chromosome	Start position	Locus tag	Gene name	Annotation	Homolog in <i>B. multivorans</i> ATCC 17616
F21	1	627814	FEP09_00578	<i>paaC</i>	1,2-pehnylacetyl-CoA epoxidase, subunit C	Bmul_0230
F27	1	1177196	FEP09_01098	<i>pyrC</i>	Dihydroorotase	Bmul_2520
F69	1	447574	FEP09_00419	<i>tctD_2</i>	Transcriptional regulatory protein TctD	Bmul_0075
D19	1	2422886	FEP09_02263	<i>ppsA</i>	Phosphoenolpyruvate synthase	Bmul_1274
D3	1	1633832	FEP09_01535	<i>hexR_2</i>	HTH-type transcriptional regulator HexR	Bmul_0558
C48	1	553519	FEP09_00508	<i>flhD</i>	Flagellar transcriptional regulator FlhD	Bmul_0160
C50	1	1884111	FEP09_01758	<i>rsmB_2</i>	Ribosomal RNA small subunit methyltransferase B	Bmul_0786
K28	3	849769	-	-	23S ribosomal rRNA	Bmul_R0082
K50	2	1763684	FEP09_05169	<i>xdhA_3</i>	Xanthine dehydrogenase molybdenum-binding subunit	Bmul_4199
K51	1	2694439	FEP09_05169	-	Hypothetical protein	Bmul_1477
K73	1	2294607	FEP09_02142	-	Hypothetical protein	Bmul_1150

3.4 Analysis of disrupted genes and possible role in planktonic cellular aggregation

The group of mutants producing apparently the smaller or lesser amount of aggregates, with the highest number of free cells, include disruption of genes involved in transcriptional regulation, carbon and energy production and pyrimidine synthesis. Figures 13, 15 and 16 display the mutated genes and neighboring genetic disposition of the first group of mutants. Disrupted gene of mutant K28 is not displayed due to the wrong annotation of this region containing an rDNA 23S gene.

K28 was disrupted by the plasmid in a sequence which appears to produce 23S rRNA. This was further supported by BLAST against reference genome of *Burkholderia multivorans* ATCC 17616 in the *Burkholderia* Genome Database and against all genomes in NCBI, both returning similar results. As such, for the purpose of this work, we will hypothesize on the results obtained from the experimental work with a 23S rDNA gene in mind.

23S rRNA, along with 5S rRNA is a component of the 50S large subunit that constitutes the 70S ribosome of prokaryotes (Lluque *et al.* 2017). It is in this rRNA that the V domain resides, providing the peptidyl transferase activity of the 50S subunit needed to catalyze peptide bond formation by peptidyl transfer (Shoji *et al.* 2015). As such it is involved in protein synthesis as well as prevention of premature polypeptide hydrolysis and aiding in protein folding.

The mutation in this region of the genome may result in altered functions of the cell due to destabilization of rRNA assembly or access to other substances. These can prevent natural occurring rRNA modifications required for normal functioning. Namely, such modifications are usually associated with antimicrobial resistance. Usually 23S rRNA has more copies of the gene within the genome, possibly able to compensate for the absence of one of the copies. Furthermore, modifications in 23S rRNA and its relationship with antimicrobial resistance is usually associated with more than one altered copy of the gene (Gomes *et al.* 2016). Therefore, this mutant might not even constitute a significant change in that regard. A link between this mutation and the observed phenotypes is therefore difficult to establish. It is, however, likely that a mutation on 23S rRNA leads to defects in translation, either through incorrect association of the subunits constituting the ribosome, and therefore the translation of transcripts or protein folding that might be players in aggregation under adverse environments.

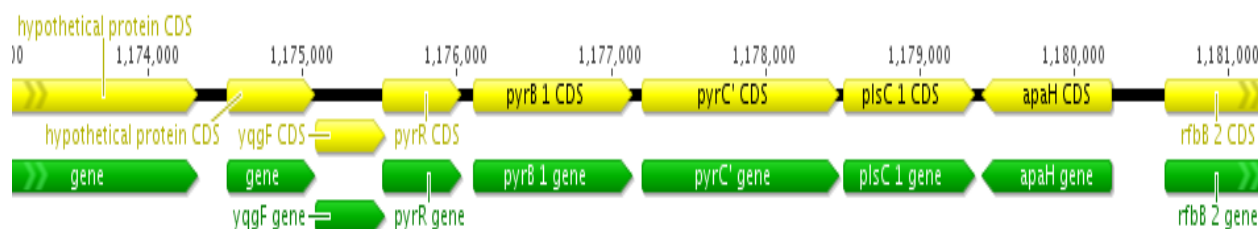


Figure 13 - In F27 mutant the plasposon is inserted in *pyrC* (Bmul_2520) gene. It belongs to the same operon as *pyrR* and *pyrB* encoding a bifunctional pyrimidine regulatory protein and an aspartate carbamoyltransferase catalytic subunit, respectively.

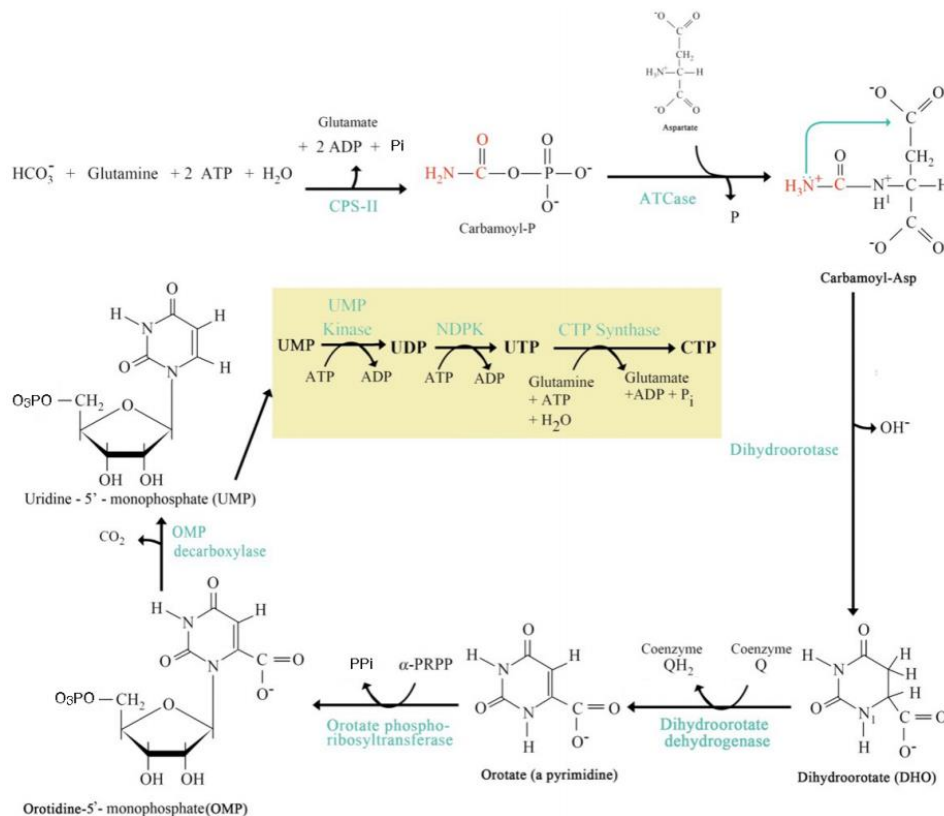


Figure 14 – De novo Synthesis of Pyrimidine Nucleotides. Retrieved from (Ahern and Rajagopal 2019). *PyrC* dihydroorotase converts Carbamoyl-L-aspartate to L-dihydroorotase in the third step of this pathway. In the final steps, UTP is converted to CTP by CTP synthase. This enzyme uses an amino group from glutamine for the reaction, balancing the relative amounts of CTP and UTP thanks to inhibition by excess CTP

Mutant F27 has the plasposon inserted into the *pyrC* gene (Fig. 13) encoding a dihydroorotase. It is the fifth gene of a 6-member putative operon in its *B. multivorans* ATCC 17616 homolog. This protein reversibly performs cyclization of carbamoyl-L-aspartate to L-dihydroorotase, the third step in the *de novo* pyrimidine nucleotide biosynthesis, producing, for example, UMP (uridine monophosphate), a nucleotide used as a monomer in RNA (Gontijo *et al.* 2014). Pyrimidines are vital since they are required as precursors for DNA and RNA synthesis and serve as energy sources under the form of UTP (uridine triphosphate) and CTP (cytosine triphosphate) (Fairbanks *et al.* 1995). Thus, this pathway is important for DNA and RNA integrity, as well as cell signaling and enzymatic reactions due to the role of their derivatives as secondary metabolites and cofactors.

PurR was described as being a repressor of this enzyme in *E. coli*, acting according to purine and pyrimidine concentration, and by association, to the ratios of GTP (a product of this pathway) to CTP, respectively, in *S. typhimurium*. When this ratio would be higher, either GTP would prevent binding of this repressor to *pyrC* or an adenine nucleotide would enhance binding of the repressor to a binding site in its own promoter. This reciprocal regulation is thought to prevent accumulation of pyrimidines and maintain a balance in the intracellular pools of purines and pyrimidines (Choi and Zalkin 1990; Jensen 1979, 1989), possibly destabilized under stress conditions. UMP degradation product was also reported to work as a feedback inducer of the pathway, including the dihydroorotase, in *Pseudomonas oleovorans* (Haugaard and West 2002; Ralli, Srivastava, and Donovan 2007).

This pathway is generally thought to be regulated at the level of enzyme synthesis (Choi and Zalkin 1990; Murahari and West 2018; Santiago and West 2002, 2003). Presence of pyrimidines, like uracil, regardless of carbon source in the media, appears to repress pyrimidine biosynthetic enzymes (Choi and Zalkin 1990; Chunduru and West 2018). However, the opposite was also suggested (Murahari and West 2018; Ralli *et al.* 2007; Santiago and West 2002). On the other hand, pyrimidine auxotrophs or pyrimidine starved microorganisms greatly induce expression of this pathway's enzymes.

In *P. aeruginosa*, two genes were found to encode this protein. The first, *pyrC*, is constitutively expressed, while the second, *pyrC2*, is presumably only expressed while the former is not functioning (Brichta *et al.* 2004). Two genes encoding this protein in the reference wild-type P0213-1 genome were also found, including the one with the inserted plasposon. It may be that under stress and biofilm induction, nutrient limitation forces the cell to save energy and thus, the constitutive *pyrC* can be shut down so that only *pyrC_2* functions, dependent on extracellular signals and according to strict survival needs of the community. In this study, it's not quite clear which one would this correspond to, nor do we know if the same functioning mechanism applies. However, we could hypothesize that it corresponds to *pyrC2* of *P. aeruginosa*, and thus, under stress conditions the *pyrC* would be shut down and *pyrC2* would take over. However, a disruption of this gene would not allow this transition, reverting back to the main expressing gene, which would take up more energy, due to constitutive expression, which would otherwise be redirected to aggregate formation. Regardless, suppression of this pathway may potentiate stress conditions, possibly similar to amino acid starvation, known to induce stringent response.

Furthermore, given the pivotal role of the pyrimidine *de novo* pathway in DNA synthesis, differential expression of this gene could have effects on eDNA produced, one of the most abundant polymers of extracellular matrix produced in *P. aeruginosa* PAO1, proven to be required for biofilm development and maturation (Shirtliff *et al.* 2002; Whitchurch 2002). As such, should eDNA be a key player in planktonic cellular aggregation in *B. multivorans* P0213-1, it is possible that abrogation of pathways that lead to its formation affect this phenotype.

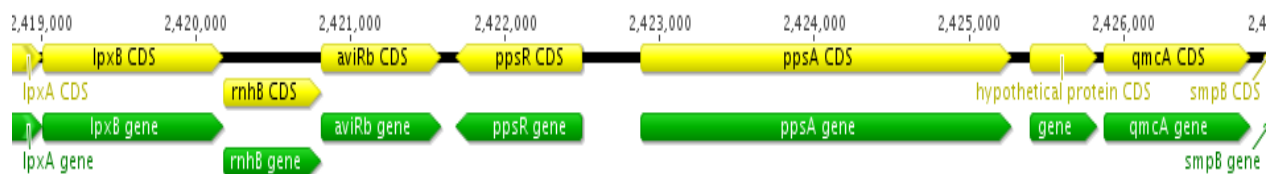


Figure 15 - In D19 mutant the plasposon is inserted in *ppsA* (Bmul_1274) gene

D19 possesses a disrupted gene, *ppsA* (Fig. 15), encoding phosphoenolpyruvate synthase, which performs the anaplerotic reaction of converting pyruvate to phosphoenolpyruvate (PEP) with expenditure of energy. The carbon source of the SM medium used, mannitol, is catabolized by the glycolytic pathway, producing phosphoenolpyruvate and then pyruvate. Since the reverse reaction is blocked, pyruvate and acetyl-CoA accumulation is likely. As such, this may overload TCA cycle activity and excess acetyl-CoA can be used to boost a number of pathways other than energy production, like lipid synthesis (Shi and Tu 2015; Takahashi *et al.* 2006; Wellen *et al.* 2009). In the case of excess pyruvate, as previously mentioned, its utilization has a role in microcolony formation and redox balancing, namely through its fermentation or release for utilization during stationary phase (Petrova *et al.* 2012). Thus, this accumulation of pyruvate may be released for posterior use or it may be fermented into lactate, allowing transition into planktonic aggregation mode of growth.

Contrary to this idea is the fact that, under normal circumstances, some pyruvate also has to be converted into phosphoenolpyruvate to serve as precursor for gluconeogenesis and thus replenish citric acid cycle intermediates and sugars necessary for polysaccharide biosynthesis (Smyer and Jeter 1989).

This enzyme may also have a role on the phosphoenolpyruvate-dependent phosphotransferase system (PTS) which enables the uptake of PTS carbohydrates, such as glucose, into the cell by active transport. This system is a phosphorylation cascade composed of a membrane-spanning protein and cytosolic proteins that transfer phosphate from PEP to the substrate carbohydrates in a sequential manner (Hornig *et al.* 2017). Mannitol is considered a PTS carbon source and as such, inability of this mutant to properly convert pyruvate back into PEP may reduce the ability of this system to function and transport sugars, possibly affecting mechanisms required for biofilm formation, like polysaccharide synthesis (Choe *et al.* 2017; Hornig *et al.* 2017).

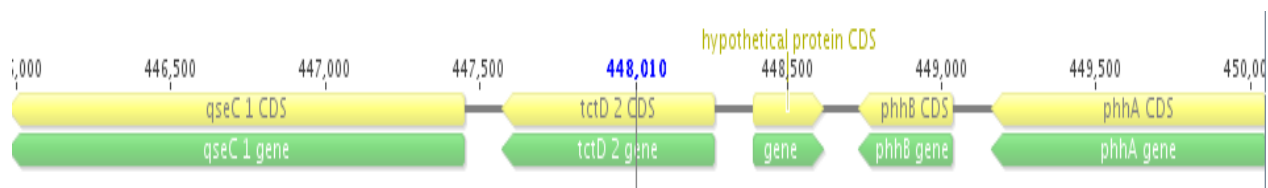


Figure 16 - In F69 mutant the plasposon is inserted in *tctD_2* (Bmul_0075) gene.

F69 mutant has the *tctD_2* (Fig. 16) disrupted gene encoding a transcriptional regulatory protein TctD according to reference genome annotation. This annotation indicates that this protein might be similar to a member of the response regulator of the two-component system TctD-TctE involved in the uptake of tricarboxylic acids, as described in *P. aeruginosa*, *Salmonella typhimurium*, *Xanthomonas campestris* pv. *Vesicatoria* (Tamber *et al.* 2007; Tamir-ariel *et al.* 2011; Widenhorn *et al.* 1988). However, this is not certain, existing the possibility of encoding something else or being

just one copy of this gene since four others encoding a protein of the same name were identified in the genome of the wild-type. After BLAST of this gene's sequence, a better homology is found with the response regulator PidR, an ortholog found in *Burkholderia glumae*, acting along the sensor histidine kinase PidS. This TCS is involved in regulation of pigmentation as well as virulence-related phenotypes (Karki *et al.* 2012). Pigments of *B. glumae* are thought to be involved in tolerance to environmental stresses like ROS and UV light, further supported by the fact that this species' TCS has significant homology with ColS-ColR of *X. campestris* pv. *campestris* and *Xanthomonas citri* ssp. *citri*, known to play a role in tolerance to environmental stresses, type III secretion system and virulence (Yan and Wang 2011; Zhang *et al.* 2008). It may be that these TCS's act on common regulatory pathways for bacterial pathogenesis under different host environments. The same or a similar TCS may be in function in *B. multivorans* P0213-1, especially considering that orthologues of PidS-PidR were found to be highly conserved among many *Burkholderia* species like *Burkholderia gladioli*, *Burkholderia mallei*, *B. pseudomallei*, and that their amino acid sequence at the N-terminal signal input domain share significant homology, suggesting recognition of the same or similar signals, and thus, similar biological functions (Karki *et al.* 2012). If such is the case, the gene disrupted in mutant F69 could be of importance in providing environmental resistance within the host, required for establishment or development of cellular aggregation. The mechanism or pathways involved could be different however, since under the tested conditions, *B. multivorans* P0213-1 does not seem to produce pigments.

The following group of mutants, forming more or bigger visible aggregates than the previous ones, but less than the wild-type strain, have their respective disrupted genes shown in Figures 17, 19, 21, 22, 23 and 24.

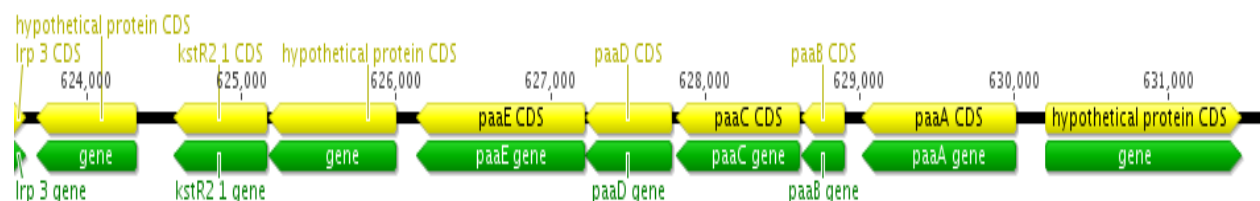


Figure 17 - In mutant F21 the plasposon is inserted in *paaC* (Bmul_0230) gene.

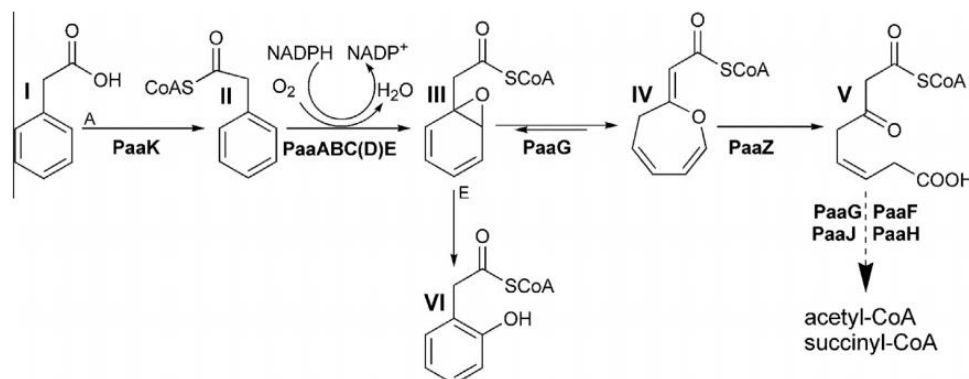


Figure 18 – Phenylacetate utilization pathway. Retrieved from (Grishin *et al.* 2013). The first step of this pathway is conversion of phenylacetate into phenylacetyl-CoA catalyzed by phenylacetate-CoA ligase (PaaK). *paaC* encodes a subunit of the PaaABC(D)E monooxygenase responsible for the second step of the pathway, converting phenylacetyl-CoA into 1,2-epoxyphenylacetyl-CoA. Final products of the pathway are TCA intermediates.

F21 has the transposon disrupting gene *paaC* (Fig. 17) which encodes for 1,2-phenylacetyl-CoA epoxidase, subunit C (Fig. 18). It presents homology with the PaaI subunit of *B. multivorans* ATCC 17616, presumably different designations for the same protein, and appears to correspond to the *paaC* gene described in *E. coli*. This gene belongs to a five-member operon, *paaABCDE*, that together encodes a complex monooxygenase that converts phenylacetyl-CoA (PA-CoA) to 1,2-epoxyphenylacetyl-CoA. This is the second step of aerobic phenylacetate catabolism, where several carbon degrading pathways converge and are directed to the Krebs cycle (Imolorhe and Cardona 2011; Luengo *et al.* 2001). The reaction it conducts consumes NADPH, implying oxygenase/reductase activity. This subunit in particular belongs to the catalytic core of the complex, however, in *E. coli* it is devoid of the catalytic centre, thus it was proposed to play a structural role in complex formation and to be essential for activity (Grishin *et al.* 2010).

The following intermediates are CoA-thioesters, typical of anaerobic rather than aerobic aromatic metabolism, constituting a hybrid pathway. At first it seems disadvantageous since in anaerobiosis there is direct profit, as it draws electrons from the reactions, facilitating ATP-dependent and other energy-driven reduction of the aromatic system. However, in aerobic degradation some intermediates due to being CoA-esters have a facilitated formation and are retained within the cell wall, being rapidly recognized and bound through CoA-binding motifs of the processing enzymes. This is important since highly reactive free epoxides would harm the cell (Teufel *et al.* 2010).

How the disruption of phenylacetate degradation pathway might lead to a decrease in size of the planktonic aggregate formation is not known, however, the highly reactive intermediates of this pathway, namely the epoxide produced by the multienzymatic complex, may harm the cell, as previously stated, and that may in turn impair aggregate size by decrease of cell viability. Despite this hypothesis, it was also found in *P. aeruginosa* Y2 that this monooxygenase was able to deoxygenate the epoxide-CoA back to PA-CoA (phenylacetate-CoA). A beneficial reaction that prevents accumulation of the unstable epoxide, which is also able to form the dead-end product 2-hydroxyphenylacetate that cannot be metabolized. Hence, this complex may harbor an escape mechanism from its own toxic product through a bifunctional oxygenase/deoxygenase (Teufel *et al.* 2012).

In several species when both phenylacetic acid (PAA) and glucose are present, the sugar is preferably used, suggesting carbon catabolite repression (CCR) of PAA metabolism by glucose. This effect was attributed to 2-keto-3-deoxy-6-phosphogluconate (KDPG) in *P. putida* KT2440, which was an inducer of glucose metabolism and identified to likely be an important signal that controls preferential utilization of glucose over other aromatic carbon sources (Kim *et al.* 2009). This effect, however, appears to be glucose specific and is reversed and controlled by cAMP or cAMP-CRP and IHF, which activate *paa* genes, possibly by binding to the promoter or intergenic region of the operon, respectively. As such, they connect expression of the *paa* genes to the metabolic and energetic status of the cell, establishing a balance according to available nutrients.

In *B. cenocepacia*, it was shown that during growth in SCFM, several genes encoding phenylacetic acid degradation enzymes were highly induced and the promoter of *paaA* gene is activated in the medium and in the presence of phenylalanine, one of the aromatic amino acids in SCFM (Hamlin *et al.* 2009; Yoder-himes *et al.* 2009). These carbon utilization routes may be of special importance during CF infection given the high concentration of aromatic amino acids found in CF sputum (Yudistira *et al.* 2011). This leads to the hypothesis that this pathway may

be involved in the transition to planktonic cellular aggregation due to its upregulation when exposed to an environment that has been shown to induce this transition, SCFM, as well as possessing an abundance of substrates for this pathway.

Another hypothesis is an involvement in QS. Since this pathway is disrupted, it might lead to accumulation of acetyl-CoA. This compound was shown, in *Prosthecomicrobium hirschii*, to be used as a substrate for a *luxI*-like AHL synthase, producing phenylacetyl-homoserine lactone which was key in controlling aggregation and biofilm formation (Liao *et al.* 2018). On the other hand, extracellular PAA was shown in *P. aeruginosa* PAO1 to work as a QS inhibitor by reducing production of AHL-dependent factors, altering pathogenicity and motility (Syed *et al.* 2012).

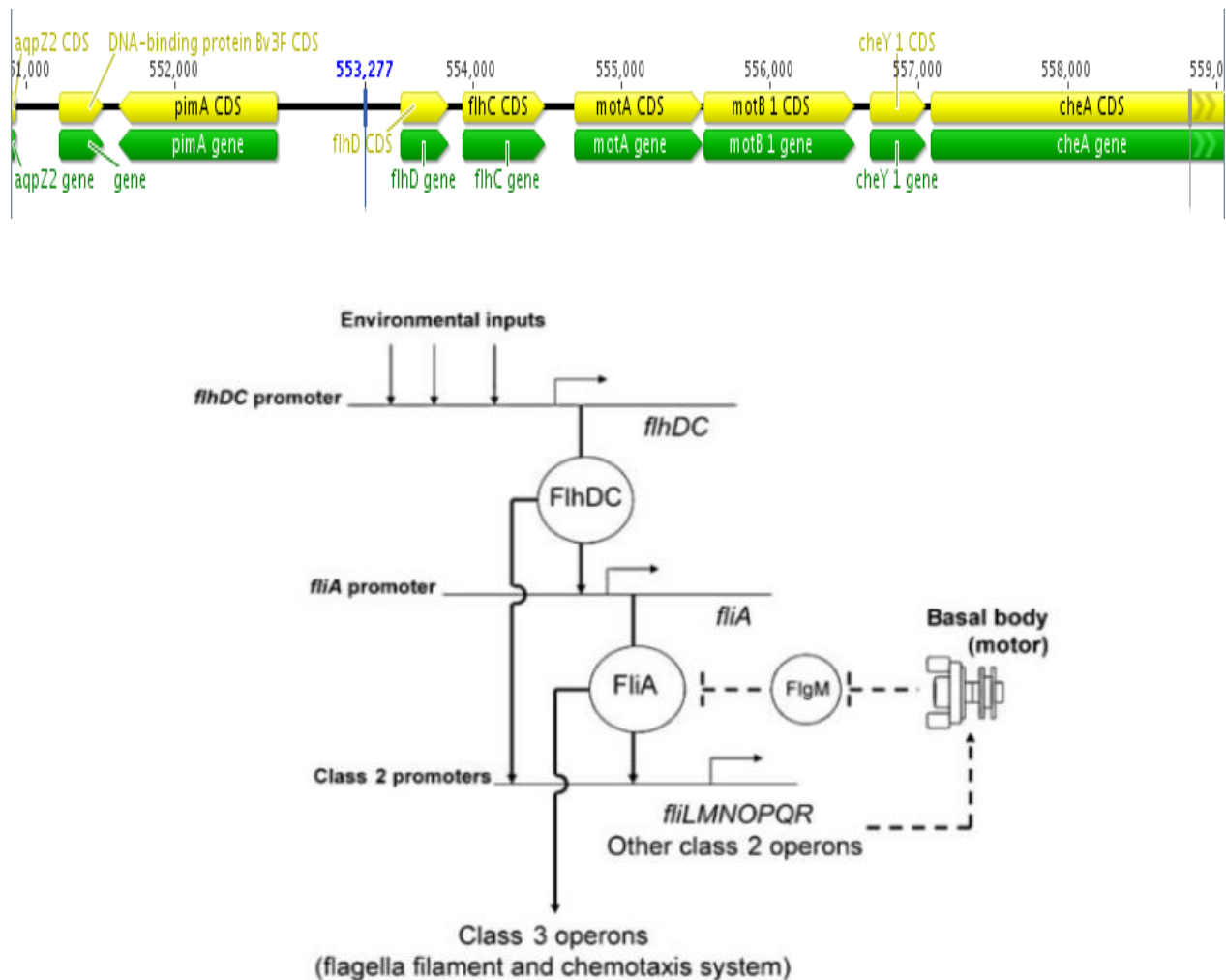


Figure 19 - Overview of FlhDC functioning. Retrieved from (Rosenfeld, Elowitz, and Alon 2002). When motility is required environmental signals are recognized by the cell, which regulates expression of master regulator *flhDC*. Being a class I operon, its expression will induce expression of class II flagellar genes, which in turn induce class 3 operon genes involved in flagella biosynthesis and chemotaxis.

In mutant C48, the transposon was found within an intergenic region between the genes encoding a GDP-mannose-dependent α -(1-2)-phosphatidylinositol and the flagellar master transcriptional regulator, FlhD (Fig. 19). However, it is roughly 577 base pairs apart from the former and 258 from the latter. Thus, due to proximity, it seems more likely

that the transposon would affect transcription of *flhD*, if at all, therefore being the gene considered for the ensuing discussion.

flhD is one of the components constituting the master regulator of flagellar genes and a global regulator of metabolism (Barker *et al.* 2004), FlhDC. It is considered a class I operon gene, which in its complex, FlhDC will induce expression of class II flagellar genes like *FliA*, which in turn will activate class III operon genes (Campos and Matsumura 2001). FlhDC, and consequently FlhD, is involved in flagella synthesis and related functions like chemotaxis, swimming and swarming motility, among other cellular processes, like anaerobic respiration and nutrient and protein transport (Amores *et al.* 2017; Claret and Hughes 2000; Eberl *et al.* 1996; Givaudan *et al.* 2000; Prüß *et al.* 2001, 2003). Stimulation of *flhD* expression results in filamentous, hyperflagellated cells, playing a central role in swarm cell differentiation as well as speed of cellular motility (Claret and Hughes 2000; Eberl *et al.* 1996). Several examples of the sort are found, as well as the loss of motility upon loss or inactivation of *flhD* (Claret and Hughes 2000; Eberl *et al.* 1996; Givaudan *et al.* 2000).

FlhD on its own does not possess DNA-binding activity but is able to regulate other non-flagellar genes involved in repression of cell septation, and thus, division rate during stationary phase (Liu and Matsumura 1994; Markovic *et al.* 1997; Prüß and Matsumura 1996). FlhC, on the other hand, acts as an allosteric effector that activates FlhD, allowing the recognition of DNA and plasticity of binding specificity according to the target, possibly by conformational change (Campos *et al.* 2001; Campos and Matsumura 2001; Claret and Hughes 2000).

The FlhDC, being a master regulator has major inputs from c-di-GMP, cAMP and (p)ppGpp, being modulated by environmental and physiological signals (Amores *et al.* 2017; Pesavento *et al.* 2008; Sommerfeldt *et al.* 2009; Valentini and Filloux 2016). This master operon is thought to be a key player in transitioning from a planktonic to biofilm structure. Biofilm formation is reported to be initiated by increasing levels of c-di-GMP and the sigma factor RpoS (Mika and Hengge 2014; Ogasawara, Yamamoto, and Ishihama 2011), which will cause inhibition of *flhD* at post-transcriptional or post-translational level (Tomoyasu *et al.* 2002). It also appears to be inhibited by catabolite repression, when glucose is present, presumably since it decreases intracellular cAMP receptor protein concentration, at the same time corresponding to enhanced biofilm formation (Maniatis *et al.* 2012; Mika and Hengge 2014; Ogasawara *et al.* 2011). Other inhibiting conditions of flagellar synthesis include high temperature, high osmolarity, low pH, high concentration of salts, carbohydrates and others (Barker *et al.* 2004). The loss of FlhDC has been shown to elevate expression of catabolic genes, providing colonization advantage (Fabich *et al.* 2011).

Only two transcription factors directly activate *flhDC* in *E. coli*, cAMP-CRP and QseB, both enhancing its transcription (Soutourina *et al.* 1999; Yokota and Gots 1970). Others control FlhD indirectly, like *ompR*, among others, which has been shown to repress *flhD* expression in *E. coli* and increase biofilm biomass (Samanta *et al.* 2013), further establishing a link between FlhDC and control of biofilm formation.

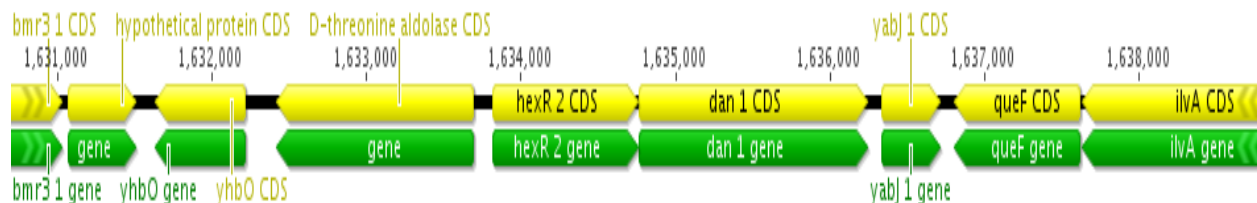


Figure 20 - In D3 mutant the plasposon is inserted in *hexR_2* (Bmul_0558) gene.

D3 has the *hexR_2* gene interrupted (Fig. 21) which encodes a HTH-type transcriptional regulator of the RpiR family, with some homology with HexR. Since it is a transcriptional regulator whose identification is not very faithful, it is difficult to designate specific genes, functions or pathways in other similar species. Its DNA binding domain is the RpiR-type HTH domain, occurring in the N-terminal, present in prokaryotic regulators of transcription. This domain is named after *E. coli* RpiR, a repressor of genes involved in sugar metabolism. In its C-terminal it contains a phosphosugar-binding domain, SIS (sugar isomerase). Most of these types of regulators are involved in sugar metabolism either as transcription repressors or activators (Leyn *et al.* 2011; Sørensen and Hove-Jensen 1996; Yamamoto *et al.* 2001). Perhaps we can highlight the homonymous HexR of *P. aeruginosa*. This is a transcriptional repressor of the *hex* regulon, involved in sugar metabolism. In turn, the *hex* regulon comprises at least three operons that encode the members of the glycolytic pathway responsible for the uptake and metabolism of glucose to glyceraldehyde 3-phosphate and pyruvate. HexR is able to repress expression of all enzymes of this regulon by binding to DNA sequences upstream of each operon, which would otherwise be constitutively expressed (Hager *et al.* 2000). It can also bind through its SIS domain to KDPG, which signals glucose availability, causing HexR to dissociate from DNA, inducing expression of its gene targets and stimulating glucose uptake and metabolism (Daddaoua *et al.* 2009).

HexR-type transcriptional regulators are also reported in other species, most of which appear to be part of central carbon metabolism regulation, namely responding to glucose concentrations (Antunes *et al.* 2016; Leyn *et al.* 2011). This is verifiable in a wide array of species, with opposing functions like the RpiR repressor of *E. coli* (Sørensen and Hove-Jensen 1996), the activator of maltose metabolism, GlvR of *Bacillus subtilis* (Yamamoto *et al.* 2001), the dual-sensing transcriptional factor-like HexR, which responds not only to KDPG but also oxidative stress in *P. putida*, and others (Kim, Jeon, and Park 2008).

These types of transcriptional regulators have also been shown to regulate genes involved in nitrogen metabolism, redox potential and denitrification (Antunes *et al.* 2016). Thus, it is suggested that although the specific identity and function of the protein encoded by the disrupted gene in this mutant is not known, it is very likely that it plays a role on metabolism, possibly carbon catabolism in addition to other processes, likely required in connecting major pathways in responses to environmental adaptation, and therefore in mode of growth transition to planktonic cellular aggregates.

Belonging to the same operon and immediately downstream of *hexR_2*, and thus susceptible to expression dysregulation upon transposon insertion, there is the *dan_1* gene, encoding a N-acyl-D-amino-acid deacylase, which is putatively involved in the hydrolyses an N-acyl-D-amino-acid into a D-amino acid. These product molecules are reported to incorporate antimicrobial peptides that provide a competition advantage when scavenging for nutrients (Hänchen *et al.* 2013). Regarding aggregate formation, some of these types of amino acids, namely D-alanine, are also constituents of the peptidoglycan, necessary to provide resistant to physical stresses and to osmotic pressure across the

cell wall (Trivedi *et al.* 2018). The peptidoglycan layer also serves as an anchorage for several surface proteins, some of which have been shown to be required for adhesion, host invasion, evasion of immune responses and biofilm formation in *S. aureus* (Foster *et al.* 2014). More importantly, in *B. cenocepacia*, the peptidoglycan-associated lipoprotein was reported to be involved in epithelial cell attachment, a trait possibly in common with adhesion to other cells for biofilm formation (Dennehy *et al.* 2016). As such, it could be that should *dan_1* gene also be influenced, there is the possibility that it may impact cell aggregation, mostly due to a lack of building blocks of peptidoglycan, and by association a reduction of peptidoglycan associated surface proteins required for cell to cell communication, as well as reduced resistance to physical stressors which may prevent proper aggregation due to compromised physical cell integrity.

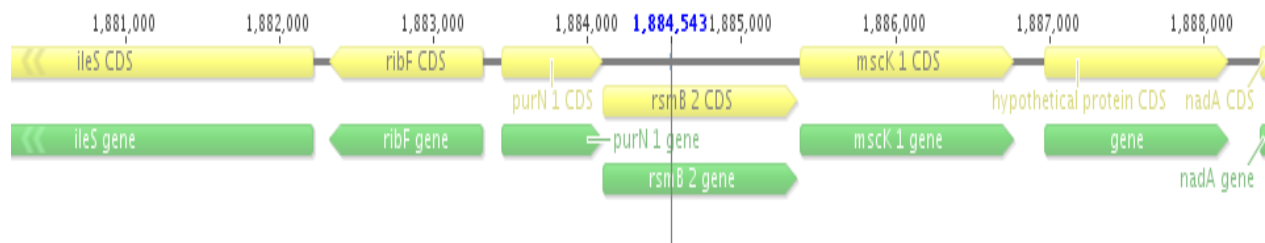


Figure 21 - In C50 mutant the plasposon is inserted in *rsmB_2* (Bmul_0786) gene.

C50 has the plasposon inserted into the *rsmB_2* gene (Fig. 22), encoding a ribosomal RNA small subunit methyltransferase subunit B in the reference genome, a similar result was obtained by BLAST in NCBI, and identified as an Fmu (Sun) domain-containing protein in *B. multivorans* ATCC 17616. The result obtained from the reference genome appears to be similar to methyltransferase RsmB of *E. coli*. As such, discussion will be based on this specific protein.

The disrupted gene encodes an enzyme thought to be involved in bacterial RNA modifications, possibly methylation of the small rRNA subunit, 30S. Modifications of rRNA consist mainly of base and sugar methylations and pseudo-uridylation (Andersen and Douthwaite 2006). Modified rRNA has been shown to have a superior performance than their unmodified counterparts (Green and Noller 1999; Khaitovich *et al.* 1999; Krzyzosiak and Ofengand 1987). It is a way of fine-tuning ribosome function. RsmB in specific is known to methylate position 5 of nucleotide C967 in 16S rRNA of the small rRNA subunit of *E. coli* and *Thermus thermophilus* (Demirci *et al.* 2010; Hikida *et al.* 2010). It has an N-terminal domain considered to be important for RNA binding, a C-terminal methyltransferase-fold domain, and a typical S-adenosyl-L-methionine (SAM) motif, responsible for donating the methyl group. Nucleotide C967 is located within the loop of a stem-loop structure which has been implicated in tRNA binding at the peptidyl site (Hikida *et al.* 2010). The recurrence of methylated residues within functionally significant sites suggests that they should fulfill some specific role, which, however, is unknown (Tscherne *et al.* 1999). RsmB specifically has been reported to be necessary for correct attenuation of tryptophan operon (Prokhorova *et al.* 2013).

In *E. coli* the expression of rRNA methyltransferases is altered by environmental stressors, including antibiotic treatment, temperature shift and oxidative treatment, supporting the importance of methyl modification of rRNA under stress conditions (Baldrige and Contreras 2013). For example, attenuation of another rRNA methyltransferase, KsgA, in *S. aureus*, proved to be more sensitive to temperature and osmotic stress, presumably due to defect of ribosome

function caused by the absence of methyl modification of 16S rRNA (Kyuma *et al.* 2015). RsmA and RsmB proteins have also been implicated in biofilm formation through QS-related genes (Burrowes *et al.* 2005). It is possible that the absence of the methyl modification destabilizes the conformation of the matured ribosome or disables ribosome biogenesis under oxidative stress conditions. Though rRNA modifications may be dispensable for all basic steps of translation, it is possible that they are needed for the control over translational efficiencies of some mRNAs under specific conditions (Prokhorova *et al.* 2013). A similar mechanism may happen with the protein of *rsmB_2* of *B. multivorans* when facing a wide array of stresses. A mutant strain of *E. coli* lacking *rsmB*, as well as *rsmD*, was shown to be cold-sensitive and have reduced fitness (Burakovsky *et al.* 2012). Ribosomes from this strain had a mild kinetic defect in selection of initiator tRNA in certain mRNA contexts, suggesting that methylations might have a differential effect on translation initiation of a subset of cellular mRNA.

An interesting study worth mentioning reports a strain of *P. aeruginosa* in which methylation of 23S rRNA of the bigger subunit was induced, blocking access of the ribosome to azithromycin, which reverted the initial reduction of virulence factor production, biofilm formation, bactericidal effects and swarming motility caused by azithromycin (Ko *et al.* 2007). Thus, “simple” rRNA modifications such as methylation may impact several phenotypes, which are not only studied in this thesis but also important for the establishment of bacteria within the host. Besides, defects such as these on the components of the small rRNA subunit may also result in similar phenotypic alterations.

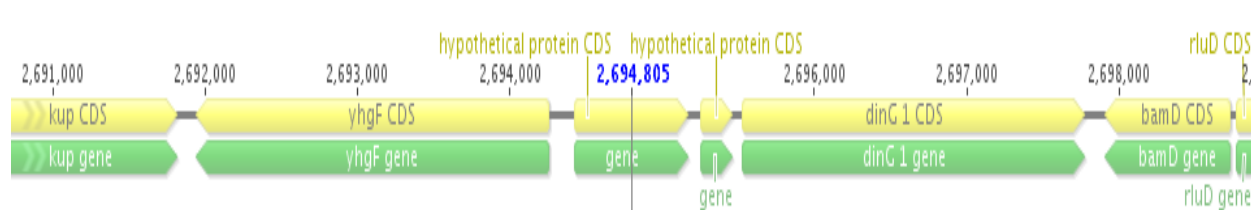


Figure 22 - In mutant K51 the plasposon is inserted in an unknown gene (Bmul_1477).

K51 has an unknown disrupted gene that encodes for a hypothetical protein (Fig. 23), thus its possible function or homology is not known. Furthermore, in the genome of the wild-type P0213-1, this gene is surrounded by other genes encoding hypothetical proteins, and in the genome of the homologous *B. multivorans* ATCC 17616 it belongs to a two-member operon whose only other constituent is yet another hypothetical protein. As such, it is not possible to relate this mutation with any of the phenotypes observed, nor hypothesize any mechanisms.

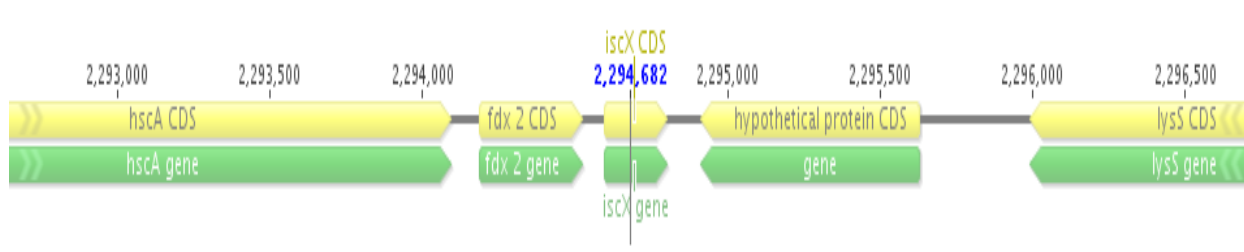


Figure 23 - In K73 mutant the plasposon is inserted in *iscX* (Bmul_1150) gene.

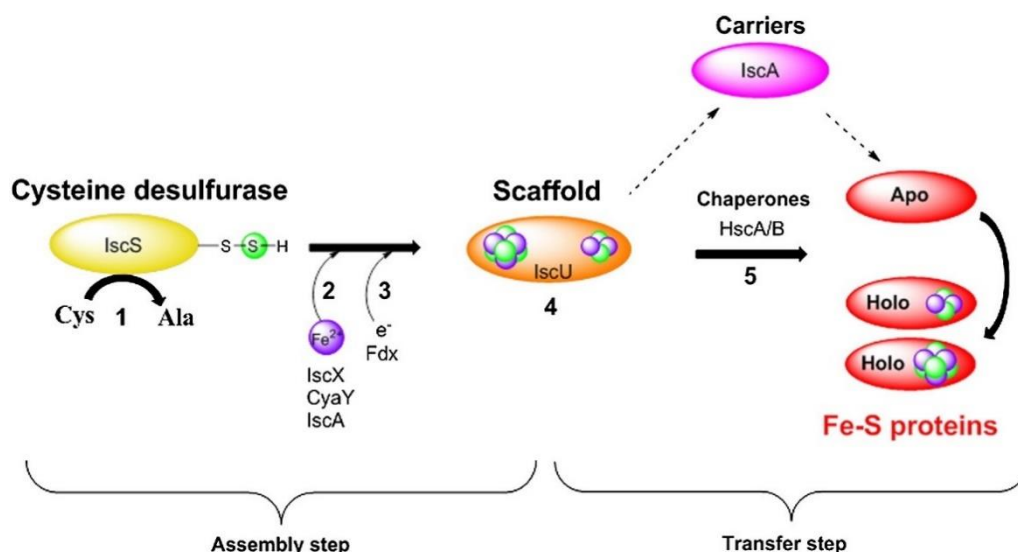


Figure 24 – Schematic view of FeS cluster biogenesis in the ISC system. Retrieved from (Blanc *et al.* 2015). Ovals represent proteins (IscS, IscU, IscA and targets). Steps 1-4 represent assembly step; step 5 represents the transfer in which FeS cluster is transferred from IscU to targets with the help of chaperones or indirectly through IscA FeS transporter.

For the last mutant of this group, disrupted gene *iscX* encoding the FeS assembly protein IscX (Fig. 24). This gene is the first of a two-gene putative operon, in which the second gene encodes a 2Fe-2S ferredoxin. IscX is also called Yfhj, its function is unknown, and it belongs to the ISC system of FeS cluster assembly (Fig. 25). It is an acidic protein, thought to be non-essential (Pastore *et al.* 2006; Tokumoto *et al.* 2002; Tokumoto and Takahashi 2001). It possesses a HTH domain, often found in transcription regulators. It has the ability to bind to iron with low affinity and to interact with IscS, the desulfurase central to FeS cluster assembly (Kim *et al.* 2014; Zhang *et al.* 2010). Its role has been proposed to be a modulator of CyaY, derepressing the effect it has on IscS, and thus, on enzymatic cluster formation. This effect is stronger at low iron concentration, with IscS being under control of IscX, and negligible at higher ones, with CyaY sensing that iron and gaining higher affinity for IscS. As such, it is thought that under iron stress conditions, CyaY is upregulated or IscS downregulated. IscX itself can also have an inhibitory effect since it possesses two binding sites in IscS. Once the first one is saturated, binding starts to occur on the second binding site, which will cause inhibition of IscS and thus, of cluster formation, possibly to prevent indiscriminate use of iron when its availability is low, since ISC generates housekeeping FeS proteins under normal conditions, or to reduce unproductive conversion of cysteine to alanine by IscS. The iron donor of the cluster is thought to be either CyaY and/or IscX (Adinolfi *et al.* 2018; Blanc *et al.* 2015; Kim *et al.* 2014).

Iron and sulfur are essential for unique redox properties. They are also highly toxic and converting them into clusters is an efficient nontoxic way to store them (Adinolfi *et al.* 2018). These clusters are present in more than 200 different types of enzymes or proteins (Bandyopadhyay *et al.* 2008). As such they are required for survival and development of cells, being involved in several conserved cellular processes such as gene expression, DNA replication and repair, ribosome biogenesis, tRNA modification, central metabolism and respiration. The prosthetic group that is a FeS cluster is required for correct folding and protein stability (Blanc *et al.* 2015).

Hydrogen peroxide is known to inactivate the ISC system in *E. coli*. This happens by oxidizing the clusters as they are assembled on or transferred from the scaffold protein (Jang and Imlay 2010). Other stresses were also shown to increase sensitivity when cluster biosynthesis was defected, such as metal, thiol and osmotic stress in *P. aeruginosa* (Romsang *et al.* 2015). However, it can only be speculated that IscX has any influence on this since it may not even be essential for iron sulfur cluster biosynthesis, especially when there is one more known system which may perform this deed, SUF. This is a system which usually takes over FeS cluster assembly under stress conditions, which doesn't change the fact that cells appear to be more sensitive in the absence of ISC (Rincon-enriquez *et al.* 2008).

As the role of IscX appears to be ambiguous, for most of the following phenotypes we can state that should this enzyme have a determinant role in FeS assembly, it is possible that it would influence them directly due to dysregulated FeS cluster assembly. As reported by Vergnes *et al.*, in a *Vibrio vulnificus* mutant lacking IscR, which regulates ISC FeS assembly, genes involved in motility and adhesion to host cells, as well as hemolytic activity and survival under oxidative stress of the pathogen during infection were upregulated (Vergnes *et al.* 2017).

The last group is only made up of mutant K50, being the only mutant that has displayed a higher ability than the wild-type to produce aggregates and presented a very distinctive structure at the microscopic level.

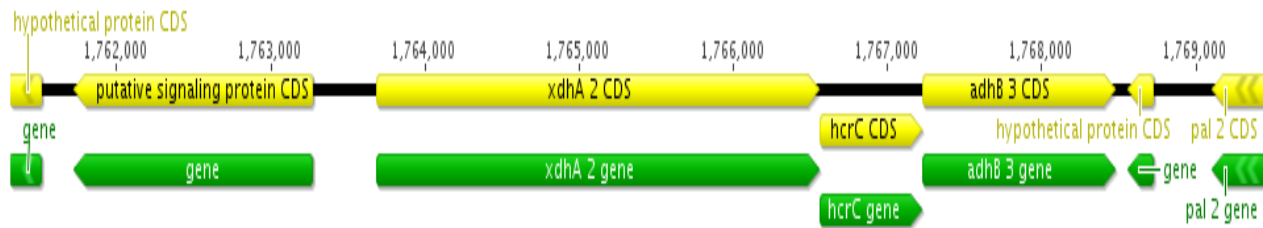


Figure 25 - In mutant K50 the plasposon is inserted in *xdhA_3* (Bmul_4199) gene

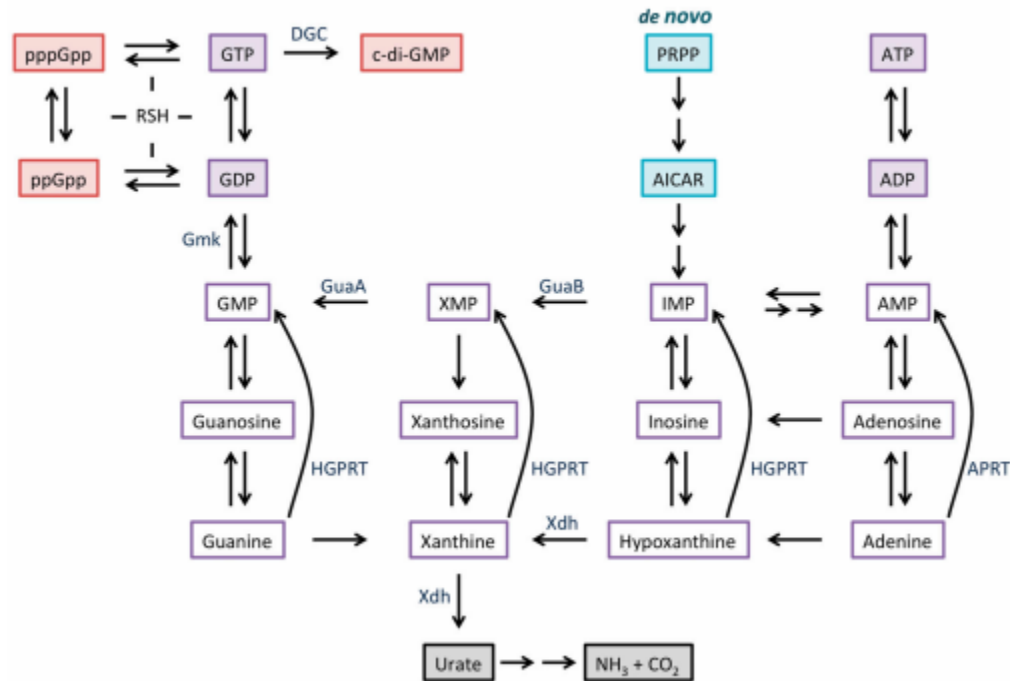


Figure 26 – Overview of purine metabolism. Retrieved from (Sivapragasam and Grove 2019). *De novo* synthesis begins in blue. Intermediates in salvage pathways are outlined in purple. Degradation of purines begins in grey.

The disrupted gene of K50 was *xdhA_3* (Fig. 26), which encodes a xanthine dehydrogenase molybdenum-binding subunit. It belongs to a three-member operon and it is required for the purine salvage pathways. Purines provide the bases required for DNA, RNA, cofactors, signaling molecules and carriers of energy. These can be obtained either through the *de novo* or salvage pathways. Their biosynthesis is an essential process for the survival of the cell, especially under limiting conditions that impose energy saving conditions on the bacterial community.

Xanthine dehydrogenase (XDH) is often described as having two active forms, dehydrogenase and oxidase, constituting an oxidoreductase. However, in prokaryotes only the dehydrogenase form has been identified. This enzyme conducts the conversion of hypoxanthine to xanthine and then xanthine to uric acid, using NAD^+ as electron acceptor (Fig. 27) (Ivanov *et al.* 2004). Besides oxidation of these substrates, it can also oxidize different endogenous metabolites and xenobiotics, like toxic substances (Pritsos and Gustafson 1994).

It is suggested that despite the role of XdhA in purine salvage, it does not participate in aerobic purine catabolism, which is somewhat in agreement with a biofilm context. The reactions conducted by XDH are a way of replenishing GMP and GTP, being an enzyme that stimulates its synthesis while distancing itself from AMP synthesis (Xi, Schneider, and Reitzer 2000).

One of the repressors of *xdhABC* operon is XdhR. Both GTP and the alarmone (p)ppGpp dissociate binding of this activator to its binding site on the intergenic region of *xdhR* and *xdhABC*. It is suggested that during exponential phase, partial derepression by GTP allows base levels of *xdhABC* expression, while in stationary phase there is an increase in production of (p)ppGpp, at the cost of GTP, which greatly counters XdhR action, thus promoting purine salvage pathways and re-establishing and maintaining GTP homeostasis and continued (p)ppGpp synthesis. This heightened expression of (p)ppGpp is also associated to the stringent response since its synthesis can occur as a result of amino acid, carbon, fatty acid, phosphate and iron limitation (Sivapragasam and Grove 2016). Furthermore, the alarmone is known to regulate certain genes like sigma factors and proteins involved in stress responses (Haugen *et al.* 2008; Magnusson *et al.* 2005; Traxler *et al.* 2011).

Disruption of this gene can therefore destabilize the ratio of GTP/GMP, and as such, the concentration of c-di-GMP, since this is usually obtained by conversion of two molecules of GTP by diguanylate cyclases, and of (p)ppGpp, that requires GTP for its synthesis (Schmid *et al.* 2017). As such, it could be expected that intracellular concentration of c-di-GMP would be reduced, as it lacks one of its synthetic pathways, and since this secondary messenger is widely associated with biofilm formation, this could translate into significant phenotype alterations such as the ones that will be discussed further on. This is possibly further potentiated by the fact that the inability to recycle purines is allied with the minimal quantities of nitrogen in the SM medium used in this study, resulting in even greater nitrogen limitation and possibly enhancement of aggregation.

c-di-GMP dysregulation might be an important consequence of this mutation. As such, for the following discussed phenotypes it is important to state that in literature, phenotypic changes associated with c-di-GMP alterations have been proposed to be due to regulation of *cepI* transcription (Schmid *et al.* 2017), and thus, of AHL-mediated gene expression and associated QS systems and the effect they may have on biofilm production, pathogenicity and virulence, as previously reported. It is not known however if QS is a factor when it comes to biofilm formation in this strain.

Similarly, to what was discussed for mutant F27, this pathway, being important in providing components for DNA synthesis may impact eDNA production and by association, possibly, aggregate formation in this strain.

3.5 *In vitro* growth of selected mutants

Growth of each selected mutant was tested repeatedly to rule out possible effect of growth impairment caused by the mutation, with the different abilities to form planktonic cellular aggregates. This was performed in the richer medium, LB, which does not favor aggregation like the SM medium, and thus optical density readings correlated with cell density are more accurate. As such, both the mutants and wild-type strain were grown in the previously described conditions and their optical density monitored hourly for the first 8 hours, and then at 23 and 24 hours.

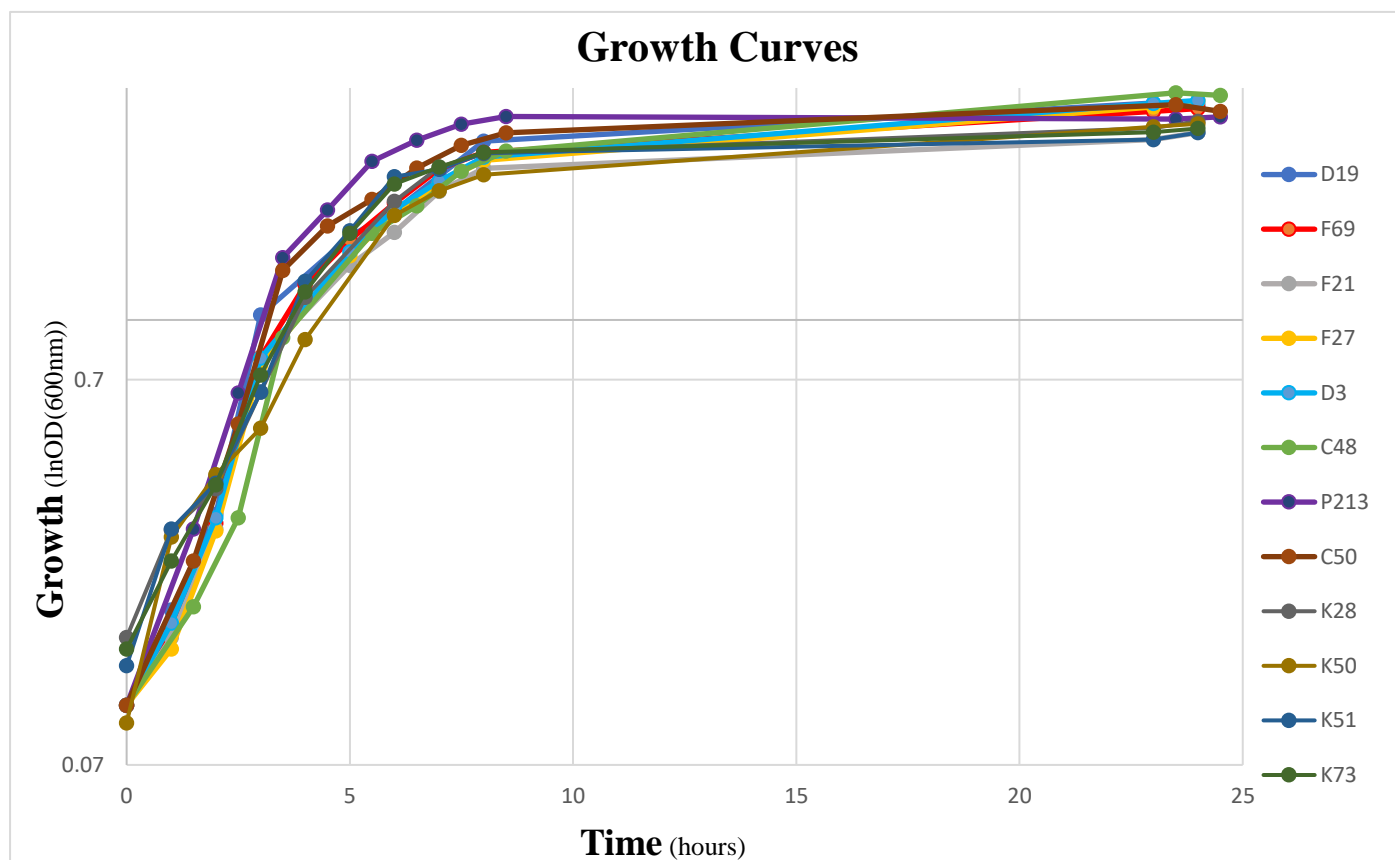


Figure 27 - Growth curves of the strains under study – Cultures were grown in LB medium at 37 °C, 250 rpm of orbital agitation, and OD_{640nm} was measured for 24 hours. Results are the means of data from three independent experiments.

By comparing with the wild-type, as seen in Figure 27, none of the mutants appears to have an evidently different growth than P0213-1, following roughly the same growth pattern. However, in Figure 28, where doubling times and growth rates are calculated, we can see that there are some significant differences in growth, namely in mutants F21, F27, D19, D3 and C48.

It would appear that for the remaining mutants the verified aggregation phenotype is not caused by differential growth, but rather with the function of the disrupted gene itself. Thus, under these conditions the disrupted genes affect planktonic cellular aggregation without affecting significantly the growth kinetics. Those significantly different might have mutations that directly affect the growth, or they may have inadvertently been subjected to slightly different conditions when the assay was underway. Therefore, it is possible that phenotypes observed were due to defective growth.

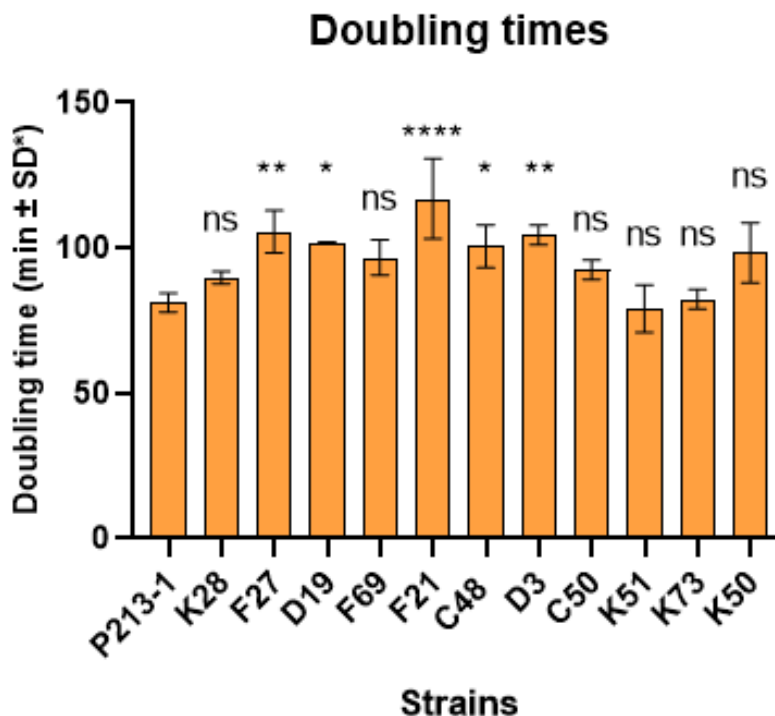


Figure 28 - Doubling time of the strains under study. Cultures were grown in LB medium at 37 °C, 180 rpm of orbital agitation and OD_{640nm} was measured for 24 hours. The doubling time was calculated from the growth rate of the exponential growth phase. Statistical difference in the doubling time of the mutant strains was tested in comparison with the wild-type strain. Significance level (one-way ANOVA followed by Dunnett's multiple comparison test): ns, not significant; *, P< 0.0332; **, P<0.0021; ****, P< 0.0001.

Despite part of the mutants not presenting significant differences in growth, some will be discussed.

K28 displayed only a slight, non-significant decrease in growth, comparing with the wild-type strain. It could be perhaps expected that destabilization of proper rRNA assembly derived from the lack of one of the copies of 23S rDNA would decrease the growth ability of the cell since protein translation is essential to vital cell functions, and that slight decrease may be what we see here. Furthermore, rRNA is proportional to growth rate, so should a defect happen in rRNA subunit assembly, it could potentially be reflected onto here. However, as stated before, this gene usually has several copies within the genome, with at least 5 found in the genome of wild-type strain. Therefore, the lack or mutation of one of the genes encoding 23S rRNA might not be enough to exert an influence on cell functioning. Similar values were obtained for a mutant of P0213-1 lacking the *rpsI* gene encoding the 30S ribosomal protein S9, involved in translation and possibly in ribosomal subunit assembly (Ferreira, 2018).

F27 mutant has a significantly slower growth than P0213-1. Reports state that in *P. aeruginosa* the independent deletion of either *pyrC* or *pyrC2*, previously mentioned, did not significantly affect growth since it is likely that the expression of one of the genes compensates for the other and that just one of them is sufficient to ensure a steady growth (Brichta *et al.* 2004). In the opportunistic fungal pathogen *Cryptococcus neoformans* a mutant strain unable to produce dihydroorotase of this pathway was shown to be unable to grow at physiological temperature of 37°C (Gontijo *et al.* 2014), this was similarly reported in the case of *Salmonella typhimurium* (Turnbough and Bochnert 1985), possibly due to accumulation of toxic intermediaries after hampering of conversion of N-carbamoyl-aspartate, as well

as *S. cerevisiae* (Yoshikawa *et al.* 2011), with reduced vegetative growth at 30°C. Opposite behavior was found in *Erwinia amylovora pyrC* mutant, which displayed a similar growth to wild-type, suggesting that its plant hosts, immature pear and apple, provide sufficient pyrimidines to support growth (Ramos *et al.* 2015).

Mutant D19 is also slightly slower in growth than the wild-type strain. It was found in *P. aeruginosa* that pyruvate fermentation alone does not sustain significant anerobic growth, expected in biofilms due to gradient formation derived from the structure itself, but it provides bacteria with the metabolic capacity for long-term survival (Eschbach *et al.* 2004), being somewhat in agreement with what is found here. Similar values for doubling time of a P0213-1 mutant lacking *ppsA*, were previously found (Ferreira, 2018).

C50 displays a not significant, yet slightly slower growth than P0213-1. As mentioned before, this mutation might have led to incorrect translational of specific mRNA required for cell division or uptake of specific nutrients needed for fitness.

K73 growth appear to be quite similar to P0213-1. According to the literature, in an *E. coli* mutant strain lacking the SUF system and IscX from the ISC system, showed no abrogation of growth, whereas deletion of any other gene of ISC system in the same genetic background resulted in severe growth defects (Tanaka *et al.* 2016). As such it appears that indeed IscX does not affect growth of bacteria, possibly because it is not essential for ISC system functioning, even when the other system is absent.

3.6 Quantification of planktonic cellular aggregation and free cells in selected mutants and overall biomass

Despite initial evaluation of cellular aggregation ability through microscopic and macroscopic observation during the screening of each mutant, quantification of each of these fractions and subsequent percentages had to be done to obtain significant data. As such, following the described methods, the dry weights of both aggregates and free cells were determined several times for each mutant. The results presented in Fig. 29 allow the creation of four categories of planktonic cellular aggregation ability (Table 4).

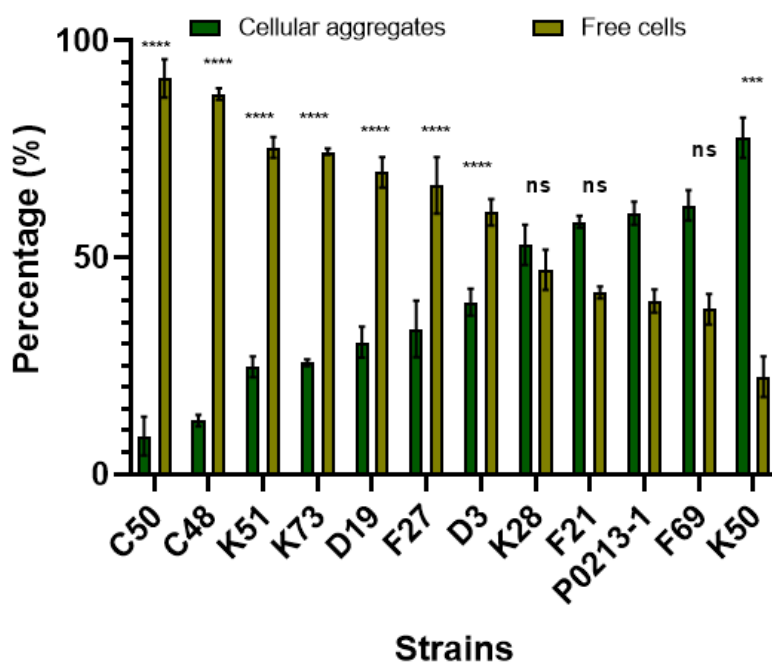


Figure 29 - Quantification of cellular aggregates and free cells of wild-type (P0213-2) and its derivative mutants. Error bars correspond to the standard deviations of the mean values of at least three independent assays. Significance level (one-way ANOVA followed by Dunnett's multiple comparison test) between cellular aggregates and free cells of the wild-type (P0213-1) and cellular aggregates and free cells of the P0213-1 derivative mutants was determined: ns, not significant; ***, $P < 0.0002$; ****, $P < 0.0001$;

Table 4 - Selected mutants were distributed into four groups. This grouping was based on the different percentage of planktonic cellular aggregates formed.

Percentage of planktonic cellular aggregates			
< 25%	> 25% and < 50%	> 50% and < 75%	> 75%
C50	D19	P0213-1	K50
C48	F27	F69	
K51	D3	F21	
	K73	K28	

According to these categories we can say that aggregation ability among mutants is highly variable. Although K50 confirms previous assessment of a very high ability to produce aggregates, some mutants fall within unexpected categories that oppose initial categorization by visual inspection. Such is the case for F69 and K28, which initially appeared to belong to a group that produced the least amount of aggregates, however they fall within the same category as the wild-type. Similar discrepancies are found in C50, C48 and K51, which during screening would appear to form more or more robust aggregates than F69 and K28, however this assay proves otherwise, belonging to those that have

the highest percentage of free cells. These differences may be due to initially unpredictable densities of the aggregates formed by each mutant, which despite being more visible, maybe due to their structure, turned out to possess a lesser quantity of cells.

To further assess aggregation ability and try to understand if discrepancies in aggregation were owed to differential overall biomass produced, this element was calculated.

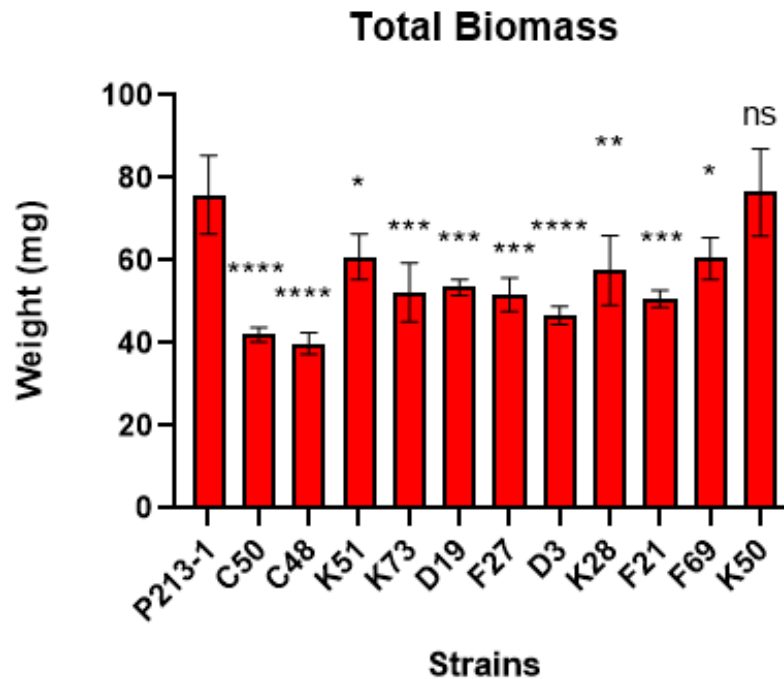


Figure 30 – Overall biomass production in 50 mL of SM medium of P0213-1 and its derivative mutants was determined by summing up the dry weights of both planktonic cellular aggregates and free cells of the quantification assay. Error bars correspond to the standard deviations of the mean values of at least three independent assays. Significance level (one-way ANOVA followed by Dunnett’s multiple comparison test) between cellular aggregates and free cells of the wild-type (P0213-1) and cellular aggregates and free cells of the P0213-1 derivative mutants was determined: ns, not significant; *, $P < 0.0332$; **, $P < 0.0021$; ***, $P < 0.0002$; ****, $P < 0.0001$

Indeed, according to Figure 30, all mutants except K50 produce significantly reduced overall biomass. However, this may explain why some of the initial visual inspections contradict quantification of the aggregates. Namely F69 and K28 which may appear at the naked eye like it has very little or few aggregates, but the proportion of aggregates to free cells is in reality similar to P0213-1. On the other hand, K51, C50 and C48 appear to produce larger aggregates but produced the least amount, also coincidental with being some of the least biomass producing mutants. It may be the in this case the observed aggregates, despite bigger, are less dense as initially thought and most of the cells are free in the medium.

Regarding F21, F27, D19, D3 and C48 specifically, they coincidentally correspond to mutants that not only produce small or less aggregates and overall biomass but were also the ones found to have a significant decrease in growth. This supports the hypothesis that the aggregation phenotype is due to an influence these mutations might have on growth.

As stated before, unlike initial assessment, K28 produces a similar quantity of aggregates to that of P0213-1, contradicting visual observation. This may be due to a production of very small aggregates in an overall similar quantity. It would seem that, like the previous hypothesis made, the mutation in one 23S rRNA encoding gene alone is not enough to alter cell functioning and thus biofilm formation. However, according to macroscopic images, it does appear to change either the size or structure. This link remains unknown.

Regarding mutant F27, it produces less aggregates than the wild-type strain. According to the literature, in *P. aeruginosa*, inhibition of the uracil biosynthetic pathway, dependent on pyrimidine production, has been demonstrated to repress biofilms, as well as all three QS pathways also involved in biofilm development, Rhl, Las and Pqs (Ueda *et al.* 2009). Such may be the case here, however a relationship between biofilm development and QS regulation is not yet established in the *Burkholderia multivorans* strain of this study.

The mutation found in mutant D19 was previously identified in similar experiments (Ferreira, 2018). Similar results were obtained for a *ppsA* mutant of this clinical isolate in that work. And like in this study, that mutant also fell within the category of >25% and <50% of planktonic cellular aggregates, being reproducible. As stated in that study, the disrupted gene, *ppsA*, is involved in central metabolism and its effect on aggregate formation is still not known due to the various associated pathways. It is possible that despite likely accumulation of pyruvate and its role in promoting microcolony formation, the lack of conversion of pyruvate to phosphoenolpyruvate leads to an adapted use of pyruvate for functions or pathways other than the ones that would promote biofilm formation. Also, considering the possible role in the PTS system, its functioning was shown to have a role on biofilm formation through regulation of eDNA and capsular polysaccharide production in *Klebsiella pneumoniae* (Hornig *et al.* 2017). Although the mechanisms are not clear, it appears that some components of this system, on which PEP may have an influence, enhance biofilm production and extracellular matrix when overexpressed, concomitant with higher amounts of eDNA and extracellular polysaccharides. This agrees with the results obtained, suggesting a possible role of eDNA in aggregate formation of this mutant.

As for mutant C48, it was one of those producing the least aggregates. Though transition to a sessile mode of growth and biofilm initiation is usually associated with the loss of motility, in this case it is possible that the lack of motility posed an obstacle for biofilm formation in that it prevented swimming of the cells towards each other and as such they are unable to overcome repulsive forces on their own, resulting in rather reduced aggregation. Therefore, the master regulator of flagella and motility appears to be necessary at least for initiation of biofilm formation, possibly losing motility during the maturation stage of biofilms.

Moreover, a study suggested that the location of mutations in *flhD* may have both positive and negative effects on motility, and reported that a mixture of cells with either type of mutation resulted in the most biofilm biomass in *E. coli* (Horne *et al.* 2016), leading to the hypothesis that motility heterogeneity in the community is what helps maintain biofilm biomass over extended periods of time, possibly by giving a degree of motility to the aggregate for nutrient scavenging, or continuous incorporation of free cells in the biofilm.

D3 produced significantly less cellular aggregates than the wild-type strain. SM medium somewhat emulates a stressful environment upon the bacteria, triggering adaptative behavior. As such, some oxidative stress may be implied. From the little that is known about this mutation, it may be a transcriptional regulator with a function similar to HexR

of *P. putida*, in which case it may be a regulator of glucose catabolism through sensing of oxidative stress (Deng *et al.* 2014). If that was the case, this would be a mutation that, according to reports, would be important for increasing NADPH production during under such conditions, and thus important to regulate redox status in addition to intracellular energy and tolerance to oxidative stress, which by not happening decreases the ability to form oxidative resistant aggregates (Kim and Park 2014).

C50 was perhaps the mutant that displayed the least amount of aggregates, a rather significant difference when compared to the control. Perhaps translation of a specific subset of mRNA required for biofilm formation was specifically affected by the impaired ability of translation of unmodified rRNA. Since the difference is so great, it may be that a great deal of biofilm inducers were affected, or perhaps a key player for that process. Another possibility is that lack of methylation of 23S rRNA may impair the ability of the cell to sense specific stressors, thus not adapting as effectively to the environment. To support this, a study has already reported that the lack of a gene not responsible for a modification, but rather for the biosynthesis of an already modified nucleotide, led to alteration of numerous bacterial properties, among them stress response, morphology, growth, antibiotic susceptibility and virulence (Shippy and Fadl 2015), all of which are associated with transition to a sessile mode of growth.

Mutant K50 was able to produce the highest amount of aggregates and concomitant lowest number of free cells, surpassing even P0213-1. This was also verified in the work of Ferreira (2018).

Although it depends on selenium, it was found that this enzyme in *Enterococcus faecalis* triggers biofilm proliferation through oxidant production (Srivastava *et al.* 2011). Furthermore, a predicted hydroxylase that increases during transition to biofilm growth was found to be stimulated in the presence of uric acid, selenium and molybdenum, parallel to an increase of *xdhA* transcription, suggesting that purine catabolic pathway stimulated biofilm production. In fact, as stated before, destabilization of c-di-GMP concentration may happen due to this mutation. This key factor is known to control transition between motile and sessile lifestyles, with high levels of it indicating biofilm mode of growth. However, this goes against the hypothesis previously made, that this mutation results in a decrease of c-di-GMP. Yet, the aggregate it produces is the most prominent of all test subjects. To support this hypothesis, reports have high concentrations of c-di-GMP resulting in reduced biofilm formation (Schmid *et al.* 2017), indicative that a low concentration might induce it, as observed for mutant K50. Furthermore, the suppression of *de novo* pyrimidine synthesis would also be expected to result in a decrease in (p)ppGpp formation, reducing positive regulation it has on RpoS, whose *rpoS* mutant in *P. aeruginosa* was shown to produce thicker biofilm structures (Shirtliff *et al.* 2002). Therefore, it may be that despite association of biofilm formation with high intracellular c-di-GMP, the opposite cannot be disregarded. As such mutant K50 appears to suggest that c-di-GMP has a role on biofilm formation. Were that the case, being a molecule used for the expression of numerous genes, and thus numerous pathways, and faced with these results and those previously reported, it becomes difficult to assign it a specific role on this phenotype. Viable scenarios are that it may have a strain specific effect on this phenotype or that it is under such strict regulation that slight condition changes in the environment might direct it to other genes than those initially expected in an attempt to increase survivability.

3.7 Surface-attached biofilm formation

Other than planktonic cellular aggregation alone, the disrupted genes of each mutant may influence other phenotypes that directly or indirectly affect or are affected by the aforementioned ability. Thus, several other phenotypes were tested for each mutant, as is the case in the production of surface-attached biofilm formation. This one is a somewhat relevant phenotype to test since surface-attached biofilms may share some of the same production mechanisms as planktonic cellular aggregates. Their production was assessed as described, through incubation for the same amount of time as the planktonic cellular aggregation assessment, after which, staining with crystal violet and measurement of absorbance at 590 nm allowed quantification of the structures at play. Results are shown in Figure 31 below.

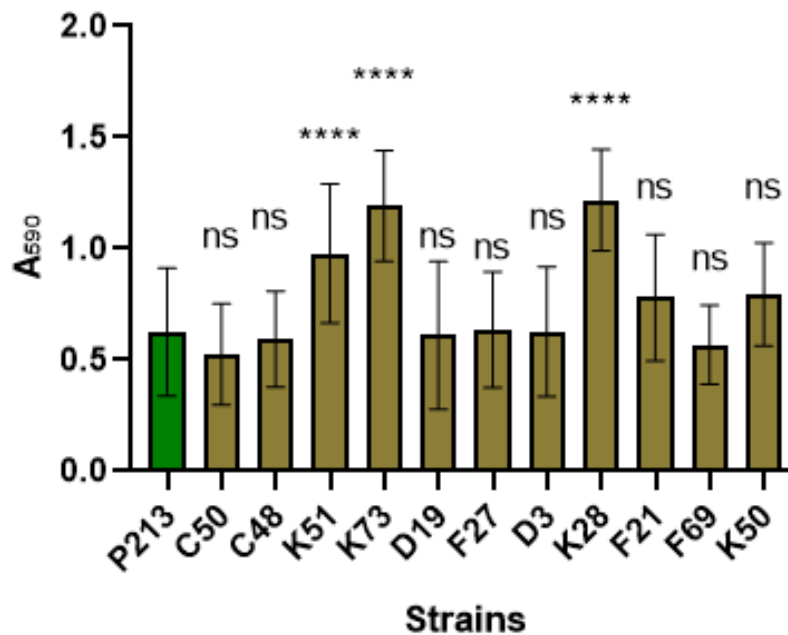


Figure 31 - Surface-attached biofilm formation of the P0213-1 and its derivative mutants was determined by absorbance measurement at 590 nm after growth for 48 hours at 37 °C in polystyrene microplates. Error bars correspond to the standard deviations of the mean values of at least fifteen replicas of two independent experiments. Significance level (one-way ANOVA followed by Dunnett's multiple comparison test) between the wild-type (P0213-1) the mutants was determined: ns, not significant; ****, $P < 0.0001$.

Of all tested mutants only K28, K51 and K73 displayed a significant difference when compared to P0213-1, in this instance, an increase. K28 produces the most amount of surface-attached biofilm, with a significant increase. It is possible that despite being only one copy of the gene, mutation in 23S rDNA may influence the adherence ability of the bacteria once in a biofilm mode of growth. However, this property in itself was not assessed for this mutant. When it comes to K51 and K73, despite producing significantly more surface-attached biofilms, they correspond to two of the mutants that produce the least amount of aggregates. In the literature, as previously stated, similar opposite cases of phenotypical display were reported, supporting the fact that despite the general consensus that the formation planktonic cellular aggregates and surface-attached biofilms share similar mechanisms, they aren't necessarily correlated within the same strain. Indeed, cell aggregation has already been reported in bacteria with biofilm inhibiting mutations (Staudinger *et al.* 2014).

3.8 Swimming and swarming motilities

Motility is yet another important phenotype to test since it may be a requirement for cellular aggregation, either by overcoming repulsive forces between cells or by having its expression and appendages regulated according to the surrounding environments, allowing cell approximation and contact or the search for more favorable conditions.

Both swimming and swarming motilities were tested in selected mutants by using appropriate plates and proceeding as described. The measured diameters that take the inoculation spot as the center and their subsequent comparison with wild-type permitted to draw a conclusion on if motility of each type was altered by the disruption of each respective gene.

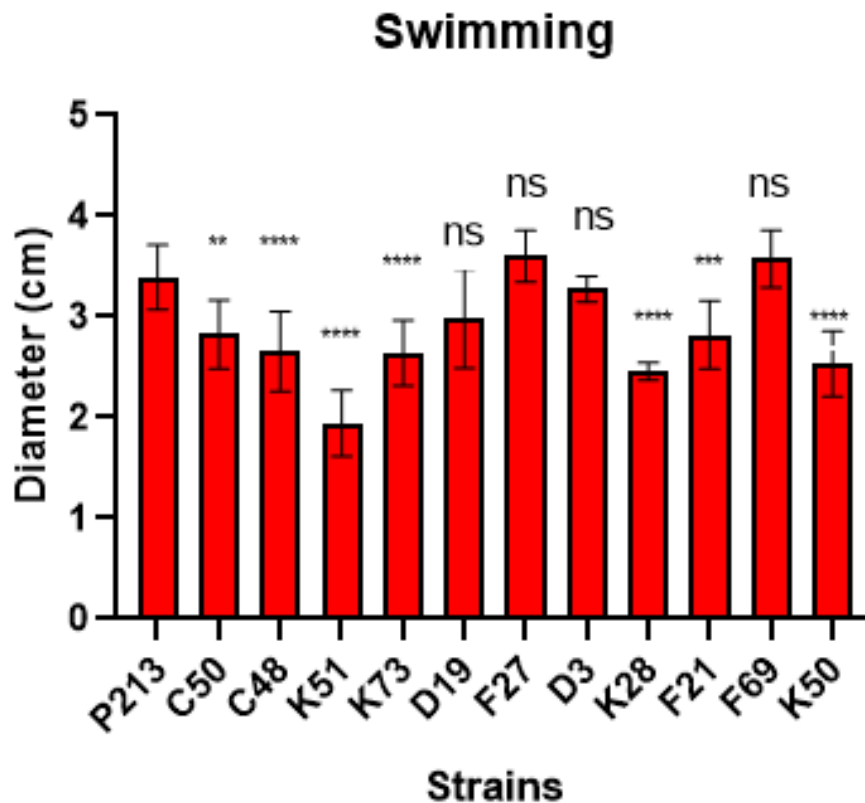


Figure 32 - Swimming ability of the P0213-1 and its derivative plasmid mutants was measured as the motility zone diameter after growth for 24 hours at 37 °C. Error bars correspond to the standard deviations of the mean values of at least 4 replicas of three independent assays. Significance level (one-way ANOVA followed by Dunnett's multiple comparison test) between cellular aggregates and free cells of the wild-type (P0213-1) and cellular aggregates and free cells of the P0213-1 derivative mutants was determined: ns, not significant; **, $P < 0.0021$; ***, $P < 0.0002$; ****, $P < 0.0001$

As seen in Figure 32, only D19, F27, F69 and D3 don't have a significant difference comparing to the wild-type strain. Of these, solely D19 appears to have a greater decrease. And of all mutants, F27 and F69 present an increase, however slight. All remaining mutants present a statistically significant decrease of swimming ability, namely C48, K73, K50, K28, and K51 as the one with the greatest decrease.

As for swarming motility (Fig. 33), despite variations of decrease and increase, F69, D3, K50 and K51 were not significantly different than P0213-1. Other than that, D19, F7, C50, F21 and C48, all present significant decrease in this motility, while K73 and K28 present a somewhat significant increase.

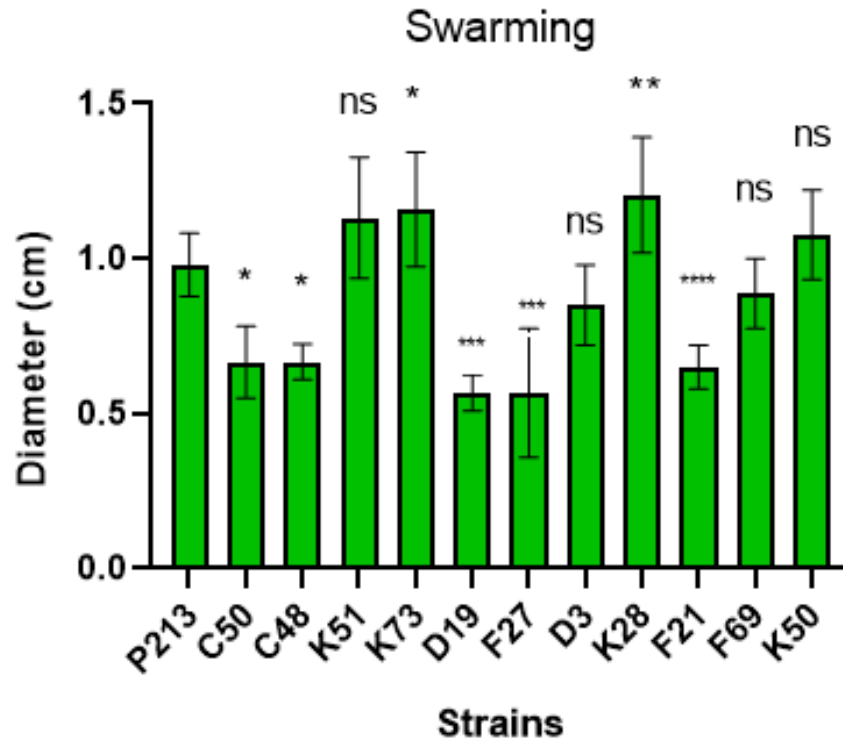


Figure 33 - Swarming motility of the P0213-1 and its derivative strains to antibiotics was measured as the motility zone diameter after growth for 24 hours at 37 °C. Error bars correspond to the standard deviations of the mean values of at least 4 replicas of three independent assays. Significance level (one-way ANOVA followed by Dunnett's multiple comparison test) between cellular aggregates and free cells of the wild-type (P0213-1) and cellular aggregates and free cells of the P0213-1 derivative mutants was determined: ns; not significant; *, $P < 0.0332$; **, $P < 0.0021$; ***, $P < 0.0002$.

In mutant K28 there was a significant decrease in the swimming ability. This is in agreement with the higher ability of this mutant to produce surface-attached biofilms, which usually implicates the loss of motility. The swarming, however, displayed a significant increase. It may be that the mutation may directly influence regulation of this type of motility or interfere with the production of a surfactant, usually required for swarming. Furthermore, since swarming motility pertains to a type of motility requiring a surface, it does not clash with the higher production of surface-attached biofilms and similar aggregation to that of the wild-type. Besides, as previously stated, production of components required for biofilm production and flagella and motility are not mutually exclusive (Rossi *et al.* 2018).

Mutant D19 displayed the same phenotype alterations, with similar values, in the same mutant of another work (Ferreira, 2018). The PTS system in which phosphoenolpyruvate takes part is also responsible for chemotaxis towards their substrates by modulating CheA autophosphorylation (Garrity *et al.* 1998). It may be that altered concentrations of phosphoenolpyruvate prevents decrease of CheA autophosphorylation, associated with a decrease in phosphoenolpyruvate concentration, hampering the movement of bacteria up the carbohydrate gradient. And this may translate into reduced swarming motility found here.

Regarding mutant F21, it had a significant decrease in swarming motility when compared to control. A reported mutant of *B. cenocepacia* lacking the monooxygenase also resulted in reduced swarming motility, likely due to inhibition of the *cepIR*, known to have an effect on motility capability (Pribytkova *et al.* 2014). Regarding swimming motility, a significant reduction was also verified. A *P. aeruginosa* PAO1 was subject to extracellular PAA, which in

this mutant might accumulate intracellularly, leading to reduced swimming motility through inhibition of QS, supporting the hypothesis that phenylacetate metabolism might impact motility through its effect on AHL-dependent factors (Syed *et al.* 2012).

C48 mutant presented reduced motility of both kinds. It seems therefore that the initial assumption that the plasposon meddled with expression of *flhD* gene rather than the GDP-mannose-dependent α -(1-2)-phosphatidylinositol encoding gene is the most likely. Being the subunit of flagellar master transcriptional regulator that directly alters downstream genetic expression, it has control over most of the genes involved in flagellar synthesis, its movement and to some extent, chemotaxis, influencing both swimming and swarming motility (Chevance *et al.* 2008; Claret and Hughes 2000; Eberl *et al.* 1996; Saini *et al.* 2008; Givaudan *et al.* 2000; Gjvskov *et al.* 1995; Ramos *et al.* 2004; Xu *et al.* 2014). So, naturally, alteration in its expression would be reflected on this phenotype, which in this case it appears to be reduced. Countless are the reports that state that loss or repression of the master regulator causes loss of motility or that overexpression increases it (Chatterjee *et al.* 2009; Fahrner and Berg 2015; Givaudan *et al.* 2000; Horne *et al.* 2016; Jozwick *et al.* 2017; Kurabayashi *et al.* 2016; Lai *et al.* 1997; Lehti *et al.* 2012; Mizushima *et al.* 1995; Singer *et al.* 2013; Xu *et al.* 2014). The phenotype observed is presumably a direct consequence of this mutation.

K50 shows a significant decrease in swimming motility, while differences in swarming motility were not significant. This appears to be in accordance with the ability of aggregation. Aggregates formed by K50 were so great that this mode of growth could potentially abolish motility to favor this mode of growth under stressful conditions. Besides, it was found in *B. cenocepacia* H111 that high intracellular c-di-GMP, associated with this gene, caused deficiency in swimming motility (Schmid *et al.* 2017). c-di-GMP, whose alteration might be implicated in this mutation, is known to influence motility in *P. aeruginosa* (Kim and Lee 2016).

3.9 Exopolysaccharide production in static media

Exopolysaccharide production has proven to be a required substance that bridges the formation of planktonic cellular aggregation in a few strains, promoting this mode of growth. Besides, it has been shown to influence other phenotypes like virulence and antimicrobial susceptibility, thus being a possibly interesting phenotype to assess.

To verify its production, all mutants were plated onto YEM agar plates and incubated for 48 hours at 37° C. By inspection at the naked eye, mucoid and non-mucoid traits could be attributed to each strain. All mutants were able to produce EPS, displaying a mucoid phenotype. Indeed, clinical isolates of *B. multivorans* frequently retain capacity for EPS production. These results (figures not shown) cannot delineate a clear relation between aggregate production and EPS production since the result is the same for the mutants producing large or small/few aggregates.

3.10 Antimicrobial susceptibility

Antibiotics may play an important role in the initial establishment of planktonic cellular aggregation, time at which they are likely the most effective. After the settlement of the bacteria however, one of the main traits of the formed structures is the resistance to a wide variety of these substances, either by mechanical limitation of access to antibiotics, a reduced metabolism or other innate biological disarmament mechanisms. Therefore, it is important to determine if any of the disrupted genes may have a role in how antibiotics are processed, as it may help identify a vulnerability in the iron-clad defense usually attributed to cellular aggregates.

Similarly, to motility assays, antimicrobial susceptibility was determined by measuring the diameter of the growth inhibition zone 24 hours after inoculation of the antibiotic, spotting of the mutant strain and incubation at 37 °C.

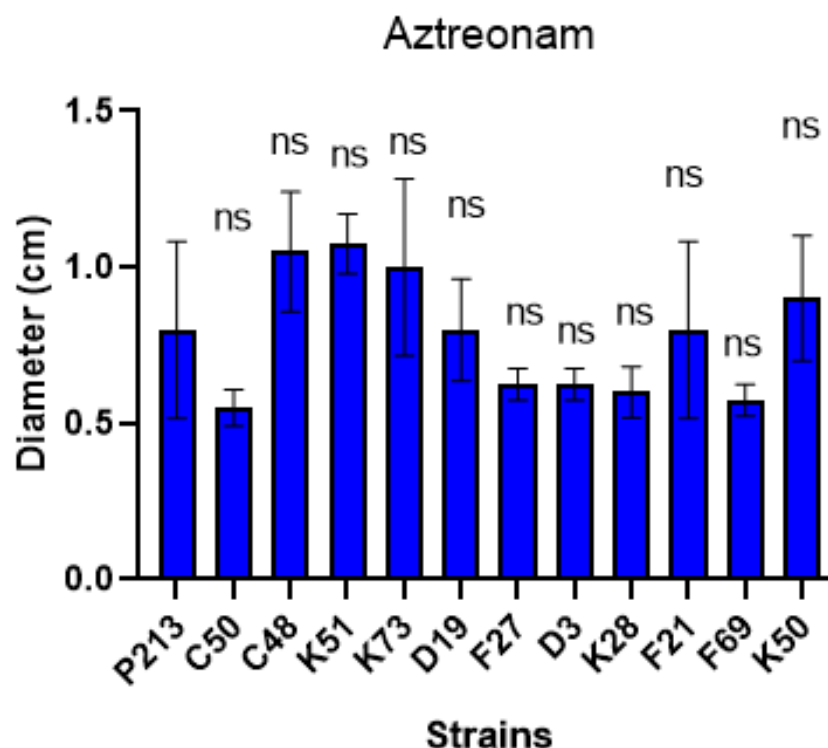


Figure 34 - Susceptibility of the P0213-1 and its derivative strains to aztreonam antibiotic was measured as the diameter of cell growth inhibition after growth for 24 hours at 37 °C. Error bars correspond to the standard deviation of the mean values of at least four replicas of 3 independent assays. Significance level (one-way ANOVA followed by Dunnett's multiple comparison test) between cellular aggregates and free cells of the wild-type (P0213-1) and cellular aggregates and free cells of the P0213-1 derivative mutants was determined: ns, not significant.

Regarding resistance to aztreonam (Fig. 34), no statistically significant differences with the wild-type strain were verified in any of the mutations. Disrupted genes appear to not have altered significantly the resistance to this antibiotic under these conditions.

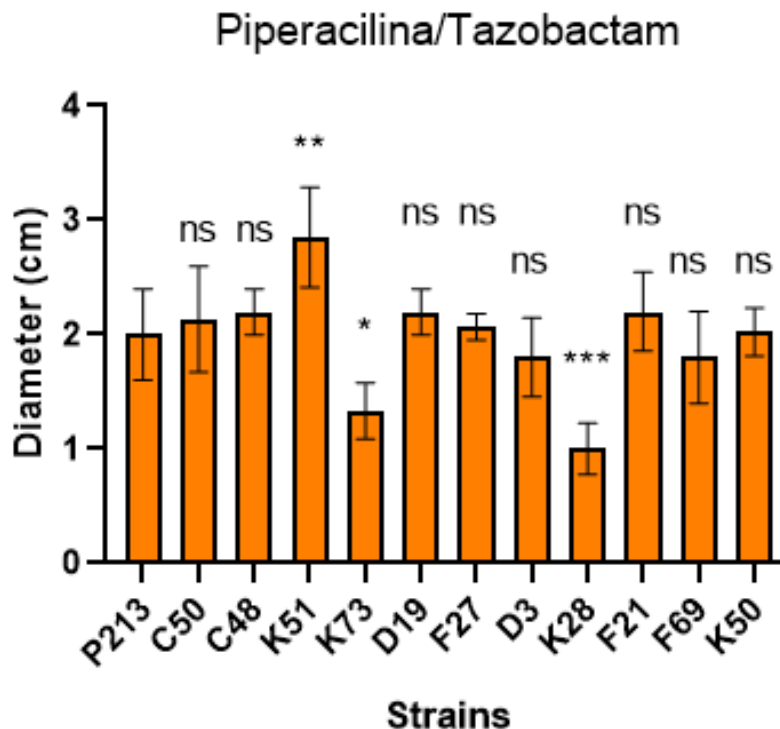


Figure 35 - Susceptibility of the P0213-1 and its derivative strains to piperacillin/tazobactam antibiotics was measured as the diameter of cell growth inhibition after growth for 24 hours at 37 °C. Error bars correspond to the standard deviation of the mean values of at least four replicas of 3 independent assays. Significance level (one-way ANOVA followed by Dunnett's multiple comparison test) between cellular aggregates and free cells of the wild-type (P0213-1) and cellular aggregates and free cells of the P0213-1 derivative mutants was determined: ns, not significant; *, $P < 0.0332$; **, $P < 0.0021$; ***, $P < 0.0002$.

As for piperacillin/tazobactam (Fig. 35), significant differences were only verified for K51, with an increase in susceptibility, and for K73 and K28, with a decrease in susceptibility.

In mutant K28, for aztreonam, no significant difference was observed, while for piperacillin/tazobactam the susceptibility to these antibiotics decreased. Regarding previous discussion of this mutation, an increase of resistance to the antibiotics could be expected, since it is through binding of the V domain of 23S rRNA that antibiotics usually act (Kannan and Mankin 2011; Marvig, Johansen, and Jelsbak 2012; Nissen *et al.* 2012; Yonezawa *et al.* 2013). Thus, a lack of this domain or alteration to its binding motif could decrease antimicrobial activity, as reported in several cases. That agrees with what is found here. As discussed earlier, this influence on antimicrobial resistance is usually associated to a mutation in more than one copy of the gene (Gomes *et al.* 2016), which does not happen here. It is possible that in this strain, disruption of one copy is enough to destabilize effective binding of antimicrobials and their activity under the tested conditions. Another possibility is that destabilization of 23S rRNA results in a defect of rRNA subunit assembly, which might affect specific mRNA transcripts essential for antimicrobial action. Despite this, V domain interaction with antibiotics usually regards macrolides, which were not the type of antibiotic used here.

For F27, there was no statistically significant difference in either antimicrobial susceptibility, only perhaps a slight decrease to the resistance to aztreonam. This may, however, be antibiotic specific. It is possible that the *de novo* pyrimidine pathway is required for the formation of structures or activation of pathways that metabolize antibiotics. It

has been suggested that nucleic acid synthesis pathways may present potential unexplored targets for intervention in treating infections, following the observation that *Cryptococcus neoformans* unable to express the dihydroorotase of this pathway, and subsequently to be deficient in uracil, led to a higher susceptibility to the antibiotic amphotericin B (Gontijo *et al.* 2014).

Although in C50 there was no significant difference in antimicrobial resistance, except for the slight reduction of resistance to aztreonam, it is quite possible that a disruption in the ability of proper translation of specific mRNAs might lead to a decreased resistance to antibiotics. Therefore, it might constitute a viable target to enhance action of antimicrobial upon the cells. Furthermore, it is generally accepted that lack of methylation in specific residues of the V domain of 23S rRNA, usually in more than one copy of the 23S rRNA (Gomes *et al.* 2016), results in inability of binding of macrolide antibiotics to the ribosome, and therefore rendered useless. Even though none of the antibiotics tested was a macrolide, the same may be happening here, yet at a very diminished degree, likely due to the mutation happening in only one of the copies.

3.11 Virulence

The establishment of planktonic cellular aggregates and their ability to circumvent several adversities imposed by the respiratory human tract grant them a certain status and degree of virulence, usually boosted or dwindled by their differential ability in the phenotypes such as the ones previously presented in this study. Thus, virulence was determined for some of the mutants and wild-type strain, using *Galleria mellonella* as the infection model. This organism is deemed appropriate since it possesses a similar innate immune system to that of mammals and it is therefore frequently used in the study of bacterial human pathogens, as is the case.

In this assay, each strain was injected in ten larvae, in triplicate. A harmless solution, also present in the bacterial concoction for this assay, was used as control. The survival of the larvae was monitored over a period of 72 hours since injection. Approximately 1×10^6 cells were injected per larvae.

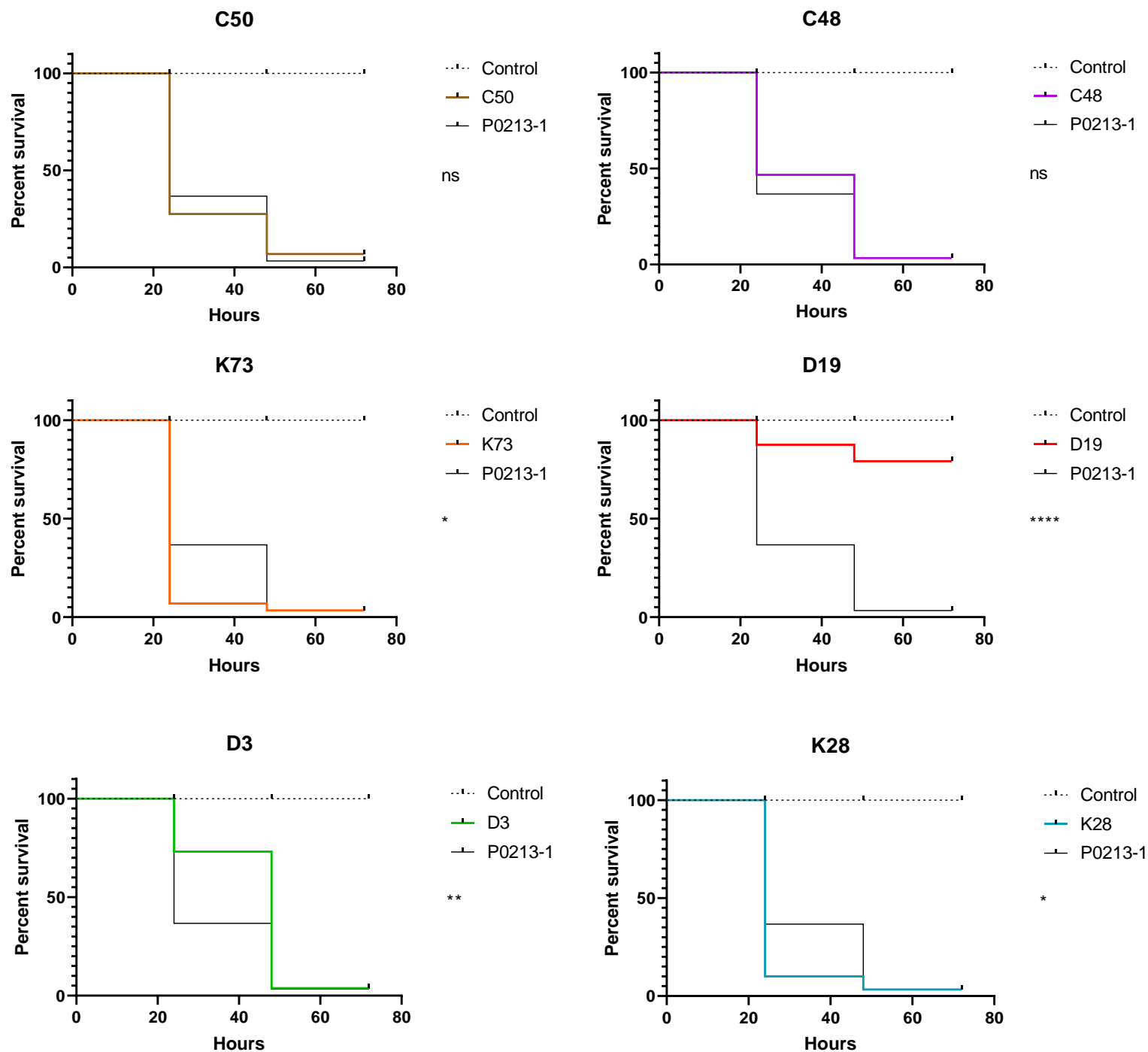


Figure 36 – Survival of *Galleria mellonella* larvae inoculated with *B. multivorans* (wild-type P0213-1 and the selected mutants). Triplicate groups of 10 larvae were inoculated with each isolate and survival was followed for three days post-infection. Larvae were injected with approximately 1×10^6 bacterial cells. The control experiment without bacteria is also represented. Statistical significance of differences between the Kaplan-Meier curve of the wild-type and its derivatives was determined: ns, not significant; *, $P < 0.0332$; **, $P < 0.0021$; ***, $P < 0.0002$; ****, $P < 0.0001$

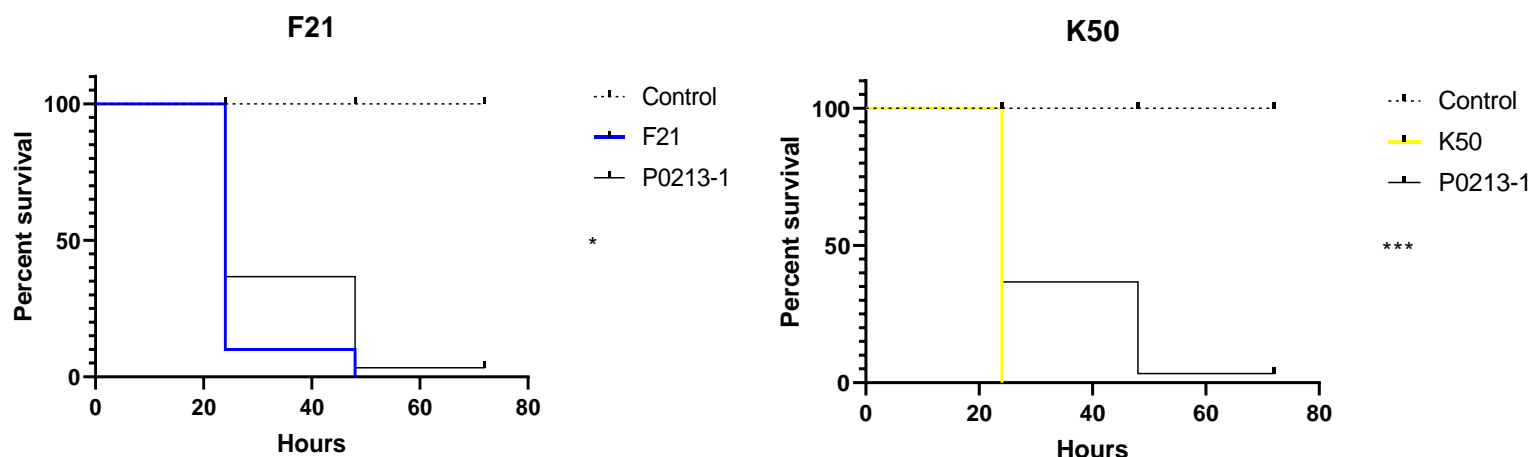


Figure 36 (continuation) - Survival of *Galleria mellonella* larvae inoculated with *B. multivorans* (wild-type P0213-1 and the selected mutants). Triplicate groups of 10 larvae were inoculated with each isolate and survival was followed for three days post-infection. Larvae were injected with approximately 1×10^6 bacterial cells. The control experiment without bacteria is also represented. Statistical significance of differences between the Kaplan-Meier curve of the wild-type and its derivatives was determined: ns, not significant; *, $P < 0.0332$; **, $P < 0.0021$; ***, $P < 0.0002$.

According to the curves on Figure 36, there was a very significant attenuation of virulence in the mutant D19. C48 and C50 presented a nearly identical phenotype to the wild-type strain. Although D3 is also very similar, considerably more larvae were still alive at 48 hours. K50 was the most virulent strain tested, killing everything at 24 hours. F21, K28 and K73 all presented a slight increase of virulence than the wild-type strain. Although K28 and K73 end up with the same alive larvae at the end of the assay as P0213-1, much more larvae are already dead at 48 hours. Mutants F27, F69 and K51 were not tested.

Regarding mutant D19, it displayed significant attenuation of virulence, the same as previously reported in a *ppsA* mutant of P0213-1 (Ferreira, 2018). In *Salmonella enterica* serovar *Typhimurium*, absence of *ppsA* was found to have no influence on virulence of the bacteria in BALB/c mice (Yimga *et al.* 2006), contradicting these results. On the other hand, disruption of this gene in *Xanthomonas campestris* pv. *Campestris* resulted in virulence reduction in its plant host, Chinese radish (Tang *et al.* 2005). As stated before, this mutation might influence the PTS system, one of whose transporters has been shown to be required for pathogenicity of *Borrelia burgdorferi* (Khajanchi *et al.* 2016). Thus, dysregulation of *ppsA* might result in abnormal phosphoenolpyruvate concentrations, which in turn affects the PTS system and the role its components might have on virulence. To further support this, in *Salmonella*, incomplete PTS caused downregulation of multiple virulence determinants like flagella genes, the *lsr* operon, pathogenicity islands and the PhoQ regulon (Lim *et al.* 2019). It was proposed by the authors that the LsrR regulator of quorum sensing could be a mediator between the PTS system and these virulence factors. An incomplete PTS system could reverse inactivation of LsrR by AI-2, which in turn could branch off to multiple regulatory circuits of the *lsr* operon, SPI-1 and the flagella cascade. According to these reports, the role of this gene on virulence is species specific or possibly it depends on the infection model used.

Concerning mutant F69, the TctD protein was shown to increase significantly in *Chlamydia pneumoniae* when they differentiated from elementary bodies, entering host epithelial cells, to metabolically active reticulate bodies able to establish chronic infections (Mukhopadhyay *et al.* 2006). In *Xanthomonas campestris* pv. *Vesicatoria*, the *citH* gene

is involved in early infection of tomato, and it is known to be positively regulated by TctDE, however, absence of this TCS did not sustain any effect on the virulence ability of the bacteria, retaining ambiguity for a possible virulence assay in this mutant (Tamir-ariel *et al.* 2011).

Mutant F21 presents increased virulence when compared to the wild-type strain. In *B. cenocepacia*, PAA degradation pathway was found to be necessary for full pathogenicity in *C. elegans* and rat infection models (Hunt *et al.* 2004; Law *et al.* 2008). More recently, in *B. cenocepacia*, *paaABCDE* mutants were found to result in accumulation of PAA-CoA, unlike the mutant of the pathway's previous step, *paaK* (Lightly *et al.* 2019). This compound's accumulation led to an avirulent phenotype in *C. elegans*, while its consume (*paaK*) maintained wild-type virulence. The same virulence phenotypes were verified when *cepIR* was also mutated in both. It would appear that PAA is not responsible for virulence attenuation since both *paaK* and *paaABCDE* mutants release high levels of PAA yet present these distinct phenotypes. This evidences a role of PAA-CoA in QS-regulated virulence. Presumably, and having reported that CepIR levels were not affected in wild type *paaABCDE* mutants, the authors suggest that when PAA-CoA accumulates, it forms a complex with an unidentified transcriptional regulator, XR, which in the presence of CepIR, will displace the complex CepR:C8-HSL, attenuating virulence. When CepIR is not present and PAA-CoA accumulates, the PAA-CoA:XR complex would have no CepR complex to displace, maintaining an avirulent phenotype, but when CepIR is absent and PAA-CoA levels are normal (as it would happen in a *paaK* mutant), XR would be free to bind virulence gene regulatory elements. This could be a relevant alternative pathway to accommodate to environmental conditions in a situation where QS signals do not accumulate but a virulent response is necessary. Despite this, an agreeable reduced virulence was not verified in mutant F21, contradicting what was reported in that work. It may be that in this strain this alternative pathway is not at play or that it may depend on the infection model. Coincidentally, PAA was proposed as an antagonist of pathogenic responses in *P. aeruginosa* and to be correlated with QS (Syed *et al.* 2012; Wang *et al.* 2013), known to be important for pathogenicity of Bcc in *C. elegans* and various virulence factors like adhesins, proteases, motility and biofilm production (Lewenza *et al.* 1999; Lewenza and Sokol 2001; Mulcahy and Lewenza 2011; Riedel *et al.* 2001; Uehlinger *et al.* 2009; Wopperer *et al.* 2006). Other studies reveal that accumulation of PAA and release onto the medium results in a chemoattractant for neutrophils, resulting in increased bacterial clearance (Bhuiyan *et al.* 2016).

Mutant C48 did not display significant changes relative to P0213-1. This is quite unexpected since motility is highly associated with virulence, being a staple for the establishment of bacterial communities within the host through chemotaxis, adhesion and invasion of host cells. Furthermore, it has been reported that certain virulence genes are under control of flagellar proteins, and therefore of FlhDC. FlhZ, for example, is a class II flagellar gene required for the activation of the *hila* gene in *S. enterica* (Lucas *et al.* 2000). FlhDC was also shown to control several virulence factors like lipolysis, extracellular hemolysis and virulence in the pathogen *Xenorhabdus nematophilus* (Givaudan *et al.* 2000) or extracellular phospholipase gene in *Serratia liquefaciens* (Gjvskov *et al.* 1995).

Other similar cases are found in the literature, in which downregulation or absence of *flhDC* results not only in the loss of motility but in decreased virulence (Givaudan *et al.* 2000; Jozwick *et al.* 2017; Stella *et al.* 2008; Teplitski *et al.* 2003; Xu *et al.* 2014). Namely, mutations abolishing flagellar motility negatively affected pathogenesis by *B. pseudomallei* and *B. cepacia* (Rossi *et al.* 2018). Despite this, opposite cases are also found, as is the case of an *flhD*

mutant of *Salmonella enteritidis*, which displayed much more invasiveness than the wild-type when administered orally to poultry (Parker and Guard-petter 2001). Yet, this is an example of hard comparison since it may produce these results due to the specific administration route or the specific immune system and the authors argue that suppression of class I regulators of flagellin biosynthesis may aid the oral infection in poultry.

The fact that virulence was not reduced, as initially expected, might be due to the absence of full motility, an energetically costly process, leading to energy savings which might be redirected towards other cellular processes like growth, which would favor infection. Besides, flagellin is a potent immune stimulator, therefore its reduction or inexistence might actually represent an advantage as it impairs recognition by the immune system of the host.

For mutant C50, virulence ability was very similar to that of wild-type strain. As previously mentioned, a study constructed an *S. aureus* mutant strain lacking a rRNA methyltransferase, KsgA, as well (Kyuma *et al.* 2015). This mutant was not only more sensitive to stresses but the viable cell number in macrophages, which subject bacteria to oxidative stress, appeared to decrease. Therefore, the role of methyltransferases in virulence cannot be disregarded.

K73 presented increased virulence when in comparison with wild-type strain at 24 hours, but the same at 48 hours. According to reports by Kalindamar *et al.* 2019, mutants of *Edwardsiella ictalurid* lacking the *iscX* gene showed attenuation of virulence, even allowing the successful development of a vaccine of these bacteria, which granted protection to fish immune system against wild-type.

Iron starvation and oxidative stress are detrimental for FeS enzyme biogenesis (Rincon-enriquez *et al.* 2008) and this is a recurring environment met by bacteria upon infection of the host. Although the specific role of IscX is undetermined in the ISC system (Adinolfi *et al.* 2018), iron-metabolizing systems are known to be required for virulence in *Erwinia chrysanthemi* at least. Under iron-limited conditions it seems, as is the case during infection, that the SUF system may take charge and thus ISC may become redundant on these occasions (Rincon-enriquez *et al.* 2008). According to Vergnes *et al.* 2017, regardless of the role of IscX, ISC machinery is required for HeLa cell invasion and virulence in mice of *Salmonella enterica*. In face of these results and reports, it may be that the ISC system, and possibly IscX, are required for invasion and initial establishment of the infection, upon which there is a transition to the SUF system, which will allow the bacterial community to develop within the host and form aggregates..

K50 is a mutant of notable results in this phenotype, it displays quite an enhancement in virulence, with all larvae dead at 24 hours. Comparing to previous assays on a mutant lacking *xdhA* (Ferreira, 2018), this is not reproducible, having resulted in attenuated virulence justified by possible defects in signaling pathways, owed to c-di-GMP and (p)ppGpp dysregulation, which could affect several cell traits like virulence. This mutation meddles with the purine catabolic pathway, and therefore with GMP, GTP and c-di-GMP concentration. Reports have shown that intracellular c-di-GMP determines the virulence of *B. cenocepacia* to *C. elegans* and *Galleria mellonella* (Schmid *et al.* 2017). In line with the proposition we made before, that disruption of this pathway may reduce intracellular c-di-GMP, Schmid *et al.* 2017 found that a high quantity of c-di-GMP attenuated virulence of *B. cenocepacia* in *G. mellonella* model, therefore, it is possible that the opposite is true, which would support the previous proposition and the idea that this pathway has a toll on pathogenicity. Inactivation of enzymes involved in (p)ppGpp metabolism have also shown to reduce the virulence of pathogenic species.

3.12 Adhesion

Although planktonic cellular aggregates don't require a surface to be established, cell-to-cell adhesion is one of the requirements for these structures to form, as well as to invade host cells. As stated before, similar modes of growth like clumping require cells to transiently interact by adhering to one another at their non-flagellated poles. The ability of P0213-1 and its mutant derivatives to adhere to mammalian cells was assessed (Fig. 37).

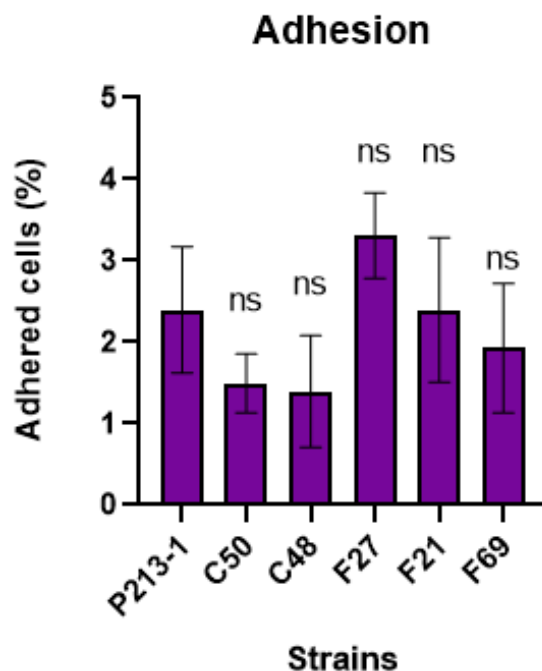


Figure 37 - Percentage of adherence of bacterial cells of each mutant to mammalian cells was determined by counting CFU and dividing adhered cells by total cells, after following described protocol. Error bars correspond to the standard deviations of the mean values of at least two independent assays. Significance level (one-way ANOVA followed by Dunnett's multiple comparison test) between cellular aggregates and free cells of the wild-type (P0213-1) and cellular aggregates and free cells of the P0213-1 derivative mutants was determined: ns, not significant.

Since no significant alterations to adhesion to animal cells were found, it appears that none of the mutations interferes with this ability, neither does it seem to be correlated with the planktonic cellular aggregation in this strain. Concurrently all strains tested here also displayed no significant alterations when it comes to the production of surface-attached biofilms, which could potentially depend on the ability to adhere. Furthermore, all of them maintained ability to produce exopolysaccharides, known in some species to be important for adhesion to surfaces, possibly also implicated in adhesion to host cells. Moreover, all of them displayed either no significant changes or an increase in motility, a phenotype shown in species to promote synthesis and functioning of motility appendages that enhance adherence of bacteria to surfaces and to each other, and once again, possibly to host cells. However, it should be noted that these results pertain to very few replicas, requiring more work to reach a more faithful conclusion.

In C48 there wasn't a significant difference when it comes to adhesion, despite appearing to have slightly reduced results. Under a general and superficial view, it would be expected that a mutation in the master regulator of the flagellar regulon would result in lesser motility, as it was proven, and thus would favor adhesion to surfaces where it would be favorable for bacteria to establish and develop. However, it might be that motility would positively regulate

expression of motility appendages required for initial adhesion, and thus the loss of the master regulator of motility would abolish that expression, and with it, reduce the capacity to overcome repulsive forces between cells and adhere. Even though that were true, neither a significant increase nor decrease in that ability was verified for this mutant, indicating that this mutation does not affect adhesion to these epithelial cells under the tested conditions.

3.13 Co-culturing of *Burkholderia* strains

Bacterial species co-exist very often in mixed communities, including in the infection environment within human hosts. The interactions between these co-localized bacteria may contribute to progressing changes of a bacterial community when it comes to its member composition, the evolution and severity of the infection, as well as mutational adaptations beyond those induced by the medium alone. Thus, it is important to study mixed cultures to develop treatment strategies that might take advantage of these intricate interactions. More frequently these studies focus on species of different genus. *Burkholderia* has been shown to form co-cultures in soil with fungal hyphae (Yang *et al.* 2017), with Gram-positive bacteria like *Bacillus amyloliquefaciens* (Boottanun *et al.* 2017), or other Gram-negative bacteria like *S. aureus* and *P. aeruginosa* (Riedel *et al.* 2001; Riedel and Reichl 2011; Rüger *et al.* 2014; Yoshida *et al.* 2009). Most of which, one way or another inflict proven alterations to certain phenotypes, such as differential growth, enhanced biofilm formation, antimicrobial susceptibility and cross communication through AHL production. However, not all mixed cultures are beneficial for the intervening species. Studies have demonstrated that the secondary metabolites of one player may kill the other (Boottanun *et al.* 2017), or that one species eventually dominates the other through more efficient substrate consumption (Rüger *et al.* 2014).

In this light, the aim of this section of the work was to try to visualize mixed cultures of different species of the *Burkholderia* genus, both previously known to be able to aggregate. And with this, test whether there was a differential ability of planktonic cellular aggregation derived from the existence of another growing species. This was done by expressing different fluorescent proteins in each of the strains and after growth for 48 hours in SM medium, observe the structures both macroscopically and microscopically. Out of all the tested pairs, the combination in which we focused, due to relatively better results, constituted of the clinical isolate *B. multivorans* P0213-1 expressing dsRed and *Burkholderia contaminans* IST 408 expressing GFP. These strains were previously co-cultured in solid medium as described to try to determine if each member of each pair would have a killing action upon the other. No such thing was apparent. The results are shown in Figure 38.

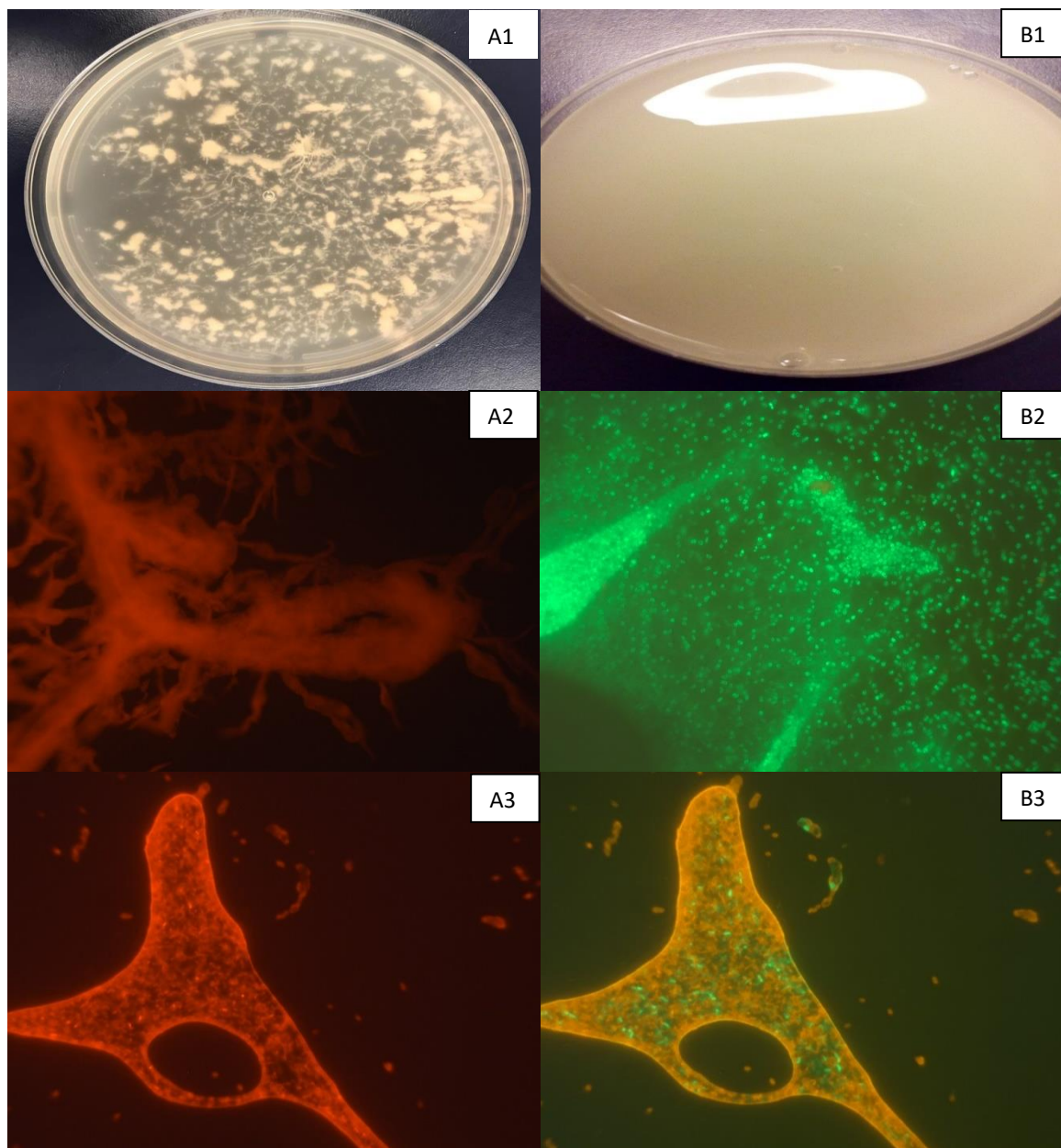


Figure 38 - Mixed and independent planktonic cellular aggregates of *B. multivorans* P0213-1 clinical isolate expressing dsRed and *B. contaminans* IST 408 expressing GFP. Both strains were grown either separately or together for 48 hours in SM medium at 37 °C, 180 rpm of orbital agitation and observed at the microscope. **A1** – P0213-1 in liquid culture on a petri dish. **B1** – *B. contaminans* IST 408 on liquid culture on a petri dish. **A2** – Microscopy image of P0213-1 expressing dsRed under appropriate fluorescence filter and a 10x magnification. **B2** – Microscopy image of *B. contaminans* IST 408 expressing GFP under appropriate fluorescence filter and a 100x magnification. **A3-A8** – Microscopy image of mixed biofilms of fluorescent strains of P0213-1 and *B. contaminans* IST 408 under appropriate filter for dsRed fluorescence and 10x magnification. **B3-B8** - Microscopy image of mixed biofilms of fluorescent strains of P0213-1 and *B. contaminans* IST 408 under appropriate filter for GFP fluorescence and 10x magnification.

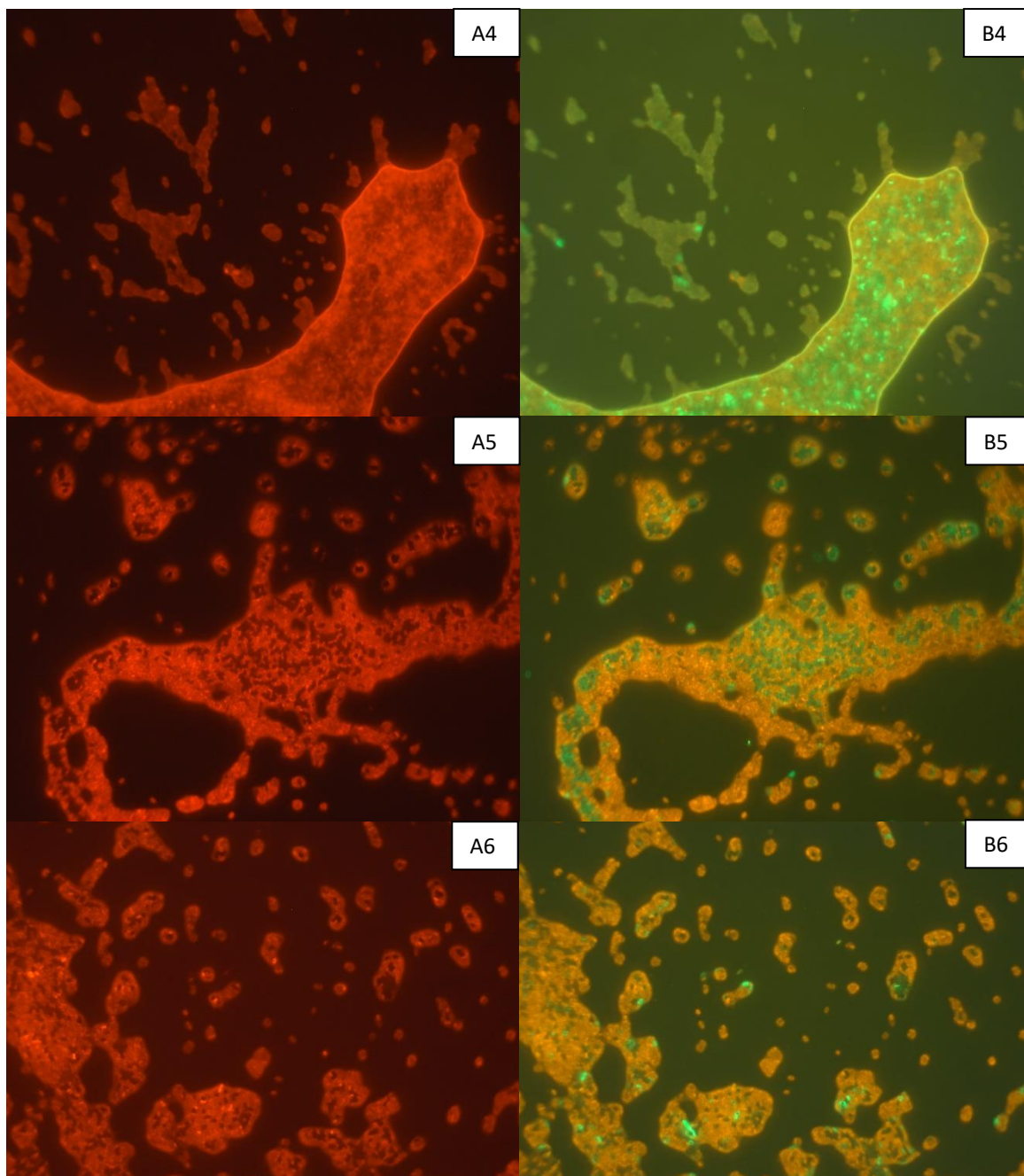


Figure 38 (continuation) – Mixed and independent planktonic cellular aggregates of *B. multivorans* P0213-1 clinical isolate expressing dsRed and *B. contaminans* IST 408 expressing GFP. Both strains were grown either separately or together for 48 hours in SM medium at 37 °C, 180 rpm of orbital agitation and observed at the microscope. **A1** – P0213-1 in liquid culture on a petri dish. **B1** – *B. contaminans* IST 408 on liquid culture on a petri dish. **A2** – Microscopy image of P0213-1 expressing dsRed under appropriate fluorescence filter and a 10x magnification. **B2** – Microscopy image of *B. contaminans* IST 408 expressing GFP under appropriate fluorescence filter and a 100x magnification. **A3-A8** – Microscopy image of mixed biofilms of fluorescent strains of P0213-1 and *B. contaminans* IST 408 under appropriate filter for dsRed fluorescence and 10x magnification. **B3-B8** - Microscopy image of mixed biofilms of fluorescent strains of P0213-1 and *B. contaminans* IST 408 under appropriate filter for GFP fluorescence and 10x magnification.

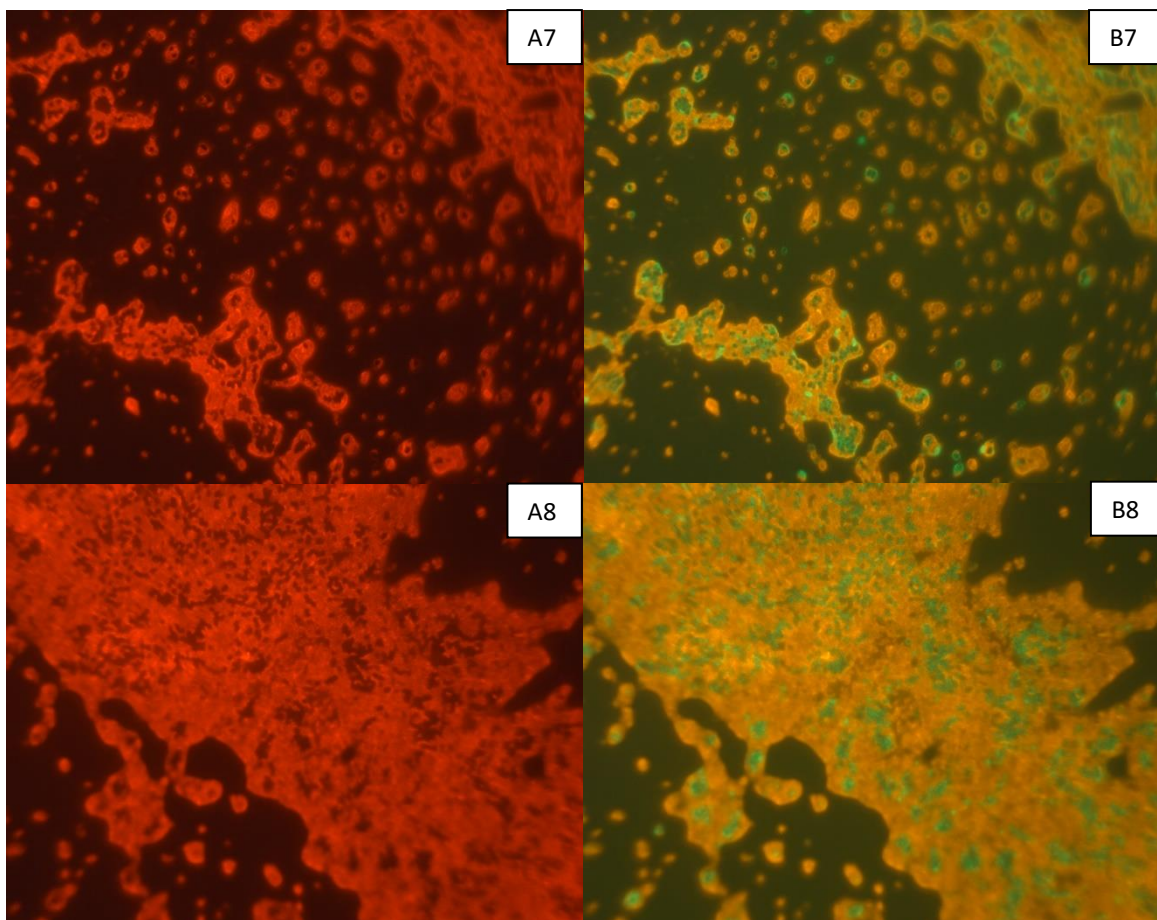


Figure 38 (continuation) – Mixed and independent planktonic cellular aggregates of *B. multivorans* P0213-1 clinical isolate expressing dsRed and *B. contaminans* IST 408 expressing GFP. Both strains were grown either separately or together for 48 hours in SM medium at 37 °C, 180 rpm of orbital agitation and observed at the microscope. **A1** – P0213-1 in liquid culture on a petri dish. **B1** – *B. contaminans* IST 408 on liquid culture on a petri dish. **A2** – Microscopy image of P0213-1 expressing dsRed under appropriate fluorescence filter and a 10x magnification. **B2** – Microscopy image of *B. contaminans* IST 408 expressing GFP under appropriate fluorescence filter and a 100x magnification. **A3-A8** – Microscopy image of mixed biofilms of fluorescent strains of P0213-1 and *B. contaminans* IST 408 under appropriate filter for dsRed fluorescence and 10x magnification. **B3-B8** – Microscopy image of mixed biofilms of fluorescent strains of P0213-1 and *B. contaminans* IST 408 under appropriate filter for GFP fluorescence and 10x magnification.

As it can be seen above (Fig. 38), the results were not quite clear. It would appear that microscopically P0213-1 dominated, possibly due to its distinctive ability of producing rather large aggregates, to a dimension to which *B. contaminans* IST408 could not achieve. It could also be that the growth rates of both species are different, thus promoting the dominance of one over the other, but specific growth assays would have to be made. Visualization of fluorescence was not certain at times, with the possibility of red regions being due to high background or the standard color produced by the matrix under the scope of the filter used, regardless of actually fluorescing or not.

Despite this, in some images it appears that both bacteria can form mixed aggregates, with the GFP expressing *B. contaminans* IST408 being predominantly enveloped by the dsRed expressing P0213-1. Even if this was confirmed, the structure of the aggregates, both at the naked eye and microscopically, does not seem to be maintained, lacking the

very branched and curly like structures of the wild-type of P0213-1, as well as the large clumps usually visible in the medium.

Although we cannot reach a conclusion regarding this topic, we determined that among the tested strains this pair appears to be the most promising one for further studies on co-cultured aggregates. Presuming that both species can indeed integrate the aggregates, it may be that this would have an effect on the capacity of the bacteria to adapt to the stressful media as the size and structure of the wild-type was not maintained. However, further tests like aggregate quantification would need to be performed to say this for sure. Other than that, there is a need to optimize the visualization of the fluorescence in aggregates, especially since the cells expressing it are easily trapped within the matrix of the aggregates' branches. Finally, different strains might have to be used. Either substitute *B. contaminans* IST408 with a better aggregating strain, comparable to that of P0213-1, or vice-versa. Using two aggregating strains with lesser ability than P0213-1 might even be the most viable solution so as to obtain less dense or rigid aggregates and facilitate visualization.

4. Conclusion and future perspectives

Despite similarities with biofilms and shared formation mechanisms in some strains, not much is known about planktonic cellular aggregation, much less in the CF affecting bacteria *Burkholderia multivorans* shadowed by the more prominent *Pseudomonas aeruginosa*. These are structures that occur not only in natural environments but also within hosts during infection, possibly being determinants in the establishment of chronic infections. Therefore, there are plenty of reasons to engage in studies dedicated to this bacterium in a CF disease context, understanding cellular behavior and seeking weaknesses that might lead to therapeutic targets.

The objective of this work was to identify genes that could possibly mediate *B. multivorans* P0213-1 aggregation, and consequently, with its ability to invade and establish infection within a host. Once identified, their mechanisms were explored, trying to find a reason how the genes affect this ability as well as other related phenotypes like motility, EPS production, antimicrobial resistance, virulence in *G. mellonella*, growth and adherence. As such, random mutants were obtained from the aggregative clinical isolate P0213-1, whose disrupted genes were posteriorly identified and studied, and their remaining phenotypes assayed, trying to further establish a relationship between them.

For many of the selected mutants, a direct link was not found. Results returned genes whose identity or function is rather general and therefore can have widespread repercussions that may or may not affect aggregation. Therefore, their specific role and mechanism towards formation of these structures remains rather ambiguous in this strain. Regardless they were identified as possible key players in this mode of growth and possible mechanisms discussed.

Confirming results of previous studies, it appears that ribosomal activity plays a key part in aggregation formation. Minding mutant C50 it is possible that abnormal ribosome composition, which may distort ability to synthesize proteins or contact exogenous substances, leads to reduced aggregation of the bacteria, possibly mediated by an interference with motility, also found to be reduced in this mutant, possibly by abnormal synthesis of chemotaxis or flagellar proteins. To complement this hypothesis, mutant C48, possibly affected in the motility master regulator, presented nearly identical phenotypes to C50. In this case the link with aggregation appears to be clear, with the formation of these structures requiring motility either initially for free cells to come together or/and after formation so as to provide a degree of mobility to the aggregates, that allows nutrient scavenging. Although mutant K28 also possibly involves the ribosomes, 23S rRNA subunit to be precise, it doesn't seem to interfere with the ratio of free cells to aggregates, but with the size of the aggregates and total biomass.

It would seem that carbon catabolism is also implicated in aggregate formation. If not for the quantity, then for the structure of the aggregates. D19 phosphoenolpyruvate is likely to be key in a pathway or specific component that may be a common factor between virulence and aggregation. Despite this, however, other mutations related to carbon catabolism, except for the possible D3, do not alter aggregation, perpetuating the mystery and complexity of central metabolism on this phenotype.

Pyrimidine synthesis identified in F27 and FeS cluster assembly identified in K73 also appear to be required for appropriate transition to planktonic cellular aggregation. However, this most likely pertains to general harmonized cell functioning rather than specific aggregation requirements since pyrimidines are essential for DNA and RNA integrity and proper cell signaling and iron-sulfur prosthetic group is required for correct functioning of the majority of enzymes. This is further supported by the fact that K73 displayed significant changes in all phenotypes, which would be expected,

in contrast to F27, as it most likely influences a much wider range of functions. However, both significantly reduced aggregation of bacteria.

Finally, intracellular messengers (p)ppGpp and c-di-GMP seem to be key in planktonic cellular aggregation, possibly due to their widespread function in sensing, activating and repressing enzyme activity, bridging intracellular and intercellular communication and response in tandem with environmental changes. It confirms several reports that implicate these molecules with an aggregation type of growth. The implication of these molecules is so dispersed that to better understand what and how it influences aggregation, following their concentration over time could be a hypothesis.

As it is, further studies are required to try to identify more genes and mechanisms that influence aggregation in *Burkholderia multivorans*. Since random mutagenesis does not seem to produce what are thought to be the most important mutants in regulating this phenotype, like quorum-sensing, ROS, exopolysaccharide production or virulence, perhaps a different approach would be to perform targeted mutagenesis on those genes and then assess the phenotypes. Furthermore, due to complexity of CF lung environment, these studies could be performed in the presence of other representative strains, more closely emulating stresses and interactions that might induce this mode of growth. Other techniques could also be employed, such as transcriptomic analysis, in order to identify active or dormant processes within the cell when comparing the wild-type with the mutants, or the wild-type under different conditions or time-points.

5. References

- Adinolfi, Salvatore, Rita Puglisi, Jason C. Crack, Clara Iannuzzi, Fabrizio Dal Piaz, Petr V Konarev, Dmitri I. Svergun, Stephen Martin, and Nick E. Le Brun. 2018. "The Molecular Bases of the Dual Regulation of Bacterial Iron Sulfur Cluster Biogenesis by CyaY and IscX." *Frontiers in Molecular Biosciences* 4:97
- Ahern, Kevin and Indira Rajagopal. n.d. "Pyrimidine de Novo Biosynthesis." Retrieved April 10, 2019 ([https://bio.libretexts.org/Bookshelves/Biochemistry/Book%3A_Biochemistry_Free_and_Easy_\(Ahern_and_Rajagopal\)/07%3A_Metabolism_II/7.10%3A_Pyrimidine_de_novo_Biosynthesis](https://bio.libretexts.org/Bookshelves/Biochemistry/Book%3A_Biochemistry_Free_and_Easy_(Ahern_and_Rajagopal)/07%3A_Metabolism_II/7.10%3A_Pyrimidine_de_novo_Biosynthesis)).
- Al-Bakri, A. G., P. Gilbert, and D. G. Allison. 2004. "Immigration and Emigration of *Burkholderia cepacia* and *Pseudomonas aeruginosa* between and within Mixed Biofilm Communities." *Journal of Applied Microbiology* 96(3):455–63.
- Alexandre, Gladys. 2015. "Chemotaxis Control of Transient Cell Aggregation." *Journal of Bacteriology* 197(20):3230–3237.
- Alhede, Morten, Kasper Nørskov Kragh, Klaus Qvortrup, Marie Allesen-Holm, Maria van Gennip, Louise D. Christensen, Peter Østrup Jensen, Anne K. Nielsen, Matt Parsek, Dan Wozniak, Søren Molin, Tim Tolker-Nielsen, Niels Høiby, Michael Givskov, and Thomas Bjarnsholt. 2011. "Phenotypes of Non-Attached *Pseudomonas aeruginosa* Aggregates Resemble Surface Attached Biofilm." *PLoS ONE* 6(11).
- Allesen-Holm, Marie, Kim Bundvig Barken, Liang Yang, Mikkel Klausen, Jeremy S. Webb, Staffan Kjelleberg, Søren Molin, Michael Givskov, and Tim Tolker-Nielsen. 2006. "A Characterization of DNA Release in *Pseudomonas aeruginosa* Cultures and Biofilms." *Molecular Microbiology* 59(4):1114–28.
- Altschul, Stephen F., Thomas L. Madden, Alejandro A. Schäffer, Jinghui Zhang, Zheng Zhang, Webb Miller, and David J. Lipman. 1997. "Gapped BLAST and PSI-BLAST: A New Generation of Protein Database Search Programs." *Nucleic Acids Research* 25(17):3389–3402.
- Amores, Gerardo Ruiz, Aitor De Heras, Ananda Sanches-medeiros, and Alistair Elfick. 2017. "Systematic Identification of Novel Regulatory Interactions Controlling Biofilm Formation in the Bacterium *Escherichia coli*." *Scientific Reports* 7(1):16768.
- Andersen, Niels Møller and Stephen Douthwaite. 2006. "YebU Is a m⁵C Methyltransferase Specific for 16 S rRNA Nucleotide 1407." *Journal of Molecular Biology* 777–86.
- Andrews, S. 2010. "FASTQC. A Quality Control Tool for High Throughput Sequence Data."
- Antunes, Ana, Giacomo Golfieri, Francesca Ferlicca, Marzia M. Giuliani, and Vincenzo Scarlato. 2016. "HexR Controls Glucose-Responsive Genes and Central Carbon Metabolism in *Neisseria meningitidis*." *Journal of Bacteriology* 198(4):644–54.
- Baldrige, Kevin C. and Lydia M. Contreras. 2014. "Functional Implications of Ribosomal RNA Methylation in Response to Environmental Stress Environmental Stress." *Critical Reviews in Biochemistry and Molecular Biology* 49(1):68–89.
- Bandyopadhyay, Sibali, Kala Chandramouli, and Michael K. Johnson. 2008. "Iron-Sulphur Cluster Biosynthesis." *Biochemical Society Transactions* 36(Pt 6):1112–19.
- Banin, Ehud, Michael L. Vasil, and E. Peter Greenberg. 2005. "Iron and *Pseudomonas aeruginosa* Biofilm Formation." *Proceedings of the National Academy of Sciences* 102(31):164.
- Barker, Clive S., Birgit M. Pru, and Philip Matsumura. 2004. "Increased Motility of *Escherichia coli* by Insertion Sequence Element Integration into the Regulatory Region of the FlhD Operon." *Journal of Bacteriology* 186(22):7529–37.
- Bateman, Alex et al. 2017. "UniProt: The Universal Protein Knowledgebase." *Nucleic Acids Research* 45(D1):D158–

- Bauer, A. W., Kirby W. M. M., J. C. Sherris, and M. Turck. 1966. "Antibiotic Susceptibility Testing By A Standardized Single Disk Method." *The American Journal of Clinical Pathology* 45(4):493–96.
- Bhuiyan, Saruar, Felix Ellett, Gerald L. Murray, Xenia Kostoulas, Gustavo M. Cerqueira, and Keith E. Schulze. 2016. "Acinetobacter baumannii Phenylacetic Acid Metabolism Influences Infection Outcome through a Direct Effect on Neutrophil Chemotaxis." *PNAS* 113(34):9599–604.
- Bible, Amber N., Gurusahai K. Khalsa-Moyers, Tanmoy Mukherjee, Calvin S. Green, Priyanka Mishra, Alicia Purcell, Anastasia Aksenova, Gregory B. Hurst, and Gladys Alexandre. 2015. "Metabolic Adaptations of *Azospirillum brasilense* to Oxygen Stress by Cell-to-Cell Clumping and Flocculation." *Applied and Environmental Microbiology* 33(7):503–10.
- Bible, Amber N., Bonnie B. Stephens, Davi R. Ortega, Zhihong Xie, and Gladys Alexandre. 2008. "Function of a Chemotaxis-like Signal Transduction Pathway in Modulating Motility, Cell Clumping, and Cell Length in the Alphaproteobacterium *Azospirillum brasilense*." *Journal of Bacteriology* 190(19):6365–75.
- Bible, Amber, Matthew H. Russell, and Gladys Alexandre. 2012. "The *Azospirillum brasilense* Che1 Chemotaxis Pathway Controls Swimming Velocity, Which Affects Transient Cell-to-Cell Clumping." *Journal of Bacteriology* 194(13):3343–55.
- Blanc, B., C. Gerez, and S. Ollagnier De Choudens. 2015. "Assembly of Fe/S Proteins in Bacterial Systems. Biochemistry of the Bacterial System." *BBA - Molecular Cell Research* 1853(6):1436–47.
- Boottanun, Patcharaporn, Chotima Potisap, Julian G. Hurdle, and Rasana W. Sermswan. 2017. "Secondary Metabolites from *Bacillus amyloliquefaciens* Isolated from Soil Can Kill *Burkholderia pseudomallei*." *AMB Express* 7:16.
- Bragonzi, Alessandra, Ilaria Farulla, Moira Paroni, Kate B. Twomey, Luisa Pirone, Irene Bianconi, Claudia Dalmastrì, Robert P. Ryan, and Annamaria Bevivino. 2012. "Modelling Co-Infection of the Cystic Fibrosis Lung by *Pseudomonas aeruginosa* and *Burkholderia cenocepacia* Reveals Influences on Biofilm Formation and Host Response." 7(12).
- Brambilla, Cecilia, Marta Llorens-Fons, Esther Julián, Estela Noguera-Ortega, Cristina Tomàs-Martínez, Miriam Pérez-Trujillo, Thomas F. Byrd, Fernando Alcaide, and Marina Luquin. 2016. "Mycobacteria Clumping Increase Their Capacity to Damage Macrophages." *Frontiers in Microbiology* 7:1562.
- Brichta, Dayna M., Kamran N. Azad, Pooja Ralli, and Gerard A. O'Donovan. 2004. "Pseudomonas aeruginosa Dihydroorotases: A Tale of Three PyrCs." *Archives of Microbiology* 182(1):7–17.
- Burakovsky, Dmitry E., Irina V Prokhorova, Petr V Sergiev, Pohl Milo, Olga V Sergeeva, Alexey A. Bogdanov, Marina V Rodnina, and Olga A. Dontsova. 2012. "Impact of Methylations of m²G966/m⁵C967 in 16S rRNA on Bacterial Fitness and Translation Initiation." *Nucleic Acids Research* 40(16):7885–95.
- Burdman, Saul, Edouard Jurkevitch, Boris Schwartzburd, Michal Hampel, and Yaacov Okon. 1998. "Aggregation in *Azospirillum brasilense*: Effects of Chemical and Physical Factors and Involvement of Extracellular Components." *Microbiology* 144(7):1989–99.
- Burrowes, Elizabeth, Abdelhamid Abbas, Aifric O. Neill, Claire Adams, and Fergal O. Gara. 2005. "Characterisation of the Regulatory RNA RsmB from *Pseudomonas aeruginosa* PAO1." *Research in Microbiology* 156(1):7–16.
- Butler, Sarah L., James W. Nelson, Ian R. Poxton, and John R. W. Govan. 1994. "Serum Sensitivity of *Burkholderia (Pseudomonas) cepacia* Isolates from Patients with Cystic Fibrosis." *FEMS Immunology and Medical Microbiology* 8(4):285–92.
- Caceres, Silvia M., Kenneth C. Malcolm, Jennifer L. Taylor-Cousar, David P. Nichols, Milene T. Saavedra, Donna L. Bratton, Samuel M. Moskowitz, Jane L. Burns, and Jerry A. Nick. 2014. "Enhanced in Vitro Formation and Antibiotic Resistance of Nonattached *Pseudomonas aeruginosa* Aggregates through Incorporation of Neutrophil Products." *Antimicrobial Agents and Chemotherapy* 58(11):6851–60.
- Cámara M., Williams P., Hardman A. 2002. "Controlling infection by tuning in and turning down the volume of

- bacterial small-talk." *The Lancet infectious Diseases* 2(11):667-76.
- Campos, Andrés and Philip Matsumura. 2001. "Extensive Alanine Scanning Reveals Protein-Protein and Protein-DNA Interaction Surfaces in the Global Regulator FlhD from *Escherichia coli*." *Molecular Microbiology* 39(3):581-94.
- Campos, Andrés, Rongguang Zhang, Randal W. Alkire, Philip Matsumura, and Edwin M. Westbrook. 2001. "Crystal Structure of the Global Regulator FlhD from *Escherichia coli* at 1.8 Å resolution." *Molecular Microbiology* 39(3):567-80.
- Castellani, Carlo and Baroukh M. Assael. 2016. "Cystic Fibrosis: A Clinical View." *Cellular and Molecular Life Sciences* 74(1):129-40.
- Chatterjee, Asita, Yaya Cui, and Arun K. Chatterjee. 2009. "RsmC of *Erwinia carotovora* Subsp . *Carotovora* Negatively Controls Motility , Extracellular Protein Production , and Virulence by Binding FlhD and Modulating Transcriptional Activity of the Master." *Journal of Bacteriology* 191(14):4582-93.
- Chevance, Fabienne F. V, Kelly T. Hughes, and Salt Lake City. 2008. "Coordinating Assembly of a Bacterial Macromolecular Machine." *Nature Reviews Microbiology* 6(6):455-65.
- Choe, Mangyu, Young-ha Park, Chang-ro Lee, Yeon-ran Kim, and Yeong-jae Seok. 2017. "The General PTS Component HPr Determines the Preference for Glucose over Mannitol." *Scientific Reports* 7:43431.
- Choi, Kang Yell and Howard Zalkin. 1990. "Regulation of *Escherichia coli* PyrC by the Purine Regulon Repressor Proteint." *Journal of Bacteriology* 172(6):3201-7.
- Chunduru, Jayendra and Thomas P. West. 2018. "Pyrimidine Nucleotide Synthesis in the Emerging Pathogen *Pseudomonas monteilii*." *Canadian Journal of Microbiology* 64(6):432-438.
- Claret, Laurent and Colin Hughes. 2000. "Functions of the Subunits in the FlhD(2)C(2) Transcriptional Master Regulator of Bacterial Flagellum Biogenesis and Swarming." *Journal of Molecular Biology* 303(4):467-78.
- Conrad, Jacinta C. 2012. "Physics of Bacterial Near-Surface Motility Using Flagella and Type IV Pili: Implications for Biofilm Formation." *Research in Microbiology* 163(9-10):619-29.
- Costerton, J. W., Philip S. Stewart, and E. P. Greenberg. 1999. "Bacterial Biofilms: A Common Cause of Persistent Infections." *Science* 284(5418):1318-22.
- Cunha, M. V. *et al* "Excpetionally high representation of *Burkholderia cepacia* among *B. cepacia* complex isolates recovered from the major Portuguese cystic fibrosis center." 2007. *Journal of Clinical Microbiology* **45**, 1628-1633.
- D'Argenio, David a D., David a D. Argenio, M. Worth Calfee, M. Worth Calfee, Paul B. Rainey, Paul B. Rainey, Everett C. Pesci, and Everett C. Pesci. 2002. "Autolysis and Autoaggregation in *Pseudomonas aeruginosa* Colony Morphology Mutants." *Journal of Bacteriology* 184(23):6481-89.
- Daddaoua, Abdelali, Tino Krell, and Juan-Luis Ramos. 2009. "Regulation of Glucose Metabolism in *Pseudomonas*: The Phosphorylative Branch and Entner-Doudoroff Enzymes Are Regulated by a Repressor Containing a Sugar Isomerase Domain." *The Journal of Biological Chemistry* 284(32):21360-68.
- Demirci, Hasan, Line H. G. Larsen, Trine Hansen, Anette Rasmussen, Ashwin Cadambi, Steven T. Gregory, Finn Kirpekar, and Gerwald Jogl. 2010. "Multi-Site-Specific 16S rRNA Methyltransferase RsmF from *Thermus thermophilus*." *RNA* 16(8):1584-96.
- Deng, Xin, Haihua Liang, Olesya A. Ulanovskaya, Quanjiang Ji, Tianhong Zhou, Fei Sun, Zhike Lu, and Alan L. Hutchison. 2014. "Steady-State Hydrogen Peroxide Induces Glycolysis in *Staphylococcus aureus* and *Pseudomonas aeruginosa*." *Journal of Bacteriology* 196(14):2499-2513.
- Denman, Carmen C. and Alan R. Brown. 2013. "Mannitol Promotes Adherence of an Outbreak Strain of *Burkholderia multivorans* via an Exopolysaccharide-Independent Mechanism That Is Associated with Upregulation of Newly Identified Fimbrial and Afimbrial Adhesins." *Microbiology* 159(4):771-81.

- Dennehy, Ruth, Maria Romano, Alessia Ruggiero, Simon L. Dignam, Cristóbal Mujica, Rita Berisio, Siobhán McClean, Máire Callaghan, and Miguel A. Valvano. 2016. "The *Burkholderia cenocepacia* Peptidoglycan - Associated Lipoprotein Is Involved in Epithelial Cell Attachment and Elicitation of Inflammation." *Cellular Microbiology* 19(5):1–16.
- Dennis, Jonathan J. and Gerben J. Zylstra. 1998. "Plasposons : Modular Self-Cloning Minitransposon Derivatives for Rapid Genetic Analysis of Gram-Negative Bacterial Genomes Plasposons : Modular Self-Cloning Minitransposon Derivatives for Rapid Genetic Analysis of Gram-Negative Bacterial Genomes." *Applied and Environmental Microbiology* 64(7):2710–15.
- Dienerowitz, Maria, Laura V. Cowan, Graham M. Gibson, Rebecca Hay, Miles J. Padgett, and Vernon R. Phoenix. 2014. "Optically Trapped Bacteria Pairs Reveal Discrete Motile Response to Control Aggregation upon Cell–Cell Approach." *Current Microbiology* 69(5):669–74.
- Diggle, S. P., Allen R.J., Gordon, V., Bjarnsholt T., Jensen, P., Irie, Y., Roberts A.E., Rodesney, C., Melaugh, G., Hutchison, J.B., Kragh, K.N. 2016. "Role of Multicellular Aggregates in Biofilm Formation." *mBio* 7(2):1–11.
- Drevinek, P. and E. Mahenthiralingam. 2010. "*Burkholderia cenocepacia* in Cystic Fibrosis: Epidemiology and Molecular Mechanisms of Virulence." *Clinical Microbiology and Infection* 16(7):821–30.
- Eberl, L. E. O., Gunna Christiansen, and Søren Molin. 1996. "Differentiation of *Serratia liquefaciens* into Swarm Cells Is Controlled by the Expression of the FlhD Master Operon." *Journal of Bacteriology* 178(2):554–59.
- Elborn, J. Stuart. 2016. "Cystic Fibrosis." *The Lancet* 59(6):438.
- Elizur, Arnon, Carolyn L. Cannon, and Thomas W. Ferkol. 2008. "Airway Inflammation in Cystic Fibrosis." *CHEST* 133(2):489–95.
- Eschbach, Martin, Kerstin Schreiber, Katharina Trunk, Jan Buer, Dieter Jahn, and Max Schobert. 2004. "Long-Term Anaerobic Survival of the Opportunistic Pathogen *Pseudomonas aeruginosa* via Pyruvate Fermentation." *Journal of Bacteriology* 186(14):4596–4604.
- Supreet Saini, Jonathon D. Brown, Phillip D. Aldridge, and Christopher V Rao. 2008. "FlhZ Is a Posttranslational Activator of FlhD(4)C(2)-Dependent Flagellar Gene Expression." *Journal of Bacteriology* 190(14):4979–88.
- Fabich, Andrew J., Mary P. Leatham, Joe E. Grissom, Graham Wiley, Hongshing Lai, Fares Najar, Bruce A. Roe, Paul S. Cohen, and Tyrrell Conway. 2011. "Genotype and Phenotypes of an Intestine-Adapted *Escherichia coli* K-12 Mutant Selected by Animal Passage for Superior Colonization □ †." *Infection and Immunity* 79(6):2430–39.
- Fahrner, Karen A. and Howard C. Berg. 2015. "Mutations That Stimulate FlhDC Expression in *Escherichia coli* K-12." *Journal of Bacteriology* 197(19):3087–96.
- Fairbanks, Lynette D., Margarita Bofill, Katarzyna Ruckemann, and H. Anne Simmonds. 1995. "Importance of Ribonucleotide Availability to Proliferating T-Lymphocytes from Healthy Humans." *The Journal of Biological Chemistry* 270(50):29682–89.
- Fazli, Mustafa, Henrik Almblad, Morten Levin Rybtke, Michael Givskov, Leo Eberl, and Tim Tolker-Nielsen. 2014. "Regulation of Biofilm Formation in *Pseudomonas* and *Burkholderia* Species." *Environmental Microbiology* 16(7):1961–81.
- Fazli, Mustafa, Morten Rybtke, Elisabeth Steiner, Elisabeth Weidel, Jens Berthelsen, Julie Groizeleau, Wu Bin, Boo Zhao Zhi, Zhang Yaming, Volkhard Kaefer, Michael Givskov, Rolf W. Hartmann, Leo Eberl, and Tim Tolker-Nielsen. 2017. "Regulation of *Burkholderia cenocepacia* Biofilm Formation by RpoN and the c-di-GMP Effector BerB." *MicrobiologyOpen* 6(4):1–13.
- Ferreira, Ana A., Inês I. Silva, Vítor V. Oliveira, Jörg J. Becker, Michael Givskov, Robert R. Ryan, Fábio Fernandes, and Leonilde M. Moreira. 2013. "Comparative Transcriptomic Analysis of the *Burkholderia cepacia* Tyrosine Kinase BceF Mutant Reveals a Role in Tolerance to Stress, Biofilm Formation, and Virulence." *Applied and Environmental Microbiology* 79(9):3009–20.
- Ferreira, Ana S., Jorge H. Leita, A. Sousa, Ana M. Cosme, and Leonilde M. Moreira. 2007. "Functional Analysis of

- Burkholderia cepacia* Genes BceD and BceF , Encoding a Phosphotyrosine Phosphatase and a Tyrosine Autokinase , Respectively : Role in Exopolysaccharide Biosynthesis and Biofilm Formation.” *Applied and Environmental Microbiology* 73(2):524–34.
- Ferreira, Ana S., Inês N. Silva, Fábio Fernandes, Ruth Pilkington, Máire Callaghan, and Siobhán Mcclean. 2015. “The Tyrosine Kinase BceF and the Phosphotyrosine Phosphatase BceD of *Burkholderia contaminans* Are Required for Efficient Invasion and Epithelial Disruption of a Cystic Fibrosis Lung Epithelial Cell Line.” *Infection and Immunity* 83(2):812–21.
- Ferreira, Ana S., Inês N. Silva, Vítor H. Oliveira, Raquel Cunha, and Leonilde M. Moreira. 2011. “Insights into the Role of Extracellular Polysaccharides in *Burkholderia* Adaptation to Different Environments.” *Frontiers in Cellular and Infection Microbiology* 1:16.
- Ferreira, Mirela. 2018. “Molecular Mechanisms of Planktonic Cellular Aggregation in *Burkholderia multivorans*.” Instituto Superior Técnico.
- Foster, Timothy J., Joan A. Geoghegan, Vannakambadi K. Ganesh, and Inflammatory Diseases. 2014. “Adhesion, Invasion and Evasion: The Many Functions of the Surface Proteins of *Staphylococcus aureus*.” *Nature Reviews Microbiology* 12(1):49–62.
- Foynes, Susan, Nick Dorrell, Stephen J. Ward, Richard A. Stabler, Andy A. McColm, Andrew N. Rycroft, and Brendan W. Wren. 2000. “*Helicobacter pylori* Possesses Two CheY Response Regulators and a Histidine Kinase Sensor, CheA, Which Are Essential for Chemotaxis and Colonization of the Gastric Mucosa.” *Infection and Immunity* 68(4):2016–23.
- Fung, Carina, Sharna Naughton, Lynne Turnbull, Pholawat Tingpej, Barbara Rose, Jonathan Arthur, Honghua Hu, Christopher Harmer, Colin Harbour, Daniel J. Hassett, Cynthia B. Whitchurch, and Jim Manos. 2010. “Gene Expression of *Pseudomonas aeruginosa* in a Mucin-Containing Synthetic Growth Medium Mimicking Cystic Fibrosis Lung Sputum Printed in Great Britain.” *Journal of Medical Microbiology* 59(Pt 9):1089–1100.
- Gambino, Michela and Francesca Cappitelli. 2016. “Mini-Review: Biofilm Responses to Oxidative Stress.” *Biofouling* 32(2):167–78.
- Garrity, Liam F., Stacey L. Schiel, Ronald Merrill, Jonathan Reizer, Milton H. Saier, and George W. Ordal. 1998. “Unique Regulation of Carbohydrate Chemotaxis in *Bacillus subtilis* by the Phosphoenolpyruvate-Dependent Phosphotransferase System and the Methyl-Accepting Chemotaxis Protein McpC.” 180(17):4475–80.
- Ghani, M. and J. S. Soothill. 1997. “Ceftazidime, Gentamicin, and Rifampicin, in Combination, Kill Biofilms of Mucoid *Pseudomonas aeruginosa*.” 43(11):999–1004.
- Givaudan, Alain, Anne Lanois, and Laboratoire De Pathologie Compare. 2000. “FlhDC , the Flagellar Master Operon of *Xenorhabdus nematophilus* : Requirement for Motility, Lipolysis, Extracellular Hemolysis, and Full Virulence in Insects.” *Journal of Bacteriology* 182(1):107–15.
- Gjyskov, Michael, Leo Eberl, Gunna Christiansen, Michael J. Benedl, and Soren Molin. 1995. “Induction of Phospholipase- and Flagellar Synthesis in *Serratia liquefaciens* Is Controlled Flagellar Master Operon FlhD.” *Molecular Microbiology* 15(3):445–54.
- Goltermann, Lise and Tim Tolker-Nielsen. 2017. “Importance of the Exopolysaccharide Matrix in Antimicrobial Tolerance of *Pseudomonas aeruginosa* Aggregates.” *Antimicrobial Agents and Chemotherapy* 61(4):1–7.
- Gomes, Cláudia, Sandra Martínez-puchol, Noemí Palma, Gertrudis Horna, Lidia Ruiz-roldán, Maria J. Pons, Joaquim Ruiz, Cláudia Gomes, Sandra Martínez-puchol, Noemí Palma, Gertrudis Horna, and Lidia Ruiz-rold. 2016. “Macrolide Resistance Mechanisms in *Enterobacteriaceae* : Focus on Azithromycin.” *Critical Reviews in Microbiology* 43(1):1-30.
- Gomes, Sara Caracol. 2018. “Genetic and Environmental Conditions Influencing Cellular Aggregates Formation in *Burkholderia multivorans*.” Instituto Superior Técnico.
- Goncz, Kaarin K., Luz Feeney, and Dieter C. Gruenert. 1999. “Differential Sensitivity of Normal and Cystic Fibrosis Airway Epithelial Cells to Epinephrine.” *British Journal of Pharmacology* 128(1):227–33.

- Gontijo, Fabiano Assis de, Renata C. Pascon, Larissa Fernandes, Joel Machado Jr^a, J. Andrew Alspaugh, and Marcelo A. Vallim. 2014. "The Role of the de Novo Pyrimidine Biosynthetic Pathway in *Cryptococcus neoformans* High Temperature Growth and Virulence." *Fungal Genetics and Biology* 70:12-23.
- Green, Rachel and Harry F. Noller. 1999. "Reconstitution of Functional 50S Ribosomes from in Vitro Transcripts of *Bacillus stearothermophilus* 23S rRNA." *Biochemistry* 38(6):1772–79.
- Grishin, Andrey M., Eunice Ajamian, Limei Tao, Mihnea Bostina, Linhua Zhang, Jean-francois Trempe, Robert Menard, Isabelle Rouiller, and Mirosław Cygler. 2013. "Family of Phenylacetyl-CoA Monooxygenases Differs in Subunit Organization from Other Monooxygenases." *Journal of Structural Biology* 184(2):147–54.
- Grishin, Andrey M., Eunice Ajamian, Linhua Zhang, and Mirosław Cygler. 2010. "Crystallization Communications Crystallization and Preliminary X-Ray Analysis of PaaAC , the Main Component of the Hydroxylase of the *Escherichia coli* Phenylacetyl-Coenzyme A Oxygenase Complex Crystallization Communications." *Acta Crystallographica Section F* 66(Pt 9):1045–49.
- Haaber, Jakob, Marianne Thorup Cohn, Dorte Frees, Thorbjørn Joest Andersen, and Hanne Ingmer. 2012. "Planktonic Aggregates of *Staphylococcus aureus* Protect against Common Antibiotics." *PLoS ONE* 7(7):1–12.
- Hager, Paul W., M. Worth Calfee, and Paul V Phibbs. 2000. "The *Pseudomonas aeruginosa* DevB / SOL Homolog , Pgl , Is a Member of the Hex Regulon and Encodes 6-Phosphogluconolactonase." *Journal of Bacteriology* 182(14):3934–41.
- Hamlin, Jason N. R., Ruhi A. M. Bloodworth, and Silvia T. Cardona. 2009. "Regulation of Phenylacetic Acid Degradation Genes of *Burkholderia*." *BMC Microbiology* 9:222.
- Hänchen, Anne, Saskia Rausch, Benjamin Landmann, Luigi Toti, and Antje Nusser. 2013. "Alanine Scan of the Peptide Antibiotic Feglymycin : Assessment of Amino Acid Side Chains Contributing to Antimicrobial Activity." *ChemBioChem* 14(5):625–32.
- Haugaard, L. E. and T. P. West. 2002. "Pyrimidine Biosynthesis in *Pseudomonas oleovorans*." *Journal of Applied Microbiology* (92):517–25.
- Haugen, Shanil P., Wilma Ross, and Richard L. Gourse. 2008. "Advances in Bacterial Promoter Recognition and Its Control by Factors That Do Not Bind DNA." *Nature Reviews Microbiology* 6(7):507–19.
- Hikida, Yasushi, Mitsuo Kuratani, Bessho Yoshitaka, Shun-ichi Sekine, and Shigeyuki Yokoyama. 2010. "Structure of an Archaeal Homologue of the Bacterial Fmu RsmB/RrmB rRNA Cytosine 5-Methyltransferase." *Acta Crystallographica Section D* 66(Pt 12):1301–7.
- Horne, Shelley M., Joseph Sayler, Nicholas Scarberry, Meredith Schroeder, Ty Lynnes, and Birgit M. Prüß. 2016. "Spontaneous Mutations in the FlhD Operon Generate Motility Heterogeneity in *Escherichia coli* Biofilm." *BMC Microbiology* 16(1):262.
- Horng, Yu-tze, Chi-jen Wang, Wen-ting Chung, Huei-jen Chao, Yih-yuan Chen, and Po-chi Soo. 2017. "Phosphoenolpyruvate Phosphotransferase System Components Positively Regulate *Klebsiella* Biofilm Formation." *Journal of Microbiology, Immunology and Infection* 51(2):174–83.
- Hunt, Tracey A., Cora Kooi, Pamela A. Sokol, and Miguel A. Valvano. 2004. "Identification of *Burkholderia cenocepacia* Genes Required for Bacterial Survival in Vivo." *Infection and Immunity* 72(7):4010–22.
- Imolorhe, Ijeme A. and Silvia T. Cardona. 2011. "3-Hydroxyphenylacetic Acid Induces the *Burkholderia cenocepacia* Phenylacetic Acid Degradation Pathway – toward Understanding the Contribution of Aromatic Catabolism to Pathogenesis." *Frontiers in Cellular and Infection Microbiology* 1:14.
- Inhülsen, Silja, Claudio Aguilar, Nadine Schmid, Angela Suppiger, Kathrin Riedel, and Leo Eberl. 2012. "Identification of Functions Linking Quorum Sensing with Biofilm Formation in *Burkholderia cenocepacia* H111." *MicrobiologyOpen* 1(2):225–42.
- Ivanov, Nikolai V, Manuela Trani, and Dale E. Edmondson. 2004. "High-Level Expression and Characterization of a Highly Functional *Comamonas acidovorans* Xanthine Dehydrogenase in *Pseudomonas aeruginosa*." *Protein*

- Jang, Soojin and James A. Imlay. 2010. “Hydrogen Peroxide Inactivates the *Escherichia coli* ISC Iron-Sulfur Assembly System, and OxyR Induces the Suf System to Compensate.” *Molecular Microbiology* 78(6):1448–67.
- Jayathilake, Pahala G., Saikat Jana, Steve Rushton, David Swailes, Ben Bridgens, Tom Curtis, and Jinju Chen. 2017. “Extracellular Polymeric Substance Production and Aggregated Bacteria Colonization Influence the Competition of Microbes in Biofilms.” *Frontiers in Microbiology* 8:1865.
- Jensen, Kaj Frank. 1979. “Apparent Involvement of Purines in the Control of Expression of *Salmonella typhimurium* *pyr* Genes : Analysis of a Leaky GuaB Mutant Resistant to Pyrimidine Analogs.” *Journal of Bacteriology* 138(3):731–38.
- Jensen, Kaj Frank. 1989. “Regulation of *Salmonella typhimurium pyr* Gene Expression : Effect of Changing Both Purine and Pyrimidine Nucleotide Pools.” *Journal of General Microbiology* (135):805–15.
- Jones, A. M., M. E. Dodd, J. R. W. Govan, V. Barcus, C. J. Doherty, J. Morris, and A. K. Webb. 2004. “*Burkholderia cenocepacia* and *Burkholderia multivorans*: Influence on Survival in Cystic Fibrosis.” *Thorax* 59(11):948–51.
- Joshi, N. A. and J. N. Fass. 2011. “Sickle: A Sliding-Window, Adaptive, Quality-Based Trimming Tool for FastQ Files (Version 1.33) [Software].”
- Jozwick, Anna K. Snyder, Joerg Graf, Timothy J. Welch, Cold Water Aquaculture, West Virginia, Cell Biology, and Cold Water Aquaculture. 2017. “The Flagellar Master Operon FlhDC Is a Pleiotropic Regulator Involved in Motility and Virulence of the Fish Pathogen *Yersinia ruckeri*.” *Journal of Applied Microbiology* 122(3), 578-588
- Kalindamar, Safak, Jingjun Lu, Hossam Abdelhamed, Hasan C. Tekedar, Mark L. Lawrence, and Attila Karsi. 2019. “Transposon Mutagenesis and Identification of Mutated Genes in Growth-Delayed *Edwardsiella ictaluri*.” *BMC Microbiology* 19(55).
- Kannan, Krishna and Alexander S. Mankin. 2011. “Macrolide Antibiotics in the Ribosome Exit Tunnel : Species-Specific Binding and Action.” *Annals of the New York Academy of Sciences* 1241:33–47.
- Karki, Hari Sharan, Inderjit Kaur Barphagha, and Jong Hyun Ham. 2012. “A Conserved Two-Component Regulatory System , PidS/PidR , Globally Regulates Pigmentation and Virulence-Related Phenotypes of *Burkholderia glumae*.” *Molecular Plant Pathology* 13(7):785–94.
- Kearse, Matthew, Richard Moir, Amy Wilson, Steven Stones-havas, Shane Sturrock, Simon Buxton, Alex Cooper, Sidney Markowitz, Chris Duran, Tobias Thierer, Bruce Ashton, Peter Meintjes, and Alexei Drummond. 2012. “Geneious Basic : An Integrated and Extendable Desktop Software Platform for the Organization and Analysis of Sequence Data.” *Bioinformatics* 28(12):1647–49.
- Kessler, Birgit, Victor de Lorenzo, and Kenneth N. Timmis. 1992. “A General System to Integrate LacZ Fusions into the Chromosomes of Gram-Negative Eubacteria: Regulation of the Pm Promoter of the TOL Plasmid Studied with All Controlling Elements in Monocopy.” *Molecular & General Genetics* 233(1–2):293–301.
- Khaitovich, Philipp, Tanel Tenson, Patricia Kloss, and Alexander S. Mankin. 1999. “Reconstitution of Functionally Active *Thermus aquaticus* Large Ribosomal Subunits with in Vitro-Transcribed rRNA.” *Biochemistry* 38(6):1780–88.
- Khajanchi, Bijay K., Evelyn Odeh, Lihui Gao, Mary B. Jacobs, Mario T. Philipp, and Tao Lin. 2016. “Modulate Gene Transcription and Virulence of *Borrelia burgdorferi*.” *Infection and Immunity* 84(3):754–64.
- Kim, Jin Hae, Jameson R. Bothe, Ronnie O. Frederick, Johnesa C. Holder, and John L. Markley. 2014. “Role of IscX in Iron – Sulfur Cluster Biogenesis in *Escherichia coli*.” *Journal of the American Chemical Society* 136(22):7933-42.
- Kim, Jisun and Woojun Park. 2014. “Oxidative Stress Response in *Pseudomonas putida*.” *Applied Microbiology and Biotechnology* 98(6):6933–46.

- Kim, Juhyun, Che Ok Jeon, and Woojun Park. 2008. "Dual Regulation of *zwf-1* by Both 2-Keto-3-Deoxy-6-Phosphogluconate and Oxidative Stress in *Pseudomonas putida*." *Microbiology* 154(Pt 12):3905–16.
- Kim, Juhyun, Jinki Yeom, Che Ok Jeon, and Woojun Park. 2009. "Intracellular 2-Keto-3-Deoxy-6-Phosphogluconate Is the Signal for Carbon Catabolite Repression of Phenylacetic Acid Metabolism in *Pseudomonas putida* KT2440." *Microbiology* 155(Pt 7):2420–28.
- Kim, Soo Kyoung and Joon Hee Lee. 2016. "Biofilm Dispersion in *Pseudomonas aeruginosa*." *Journal of Microbiology* 54(2):71–85.
- Ko, Thilo, Jean-luc Dumas, and Christian Van Delden. 2007. "Ribosome Protection Prevents Azithromycin-Mediated Quorum-Sensing Modulation and Stationary-Phase Killing of *Pseudomonas aeruginosa*." *Antimicrobial Agents and Chemotherapy* 51(12):4243–48.
- Krzyzosiak, W. and J. Ofengand. 1987. "In Vitro Synthesis of 16S Ribosomal RNA Containing Single Base Changes and Assembly into a Functional 30S Ribosome." *Biochemistry* 26(8):2353–64.
- Kurabayashi, Kumiko, Tomohiro Agata, Hirofumi Asano, and Haruyoshi Tomita. 2016. "Fur Represses Adhesion to, Invasion of, and Intracellular Bacterial Community Formation within Bladder Epithelial Cells and Motility in Uropathogenic *Escherichia coli*." *Infection and Immunity* 84(11):3220–31.
- Kyuma, Tatsuhiko, Hayato Kizaki, Hiroki Ryuno, Kazuhisa Sekimizu, and Chikara Kaito. 2015. "16S rRNA Methyltransferase KsgA Contributes to Oxidative Stress Resistance and Virulence in *Staphylococcus aureus*." *Biochimie* 119:166–74.
- Laganenka, Leanid, Remy Colin, and Victor Sourjik. 2016. "Chemotaxis towards Autoinducer 2 Mediates Autoaggregation in *Escherichia coli*." *Nature Communications* 7:12984.
- Lai, Hsin-chih, Jwu-ching Shu, Sunny Ang, Meng-jiun Lai, Birei Fruta, Shiming Lin, Kun-tay Lu, and Shen-wu Ho. 1997. "Effect of Glucose Concentration on Swimming Motility in Enterobacteria." *Biochemical and Biophysical Research Communications* 695(231):692–95.
- Lai, Sandra, Julien Tremblay, and Eric Déziel. 2009. "Swarming Motility: A Multicellular Behaviour Conferring Antimicrobial Resistance." *Environmental Microbiology* 11(1):126–36.
- Lam, J., R. Chan, K. Lam, and J. W. Costerton. 1980. "Production of Muroid Microcolonies by *Pseudomonas aeruginosa* within Infected Lungs in Cystic Fibrosis." *Infection and Immunity* 28(2):546–56.
- Larkin, Angelyn, Michelle Chang, Garrett Whitworth, and Barbara Imperiali. 2015. "Origins of Cystic Fibrosis Lung Disease." *The New England Journal of Medicine* 9(6):367–73.
- Law, Robyn J., Jason N. R. Hamlin, Aida Sivo, Stuart J. Mccorrister, Georgina A. Cardama, Silvia T. Cardona, and L. A. W. E. T. Al. 2008. "A Functional Phenylacetic Acid Catabolic Pathway Is Required for Full Pathogenicity of *Burkholderia cenocepacia* in the *Caenorhabditis elegans* Host Model." *Journal of Bacteriology* 190(21):7209–18.
- Leclarasamee, Amorn. 1998. "*Burkholderia pseudomallei*: The Unbeatable Foe?" *The Southeast Asian Journal of Tropical Medicine and Public Health* 29(2):410–15.
- Lehti, Timo A., Philippe Bauchart, Ulrich Dobrindt, Timo K. Korhonen, Benita Westerlund-wikstro, and Benita Westerlund-wikstro. 2012. "The Fimbriae Activator MatA Switches off Motility in *Escherichia coli* by Repression of the Flagellar Master Operon FlhDC." *Microbiology* 158(Pt 6):1444–55.
- Lewenza, Shawn, Barbara Conway, E. P. Greenberg, and Pamela A. Sokol. 1999. "Quorum Sensing in *Burkholderia cepacia*: Identification of the LuxRI Homologs CepRI." *Journal of Bacteriology* 181(3):748–56.
- Lewenza, Shawn and Pamela A. Sokol. 2001. "Regulation of Ornibactin Biosynthesis and N-Acyl-L-Homoserine Lactone Production by CepR in *Burkholderia cepacia*." 183(7):2212–18.
- Leyn, Semen A., Xiaoqing Li, Qingxiang Zheng, Pavel S. Novichkov, Samantha Reed, Margaret F. Romine, James K. Fredrickson, Chen Yang, Andrei L. Osterman, and Dmitry A. Rodionov. 2011. "Control of Proteobacterial

- Central Carbon Metabolism by The HexR Transcriptional Regulator: A Case Study in *Shewanella oneidensis*.” 286(41):35782–94.
- Li, Heng and Richard Durbin. 2010. “Fast and Accurate Long-Read Alignment with Burrows – Wheeler Transform.” 26(5):589–95.
- Li, Hongyu, Emanuela Pesce, David N. Sheppard, Ashvani K. Singh, and Nicoletta Pedemonte. 2017. “Therapeutic Approaches to CFTR Dysfunction: From Discovery to Drug Development.” *Journal of Cystic Fibrosis* 17(2S):S14–S21.
- Liao, Lisheng, Amy L. Schaefer, Bruna G. Coutinho, Pamela J. B. Brown, and E. Peter Greenberg. 2018. “An Aryl-Homoserine Lactone Quorum-Sensing Signal Produced by a Dimorphic Prothecate Bacterium.” *PNAS* 115(29):7587–92.
- Lightly, Tasia Joy, Kara L. Frejuk, Marie-Christine Groleau, Laurent R. Chiarelli, Cor Ras, Silvia Buroni, Eric Déziel, John L. Sorensen, and Silvia T. Cardona. 2019. “Phenylacetyl-CoA, Not Phenylacetic Acid, Attenuates CepIR-Regulated Virulence in *Burkholderia cenocepacia*.” *Applied and Environmental Microbiology* AEM.01594-19.
- Lim, Sangyoung, Ho Seong, Jisu Jeong, and Hyunjin Yoon. 2019. “Understanding the Multifaceted Roles of the Phosphoenolpyruvate : Phosphotransferase System in Regulation of *Salmonella* Virulence Using a Mutant Defective in *PtsI* and *Crr* Expression.” *Microbiological Research* 223–225:63–71.
- Liu, Xiaoying and Philip Matsumura. 1994. “The FlhD/FlhC Complex, a Transcriptional Activator of the *Escherichia coli* Flagellar Class II Operons.” *Journal of Bacteriology* 176(23):7345–51.
- Lluque, Angela, Maribel Riveros, Ana Prada, Theresa J. Ochoa, and Joaquim Ruiz. 2017. “Virulence and Antimicrobial Resistance in *Campylobacter* Spp. from a Peruvian Pediatric Cohort.” *Scientifica (Cairo)* 2017:7848926.
- Lucas, Robin L., C. Phoebe Lostroh, Concetta C. D. I. Russo, Michael P. Spector, Barry L. Wanner, and Catherine A. Lee. 2000. “Multiple Factors Independently Regulate HilA and Invasion Gene Expression in *Salmonella enterica* Serovar Typhimurium.” *Journal of Bacteriology* 182(7):1872–82.
- Luengo, José M., José L. Garcõ, and Elías L. Oliveira. 2001. “The Phenylacetyl-CoA Catabolon: A Complex Catabolic Unit with Broad Biotechnological Applications.” *Molecular Microbiology* 39(6):1434–42.
- Maeyama, R., Muznoe, Y., Anderson, J. M., Tanaka, M. & Matsuda, T. 2004. "Confocal imaging of biofilm formation process using fluoroprobed *Escherichia coli* and fluoro-stained exopolysaccharide." *Journal of Biomedical Materials Research Part A* 1;70(2):274-82
- Magnusson, Lisa U., Anne Farewell, and Thomas Nystro. 2005. “PpGpp : A Global Regulator in *Escherichia coli*.” *Trends in Microbiology* 13(5):236-42.
- Mahenthalingam, E. and P. Vandamme. 2005. “Taxonomy and Pathogenesis of the *Burkholderia cepacia* Complex.” *Chronic Respiratory Disease* 2(4):209–17.
- Mahenthalingam, Eshwar, Teresa A. Urban, and Joanna B. Goldberg. 2005. “The Multifarious, Multireplicon *Burkholderia cepacia* Complex.” *Nature Reviews Microbiology* 3(2):144–56.
- Maniatis, T., J. Sambrook, and E. F. Fritsch. 2012. *Molecular Cloning: A Laboratory Manual*. Vol. 1.
- Markovic, Dubravka, Birgit M. Prüß, and Philip Matsumura. 1997. “The *Escherichia coli* Flagellar Transcriptional Activator FlhD Regulates Cell Division through Induction of the Acid Response Gene CadA.” *Journal of Bacteriology* 179(11):3818–21.
- Marvig, Rasmus Lykke, Helle Krogh Johansen, and Lars Jelsbak. 2012. “Mutations in 23S rRNA Confer Resistance against Azithromycin in *Pseudomonas aeruginosa*.” 56(8):4519–21.
- Meade, Harry M., Sharon R. Long, Gary B. Ruvkun, Susan E. Brown, and M. Ausubel. 1982. “Physical and Genetic Characterization of Symbiotic and Auxotrophic Mutants of *Rhizobium Meliloti* Induced by Transposon TnS Mutagenesis.” *Journal of Bacteriology* 149(1):114–22.

- Melaugh, Gavin, Jaime Hutchison, Kasper Nørskov Kragh, Yasuhiko Irie, Aled Roberts, Thomas Bjarnsholt, Stephen P. Diggle, Vernita D. Gordon, and Rosalind J. Allen. 2016. "Shaping the Growth Behaviour of Biofilms Initiated from Bacterial Aggregates." *PLoS ONE* 11(3):1–18.
- Mesureur, Jennifer, Joana R. Feliciano, Nelly Wagner, Margarida C. Gomes, Lili Zhang, Monica Blanco-Gonzalez, Michiel van der Vaart, David O'Callaghan, Annemarie H. Meijer, and Annette C. Vergunst. 2017. "Macrophages, but Not Neutrophils, Are Critical for Proliferation of *Burkholderia Cenocepacia* and Ensuing Host-Damaging Inflammation." *PLoS Pathogens* 13(6):1–29.
- Mika, Franziska and Regine Hengge. 2014. "Small RNAs in the Control of RpoS , CsgD , and Biofilm Architecture of *Escherichia coli*." *RNA Biology* 11(5):494–507.
- Miller, J. K., Justin S. Brantner, Curtis Clemons, K. L. Kreider, Amy Milsted, Pat Wilber, Yang H. Yun, Wiley J. Youngs, Gerald Young, Hope T. Badawy, Amy Milsted, Curtis Clemons, K. L. Kreider, Pat Wilber, Gerald Young, and Yang H. Yun. 2014. "Mathematical Modelling of *Pseudomonas aeruginosa* Biofilm Growth and Treatment in the Cystic Fibrosis Lung." *Mathematical Medicine and Biology* (31):179–204.
- Mizushima, Tohru, Rimiko Koyanagi, Emi Suzuki, Arihiro Tomura, Kazuhiro Kutsukake, Takeyoshi Miki, and Kazuhisa Sekimizu. 1995. "Control by Phosphatidylglycerol of Expression of the FlhD Gene in *Escherichia coli*." *Biochimica et Biophysica Acta* 1245(3):397–401.
- Mukhopadhyay, Sanghamitra, David Good, Richard D. Miller, James E. Graham, Sarah A. Mathews, Peter Timms, and James T. Summersgill. 2006. "Identification of *Chlamydia pneumoniae* Proteins in the Transition from Reticulate to Elementary Body Formation." *Molecular and Cellular Proteomics* 5(12):2311–18.
- Mulcahy, Heidi and Shawn Lewenza. 2011. "Magnesium Limitation Is an Environmental Trigger of the *Pseudomonas aeruginosa* Biofilm Lifestyle." *PLoS ONE* 6(8):e23307.
- Murahari, Eswara C. and Thomas P. West. 2018. "The Pyrimidine Biosynthetic Pathway and Its Regulation in *Pseudomonas* Jessenii." *Antonie van Leeuwenhoek* 112(3):461–469.
- Nemoto, Ken, Katsuhiko Hirota, Keiji Murakami, Kazuko Taniguti, Hiromi Murata, Darija Viducic, and Yoichiro Miyake. 2003. "Effect of Varidase (Streptodornase) on Biofilm Formed by *Pseudomonas aeruginosa*." *Chemotherapy* 49(3):121–25.
- Nielsen, Alex T., Tim Tolker-nielsen, and Kim B. Barken. 2000. "Role of Commensal Relationships on the Spatial Structure of a Surface-Attached Microbial Consortium." 2(1):59–68.
- Nissen, Poul, Poul Nissen, Jeffrey Hansen, Nenad Ban, and Peter B. Moore. 2000. "The Structural Basis of Ribosome Activity in Peptide Bond Synthesis." *Science* 289(5481):920–930.
- O'Grady, Eoin and Pamela A. Sokol. 2011. "*Burkholderia cenocepacia* Differential Gene Expression during Host–Pathogen Interactions and Adaptation to the Host Environment." *Frontiers in Cellular and Infection Microbiology* 1:15.
- Ogasawara, Hiroshi, Kaneyoshi Yamamoto, and Akira Ishihama. 2011. "Role of the Biofilm Master Regulator CsgD in Cross-Regulation between Biofilm Formation and Flagellar Synthesis." *Journal of Bacteriology* 193(10):2587–97.
- Oh, Euna, Jong Chul Kim, and Byeonghwa Jeon. 2016. "Stimulation of Biofilm Formation by Oxidative Stress in *Campylobacter jejuni* under Aerobic Conditions." *Virulence* 7(7):846–51.
- Parker, Craig T. and Jean Guard-petter. 2001. "Contribution of Fagella and Invasion Proteins to Pathogenesis of *Salmonella enterica* Serovar *Enteritidis* in Chicks." *FEMS Microbiology Letters* 204(2):287–91.
- Pastore, Chiara, Salvatore Adinolfi, Martijn A. Huynen, Vladimir Rybin, Stephen Martin, Mathias Mayer, and Bernd Bukau. 2006. "YfhJ, a Molecular Adaptor in Iron-Sulfur Cluster Formation or a Frataxin-like Protein?" *Structure* 14(5):857–67.
- Peeters, Charlotte, Vaughn S. Cooper, Philip J. Hatcher, Bart Verheyde, Aureâlien Carlier, and Peter Vandamme. 2017. "Comparative Genomics of *Burkholderia multivorans*, a Ubiquitous Pathogen with a Highly Conserved

- Genomic Structure.” *PLoS ONE* 12(4):e0176191.
- Peralta, Diego P., Aymara Y. Chang, Angie Ariza-Hutchinson, and Catherine A. Ho. 2018. “*Burkholderia multivorans*: A Rare yet Emerging Cause of Bacterial Meningitis.” *IDCases* 11:61–63.
- Pesavento, Christina, Gisela Becker, Nicole Sommerfeldt, Alexandra Possling, Natalia Tschowri, Anika Mehlis, and Regine Hengge. 2008. “Inverse Regulatory Coordination of Motility and Curli-Mediated Adhesion in *Escherichia coli*.” *Genes Dev.* 22(17):2434–46.
- Pessoa, Filipa Duarte. 2017. “Long-Term Evolution of *Burkholderia multivorans* Bacteria during Chronic Respiratory Infections of Cystic Fibrosis Patients.” Instituto Superior Técnico.
- Petrova, Olga E., Jill R. Schurr, Michael J. Schurr, and Karin Sauer. 2012. “Microcolony Formation by the Opportunistic Pathogen *Pseudomonas aeruginosa* Requires Pyruvate and Pyruvate Fermentation.” *Mol. Microbiol.* 86(4):819–35.
- Pönisch, Wolfram, Kelly B. Eckenrode, Khaled Alzurqa, Hadi Nasrollahi, Christoph Weber, Vasily Zaburdaev, and Nicolas Biais. 2018. “Pili Mediated Intercellular Forces Shape Heterogeneous Bacterial Microcolonies Prior to Multicellular Differentiation.” *Scientific Reports* 8(1):16567.
- Porter, Steven L., George H. Wadhams, and Judith P. Armitage. 2011. “Signal Processing in Complex Chemotaxis Pathways.” *Nature Reviews Microbiology* 9(3):153–65.
- Pratt, Leslie A. and Roberto Kolter. 1998. “Genetic Analysis of *Escherichia coli* Biofilm Formation: Roles of Flagella, Motility, Chemotaxis and Type I Pili.” *Molecular Microbiology* 30(2):285–93.
- Pribytkova, Tanya, Tasia Joy Lightly, Brijesh Kumar, Steve P. Bernier, John L. Sorensen, Michael G. Surette, and Silvia T. Cardona. 2014. “The Attenuated Virulence of a *Burkholderia Cenocepacia* PaaABCDE Mutant Is Due to Inhibition of Quorum Sensing by Release of Phenylacetic Acid.” *Molecular Microbiology* 94(3):522–36.
- Pritsos, C. A. and D. L. Gustafson. 1994. “Xanthine Dehydrogenase and Its Role in Cancer Chemotherapy.” *Oncology Research* (6):477–81.
- Prokhorova, Irina V, Ilya A. Osterman, Dmitry E. Burakovsky, Marina V Serebryakova, Maria A. Galyamina, Olga V Pobeguts, Ilya Altukhov, Sergey Kovalchuk, Dmitry G. Alexeev, Vadim M. Govorun, Alexey A. Bogdanov, Petr V Sergiev, and Olga A. Dontsova. 2013. “Modified Nucleotides M²G966/M⁵C967 of *Escherichia coli* 16S rRNA Are Required for Attenuation of Tryptophan Operon.” *Sci. Rep* 3:3236.
- Prüß, Birgit M. and Philip Matsumura. 1996. “A Regulator of the Flagellar Regulon of *Escherichia coli*, FlhD, Also Affects Cell Division.” *Journal of Bacteriology* 178(3):668–74.
- Prüß, Birgit M., John W. Campbell, Tina K. Van Dyk, Charles Zhu, Yakov Kogan, and Philip Matsumura. 2003. “FlhD/FlhC Is a Regulator of Anaerobic Respiration and the Entner-Doudoroff Pathway through Induction of the Methyl-Accepting Chemotaxis Protein Aer.” *Journal of Bacteriology* 185(2):534–43.
- Prüß, Birgit M., Xiaojin Liu, William Hendrickson, and Philip Matsumura. 2001. “FlhD/FlhC-Regulated Promoters Analyzed by Gene Array and LacZ Gene Fusions.” *FEMS Microbiology Letters* 197(1):91–97.
- Ralli, Pooja, Avinash C. Srivastava, and Gerard O. Donovan. 2007. “Regulation of the Pyrimidine Biosynthetic Pathway in a PyrD Knockout Mutant of *Pseudomonas aeruginosa*.” *Journal of Basic Microbiology* (1968):165–73.
- Ramos, Hugo Cruz, Martin Rumbo, and Jean-claude Sirard. 2004. “Bacterial Flagellins: Mediators of Pathogenicity and Host Immune Responses in Mucosa.” *Trends in Microbiology* 12(11):509–17.
- Ramos, L. S., J. P. Sinn, B. L. Lehman, E. E. Pfeufer, K. A. Peter, and T. W. Mcnellis. 2015. “*Erwinia amylovora* PyrC Mutant Causes Fire Blight despite Pyrimidine Auxotrophy.” *Letters in Applied Microbiology* 60(6):572–9.
- Rhodes, Katherine A., Herbert P. Schweizer, Emerging Pathogens, Biomedical Sciences, and Fort Collins. 2016. “Antibiotic Resistance in *Burkholderia* Species.” *Drug Resistance Updates* 28:82–90.

- Ricker, Erica B. and Eric Nuxoll. 2015. "Thermal Mitigation of *Pseudomonas aeruginosa* Biofilms." *Biofouling* 15(5):477–91.
- Riedel, Kathrin, Morten Hentzer, Otto Geisenberger, Birgit Huber, Anette Steidle, Hong Wu, Niels Højby, Michael Givskov, Søren Molin, and Leo Eberl. 2001. "N -Acylhomoserine-Lactone-Mediated Communication between *Pseudomonas aeruginosa* and *Burkholderia cepacia* in Mixed Biofilms." *Mirobiology* (147):3249–62.
- Riedele, Christian and Udo Reichl. 2011. "Interspecies Effects in a Ceftazidime-Treated Mixed Culture of *Pseudomonas aeruginosa* , *Burkholderia cepacia* and *Staphylococcus aureus* : Analysis at the Single-Species Level." *Journal of Antimicrobial Chemotherapy* 66(1):138–45.
- Rincon-enriquez, Gabriel, Patrice Crété, Frédéric Barras, and Béatrice Py. 2008. "Biogenesis of Fe/S Proteins and Pathogenicity: IscR Plays a Key Role in Allowing *Erwinia Chrysanthemi* to Adapt to Hostile Conditions." *Molecular Microbiology* 67(6):1257–73.
- Romsang, Adisak, Jintana Duang-nkern, and Wilaiwan Wirathorn. 2015. "*Pseudomonas aeruginosa* IscR-Regulated Ferredoxin NADP (+) Reductase Gene (FprB) Functions in Iron-Sulfur Cluster Biogenesis and Multiple Stress Response." *PLoS ONE* 10(7):e0134374.
- Rosenfeld, Nitzan, Michael B. Elowitz, and Uri Alon. 2002. "Negative AR Motif Speeds up the Response of Transcription Networks." *Journal of Molecular Biology* 323(5):793:785–93.
- Rossi, E., M. Paroni, and P. Landini. 2018. "Biofilm and Motility in Response to Environmental and Host-Related Signals in Gram Negative Opportunistic Pathogens." *Journal of Applied Microbiology* 125(6):1587–1602.
- Rüger, Marc, Mandy Ackermann, and Udo Reichl. 2014. "Species-Specific Viability Analysis of *Pseudomonas aeruginosa* , *Burkholderia cepacia* and *Staphylococcus aureus* in Mixed Culture by Flow Cytometry." *BMC Microbiology* 14:56.
- Russel, J. S. 2001. *Molecular Cloning: A Laboratory Manual*. New York.
- Samanta, Priyankar, Emily R. Clark, Katie Knutson, Shelley M. Horne, and Birgit M. Prüß. 2013. "OmpR and RcsB Abolish Temporal and Spatial Changes in Expression of FlhD in *Escherichia coli* Biofilm." *BMC Microbiology* 13(1):1.
- Santiago, Manuel F. and Thomas P. West. 2002. "Control of Pyrimidine Formation in *Pseudomonas putida* ATCC 17536." *Canadian Journal of Microbiology* 48(12):1076–81.
- Santiago, Manuel F. and Thomas P. West. 2003. "Short Communication Effect of Carbon Source on Pyrimidine Biosynthesis in *Pseudomonas alcaligenes* ATCC 14909." *Microbiological Research* 158(2):195–99.
- Schleheck, D, et al 2009 "*Pseudomonas aeruginosa* PAO1 preferentially grows as aggregates in liquid batch cultures and disperses upon starvation." *PLoS One* 4(5):e5513
- Schmerk, Crystal L. and Miguel A. Valvano. 2013. "*Burkholderia multivorans* Survival and Trafficking within Macrophages." *Journal of Medical Microbiology* 62(Pt 2):173–84.
- Schmid, Nadine, Angela Suppiger, Elisabeth Steiner, Gabriella Pessi, Volkhard Kaever, Mustafa Fazli, Tim Tolker-nielsen, Urs Jenal, and Leo Eberl. 2017. "High Intracellular c-di-GMP Levels Antagonize Quorum Sensing and Virulence Gene Expression in *Burkholderia cenocepacia*." *Microbiology* 163(5):754–64.
- Schwab, Ute, Lubna H. Abdullah, Olivia S. Perlmutter, Daniel Albert, Roland R. Davis, C. William, Arnold, Jamer R. Yankaskas, Peter Gilligan, Heiner Neubauer, Scott H. Randell, and Richard C. Boucher. 2014. "Localization of *Burkholderia cepacia* Complex Bacteria in Cystic Fibrosis Lungs and Interactions with *Pseudomonas aeruginosa* in Hypoxic Mucus." *Infection and Immunity* 82(11):1468–75.
- Seed, Kimberley D. and Jonathan J. Dennis. 2008. "Development of *Galleria Mellonella* as an Alternative Infection Model for the *Burkholderia cepacia* Complex." *Infection and Immunity* 76(3):1267–75.
- Shi, Lei and Benjamin P. Tu. 2015. "Acetyl-CoA and the Regulation of Metabolism: Mechanisms and Consequences." *Current Opinion in Cell Biology* 33:125-131.

- Shippy, Daniel C. and Amin A. Fadl. 2015. "Microbial Pathogenesis RNA Modification Enzymes Encoded by the Gid Operon: Implications in Biology and Virulence of Bacteria." *Microbial Pathogenesis* 89:100–107.
- Shirtliff, Mark E., Jon T. Mader, and Anne K. Camper. 2002. "Molecular Interactions in Biofilms." *Chemistry and Biology* 9(8):859–71.
- Shoji, Tatsuma, Akiko Takaya, Yoshiharu Sato, Satoshi Kimura, Tsutomu Suzuki, and Tomoko Yamamoto. 2015. "RlmCD-Mediated U747 Methylation Promotes Efficient G748 Methylation by Methyltransferase RlmA II in 23S rRNA in *Streptococcus pneumoniae*; Interplay between Two rRNA Methylations Responsible for Telithromycin Susceptibility." *Nucleic Acids Research* 43(18):8964–72.
- Silva, Inês N., Marcelo J. Ramires, Lisa A. Azevedo, Ana R. Guerreiro, Andreia C. Tavares, Jorg D. Becker, and Leonilde M. Moreira. 2017. "Regulator LdhR and D-Lactate Dehydrogenase LdhA of *Burkholderia multivorans* Play Roles in Carbon Overflow and in Planktonic Cellular Aggregate Formation." *Applied and Environmental Microbiology* 83(19):1–24.
- Silva, Inês N., Pedro M. Santos, Mário R. Santos, James E. A. Zlosnik, David P. Speert, Sean W. Buskirk, Eric L. Bruger, Christopher M. Waters, S. Cooper, Vaughn, and Leonilde M. Moreira. 2016. "Long-Term Evolution of *Burkholderia multivorans* during a Chronic Cystic Fibrosis Infection Reveals Shifting Forces of Selection." *MSystems* 10(35):1–5.
- Singer, Hanna M., Marc Erhardt, and T. Hughes. 2013. "RfIM Functions as a Transcriptional Repressor in the Autogenous Control of the Salmonella Flagellar Master Operon FlhDC." *Journal of Bacteriology* 195(18):4274–82.
- Sivapragasam, Smitha and Anne Grove. 2016. "Streptomyces Coelicolor XdhR Is a Direct Target of (p)ppGpp That Controls Expression of Genes Encoding Xanthine Dehydrogenase to Promote Purine Salvage." *Molecular Microbiology* 100(4):701–18.
- Sivapragasam, Smitha and Anne Grove. 2019. "The Link between Purine Metabolism and Production of Antibiotics in Streptomyces." *Antibiotics (Basel)* 8(2). pii:E76.
- Smyer, J. Robert and Randall M. Jeter. 1989. "Characterization of Phosphoenolpyruvate Synthase Mutants in *Salmonella typhimurium*." *Archives of Microbiology* 153(1):26–32.
- Sommerfeldt, Nicole, Alexandra Possling, Gisela Becker, Christina Pesavento, Natalia Tschowri, and Regine Hengge. 2009. "Gene Expression Patterns and Differential Input into Curli Fimbriae Regulation of All GGDEF/EAL Domain Proteins in *Escherichia coli*." *Microbiology* 155(Pt 4):1318–31.
- Sørensen, Kim I. and Bjarne Hove-Jensen. 1996. "Ribose Catabolism of *Escherichia coli*: Characterization of the RpiB Gene Encoding Ribose Phosphate Isomerase B and of the RpiR Gene, Which Is Involved in Regulation of RpiB Expression." *Journal of Bacteriology* 178(4):1003–11.
- Soutourina, O., A. Kolb, E. Krin, S. Rimsky, A. Danchin, and P. Bertin. 1999. "Multiple Control of Flagellum Biosynthesis in *Escherichia coli*: Role of H-NS Protein and the Cyclic AMP-Catabolite Activator Protein Complex in Transcription of the FlhDC Master Operon." *Journal of Bacteriology* 181(24):7500–7508.
- Sriramulu, Dinesh D., Heinrich Lünsdorf, Joseph S. Lam, and Ute Römling. 2005. "Microcolony Formation: A Novel Biofilm Model of *Pseudomonas aeruginosa* for the Cystic Fibrosis Lung." *Journal of Medical Microbiology* 54(7):667–76.
- Srivastava, Milan, Chris Mallard, Theresa Barke, Lynn E. Hancock, and William T. Self. 2011. "A Selenium-Dependent Xanthine Dehydrogenase Triggers Biofilm Proliferation in *Enterococcus faecalis* through Oxidant Production." *Journal of Bacteriology* 193(7):1643–52.
- Staudinger, Benjamin J., Jocelyn Fraga Muller, Skarpheóinn Halldórsson, Blaise Boles, Angus Angermeyer, Dao Nguyen, Henry Rosen, Ólafur Baldursson, Magnus Gottfreosson, Guomundur Hrafn Guomundsson, and Pradeep K. Singh. 2014. "Conditions Associated with the Cystic Fibrosis Defect Promote Chronic *Pseudomonas aeruginosa* Infection." *American Journal of Respiratory and Critical Care Medicine* 189(7):812–24.
- Stella, Nicholas A., Eric J. Kalivoda, Dawn M. O'Dee, Gerard J. Nau, and Robert M. Q. Shanks. 2008. "Catabolite

- Repression Control of Flagellum Production by *Serratia marcescens*.” *Research in Microbiology* 159(7-8):562–68.
- Syed, Khadar, Musthafa Bhagavathi, and Sundaram Sivamaruthi. 2012. “Quorum Sensing Inhibition in *Pseudomonas aeruginosa* PAO1 by Antagonistic Compound Phenylacetic Acid.” *Current Microbiology* 65(5):475–80.
- Takahashi, Hidekazu, J. Michael McCaffery, Rafael A. Irizarry, and Jef D. Boeke. 2006. “Nucleocytoplasmic Acetyl-Coenzyme A Synthetase Is Required for Histone Acetylation and Global Transcription.” *Molecular Cell* 23(2):207–17.
- Tamber, Sandeep, Elke Maier, Roland Benz, and Robert E. W. Hancock. 2007. “Characterization of OpdH , a *Pseudomonas aeruginosa* Porin Involved in the Uptake of Tricarboxylates.” *Journal of Bacteriology* 189(3):929–39.
- Tamir-ariel, Dafna, Tally Rosenberg, and Saul Burdman. 2011. “The *Xanthomonas campestris* Pv . *Vesicatoria* CitH Gene Is Expressed Early in the Infection Process of Tomato and Is Positively Regulated by the TctDE Two-Component Regulatory System.” *Molecular Plant Pathology* 12(1):57–71.
- Tanaka, Naoyuki, Miaki Kanazawa, Keitaro Tonosaki, Nao Yokoyama, Tomohisa Kuzuyama, and Yasuhiro Takahashi. 2016. “Novel Features of the ISC Machinery Revealed by Characterization of *Escherichia coli* Mutants That Survive without Iron – Sulfur Clusters.” *Molecular Microbiology* 99(5):835–48.
- Tang, Dong-jie, Yong-qiang He, Jia-xun Feng, Bao-ren He, Bo-le Jiang, Guang-tao Lu, and Baoshan Chen. 2005. “*Xanthomonas campestris* Pv. *Campestris* Possesses a Single Gluconeogenic Pathway That Is Required for Virulence.” *Journal of Bacteriology* 187(17):6231–37.
- Teplitski, Max, Robert I. Goodier, and Brian M. M. Ahmer. 2003. “Pathways Leading from BarA/SirA to Motility and Virulence Gene Expression in *Salmonella*.” *Journal of Bacteriology* 185(24):7257–65.
- Teufel, R., V. Mascaraque, W. Ismail, M. Voss, J. Perera, W. Eisenreich, W. Haehnel, and G. Fuchs. 2010. “Bacterial Phenylalanine and Phenylacetate Catabolic Pathway Revealed.” *Proceedings of the National Academy of Sciences* 107(32):14390–95.
- Teufel, Robin, Thorsten Friedrich, and Georg Fuchs. 2012. “An Oxygenase That Forms and Deoxygenates Toxic Epoxide.” *Nature* 483(7389):359–65.
- Tokumoto, Umechiyo, Shinobu Nomura, Yoshiko Minami, Hisaaki Mihara, Shin-ichiro Kato, Tatsuo Kurihara, Nobuyoshi Esaki, Hiroshi Kanazawa, Matsubara Hiroshi, and Yasuhiro Takahashi. 2002. “Network Assembly of Protein-Protein Interactions Proteins in *Escherichia coli* among Cluster.” *Journal of Biochemistry* 131(5):713–19.
- Tokumoto, Umechiyo and Yasuhiro Takahashi. 2001. “Genetic Analysis of the Isc Operon Biogenesis of Cellular in *Escherichia coli* Involved in The.” *Journal of Biochemistry* 130(1):63–71.
- Tomich, Mladen and Christian D. Mohr. 2003. “Adherence and Autoaggregation Phenotypes of a *Burkholderia cenocepacia* Cable Pilus Mutant.” *FEMS Microbiology Letters* 228(2):287–97.
- Tomoyasu, Toshifumi, Tomiko Ohkishi, Yoshifumi Ukyo, Akane Tokumitsu, Akiko Takaya, Masato Suzuki, Kachiko Sekiya, Hidenori Matsui, and Kazuhiro Kutsukake. 2002. “The ClpXP ATP-Dependent Protease Regulates Flagellum Synthesis in *Salmonella enterica* Serovar *Typhimurium*.” *Journal of Bacteriology* 184(3):645–53.
- Traverse, Charles. Traverse, Leslie M. Mayo-Smith, Steffen R. Poltak, and Vaughn S. Cooper. 2012. “Tangled Bank of Experimentally Evolved *Burkholderia* Biofilms Reflects Selection during Chronic Infections.” *Proceedings of the National Academy of Sciences* 110(3):E250-9.
- Traxler, Matthew F., Vineetha M. Zacharia, Stafford Marquardt, Sean M. Summers, Tran Nguyen, S. Elizabeth Stark, and Tyrrell Conway. 2011. “Discretely Calibrated Regulatory Loops Controlled by ppGpp Partition Gene Induction across the ‘feast to Famine’ Gradient in *Escherichia coli*.” *Molecular Microbiology* 79(4):830–45.
- Tripathi, Lakshmi, Yan Zhang, and Zhanglin Lin. 2014. “Bacterial Sigma Factors as Targets for Engineered or Synthetic Transcriptional Control.” *Frontiers in Bioengineering and Biotechnology* 2:33.

- Trivedi, Rishi R., John A. Crooks, George K. Auer, Joel Pendry, Ilona P. Foik, Albert Siryaporn, Nicholas L. Abbott, Zemer Gitai, and Douglas B. Weibel. 2018. "Mechanical Genomic Studies Reveal the Role of D-Alanine Metabolism in *Pseudomonas aeruginosa* Cell Stiffness." *MBio* 9(5). pii: e01340-18.
- Tscherne, Joan S., Kelvin Nurse, Paul Popienick, Hanspeter Michel, Marek Sochacki, and James Ofengand. 1999. "Purification, Cloning, and Characterization of the 16S RNA m⁵C967 Methyltransferase from *Escherichia coli*." *Biochemistry* 38(6):1884–92.
- Tseng, Boo Shan, Charlotte D. Majerczyk, Daniel Passos da Silva, Josephine R. Chandler, E. Peter Greenberg, and Matthew R. Parsek. 2016. "Quorum Sensing Influences *Burkholderia thailandensis* Biofilm Development and Matrix Production." *Journal of Bacteriology* 198(19):2643–50.
- Turnbough, Charles L. and Barry R. Bochnert. 1985. "Toxicity of the Pyrimidine Biosynthetic Pathway Intermediate Carbamyl Aspartate in *Salmonella typhimurium*." *Journal of Bacteriology* 163(2):500–505.
- Ueda, Akihiro, Can Attila, Marvin Whiteley, and Thomas K. Wood. 2009. "Uracil Influences Quorum Sensing and Biofilm Formation in *Pseudomonas aeruginosa* and Fluorouracil Is an Antagonist." *Microbial Biotechnology* 2(1):62–74.
- Uehlinger, Susanne, Stephan Schwager, Steve P. Bernier, Kathrin Riedel, David T. Nguyen, Pamela A. Sokol, and Leo Eberl. 2009. "Identification of Specific and Universal Virulence Factors in *Burkholderia cenocepacia* Strains by Using Multiple Infection Hosts." *Infection and Immunity* 77(9):4102–10.
- Valentini, Martina and Alain Filloux. 2016. "Biofilms and Cyclic di-GMP (c-di-GMP) Signaling : Lessons from *Pseudomonas aeruginosa* and Other Bacteria." *The Journal of Biological Chemistry* 291(24):12547–55.
- Vergnes, Alexandra, Julie P. M. Viala, Rabah Ouadah, Tsabet Bérengère, Laurent Loiseau, Stéphane Méresse, Frédéric Barras, and Laurent Aussel. 2017. "The Iron–Sulfur Cluster Sensor IscR Is a Negative Regulator of SpiI Type III Secretion System in *Salmonella enterica*." *Cellular Microbiology* 19(4).
- Wang, Jianhe, Yihu Dong, Tielin Zhou, Xiaoling Liu, Yinyue Deng, Chao Wang, and Jasmine Lee. 2013. "*Pseudomonas aeruginosa* Cytotoxicity Is Attenuated at High Cell Density and Associated with the Accumulation of Phenylacetic Acid." *PLoS ONE* 8(3):2–9.
- Wellen, Kathryn E., Georgia Hatzivassiliou, Uma M. Sachdeva, Thi V Bui, R. Justin, and Craig B. Thompson. 2009. "ATP-Citrate Lyase Links Cellular Metabolism to Histone Acetylation." *Science* 324(5930):1076–80.
- Whitchurch, Cynthia B. 2002. "Extracellular DNA Required for Bacterial Biofilm Formation." *Science* 295(5559):1487–1487.
- Widenhorn, K. A., J. M. Somers, and W. W. Kay. 1988. "Expression of the Divergent Tricarboxylate Transport Operon (TctI) of *Salmonella typhimurium*." *Journal of Bacteriology* 170(7):3223–27.
- Wopperer, Julia, Silvia T. Cardona, Birgit Huber, Christoph A. Jacobi, Miguel A. Valvano, and Leo Eberl. 2006. "A Quorum-Quenching Approach To Investigate the Conservation of Quorum-Sensing-Regulated Functions within the *Burkholderia cepacia* Complex." *Applied and Environmental Microbiology* 72(2):1579–87.
- Worlitzsch, Dieter, Robert Tarran, Martina Ulrich, Ute Schwab, Aynur Cekici, Keith C. Meyer, Peter Birrer, Gabriel Bellon, Jürgen Berger, Tilo Weiss, Konrad Botzenhart, James R. Yankaskas, Scott Randell, and Richard C. Boucher. 2002. "Effects of Reduced Mucus Oxygen Concentration in Airway *Pseudomonas* Infections of Cystic Fibrosis Patients." *Journal of Clinical Investigation* 109(3):317–25.
- Xi, Hualin, Barbara L. Schneider, and Larry Reitzer. 2000. "Purine Catabolism in *Escherichia coli* and Function of Xanthine Dehydrogenase in Purine Salvage." *Journal of Bacteriology* 182(19):5332–41.
- Xu, T., Y. Su, Y. Xu, Y. He, B. Wang, X. Dong, Y. Li, and X. Zhang. 2014. "Mutations of Flagellar Genes FliC12, FliA and FlhDC of *Edwardsiella tarda* Attenuated Bacterial Motility, Biofilm Formation and Virulence to Fish." *Journal of Applied Microbiology* 116(2):236–44.
- Yamamoto, Hiroki, Masakuni Serizawa, and John Thompson. 2001. "Regulation of the Glv Operon in *Bacillus subtilis* : YfiA (GlvR) Is a Positive Regulator of the Operon That Is Repressed through CcpA and Cre." *Journal*

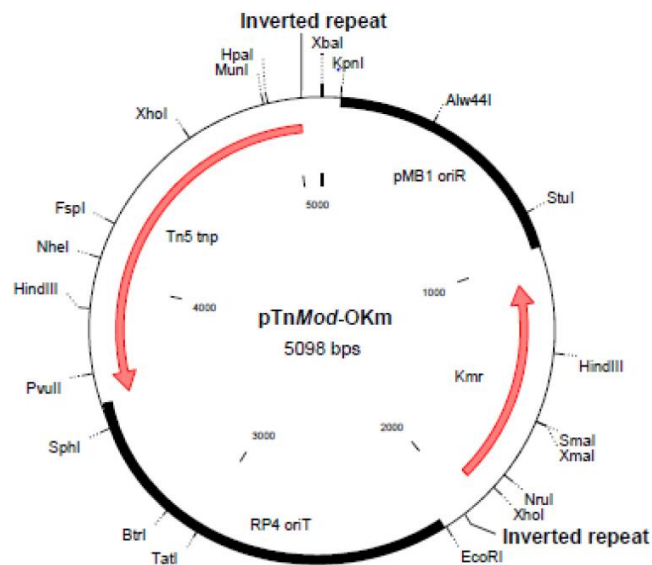
of *Bacteriology* 183(17):5110–21.

- Yan, Qing and Nian Wang. 2011. “The ColR/ColS Two-Component System Plays Multiple Roles in the Pathogenicity of the Citrus Canker Pathogen *Xanthomonas citri* Subsp. *Citri*.” *Journal of Bacteriology* 193(7):1590–99.
- Yang, Liang, Kim B. Barken, Mette E. Skindersoe, Allan B. Christensen, Michael Givskov, and Tim Tolker-Nielsen. 2007. “Effects of Iron on DNA Release and Biofilm Development by *Pseudomonas aeruginosa*.” *Microbiology* 153(5):1318–28.
- Yang, Pu, Miaozhi Zhang, and Jan Dirk Van Elsas. 2017. “Role of Flagella and Type Four Pili in the Co-Migration of *Burkholderia terrae* BS001 with Fungal Hyphae through Soil.” *Scientific Reports* 7:2997.
- Yimga, Merlin Tchawa, Mary P. Leatham, James H. Allen, David C. Laux, Tyrrell Conway, and Paul S. Cohen. 2006. “Role of Gluconeogenesis and the Tricarboxylic Acid Cycle in the Virulence of *Salmonella enterica* Serovar Typhimurium in BALB/c Mice.” *Infection and Immunity* 74(2):1130–40.
- Yoder-himes, D. R., P. S. G. Chain, Y. Zhu, O. Wurtzel, E. M. Rubin, James M. Tiedje, and R. Sorek. 2009. “Mapping the *Burkholderia cenocepacia* Niche Response via High-Throughput Sequencing.” *PNAS* 106(10):3976–81.
- Yokota, Takeshi and Joseph S. Gots. 1970. “Requirement of Adenosine 3', 5'-Cyclic Phosphate for Flagella Formation in *Escherichia coli* and *Salmonella typhimurium*.” *Journal of Bacteriology* 103(2):513–16.
- Yonezawa, Hideo, Takako Osaki, Tomoko Hanawa, Satoshi Kurata, and Kuniyasu Ochiai. 2013. “Impact of *Helicobacter pylori* Biofilm Formation on Clarithromycin Susceptibility and Generation of Resistance Mutations.” *PLoS ONE* 8(9):e73301.
- Yoshida, S., N. Ogawa, T. Fujii, and S. Tsushima. 2009. “Enhanced Biofilm Formation and 3-Chlorobenzoate Degrading Activity by the Bacterial Consortium of *Burkholderia* Sp. NK8 and *Pseudomonas aeruginosa* PAO1.” *Journal of Applied Microbiology* 106(3):790–800.
- Yoshikawa, Katsunori, Tadamasa Tanaka, Yoshihiro Ida, Chikara Furusawa, and Takashi Hirasawa. 2011. “Comprehensive Phenotypic Analysis of Single-Gene Deletion and Overexpression Strains of *Saccharomyces cerevisiae*.” *Yeast* 28(5):349–61.
- Yudistira, Harry, Leigh McClarty, Ruhi A. M. Bloodworth, Sydney A. Hammond, Haley Butcher, Brian L. Mark, and Silvia T. Cardona. 2011. “Microbial Pathogenesis Phenylalanine Induces *Burkholderia cenocepacia* Phenylacetic Acid Catabolism through Degradation to Phenylacetyl-CoA in Synthetic Cystic Fibrosis Sputum Medium.” *Microbial Pathogenesis* 51(3):186–93.
- Zhang, Linhua, Allan Matte, M. Eugenia Armengod, and Mirosław Cygler. 2010. “Structural Basis for Fe–S Cluster Assembly and tRNA Thiolation Mediated by IscS Protein–Protein Interactions.” *PLoS Biology* 8(4):e1000354.
- Zhang, Sui-sheng, Yong-qiang He, Li-ming Xu, Bo-wen Chen, and Bo-le Jiang. 2008. “A Putative colR(XC1049)-colS(XC1050) Two-Component Signal Transduction System in *Xanthomonas campestris* Positively Regulates HrpC and HrpE Operons and Is Involved in Virulence, the Hypersensitive Response and Tolerance to Various Stresses.” *Research in Microbiology* 159(7-8):569–78.
- Zlosnik, James E. A., Trevor J. Hird, Monica C. Fraenkel, Leonilde M. Moreira, Deborah A. Henry, and David P. Speert. 2008. “Differential Mucoid Exopolysaccharide Production by Members of the *Burkholderia cepacia* Complex.” *Journal of Clinical Microbiology* 46(4):1470–73.
- Zlosnik, James E. A., Guohai Zhou, Rollin Brant, Deborah A. Henry, Trevor J. Hird, Eshwar Mahenthiralingam, Mark A. Chilvers, Pearce Wilcox, and David P. Speert. 2015. “*Burkholderia* Species Infections in Patients with Cystic Fibrosis in British Columbia, Canada: 30 Years' Experience.” *Annals of the American Thoracic Society* 12(1):70–78.

6. Supplementary Material

Table S5 - Primers used in this work

Primers	Sequences
pTnMod Ω Km – fw (Dennis 1998)	5' GCAGAGCGAGGTATGTAGGC '3
pTnMod Ω Km – rev (Dennis 1998)	5' TTATGCCTCTTCCGACCATC '3
KmR	5' CCTTTTACGGTTCCTGGCCT '3
OriR	5' GTGCAATGTAACATCAGAG '3



(Bateman *et al.* 2017)

Figure S39 - Physical map of transposon pTnMod Ω Km. Retrieved from Bateman *et al.* 2017. Transposon is composed of genes that encode a transposase, two inverted repeats and a selectable marker, kanamycin in this case. The sequence between inverted repeats is the unique part of the transposon that remains inserted in the genome. Size is roughly 2000 bp.

Table S6 - Plasposon flanking sequences obtained from the plasmids recovered from the F21 mutant. Sequences A and C were obtained by primer oriR and sequences B and D with primer kmR.

F21 mutant	
Seq A	GGCCAGATCTGATCAAGAGACAGCGGCCCGGTCCTCGAGGAAGACATCGCGCTCACCAACATGAGCCTCGACCTGATCGGCCAGGC GCGCATGTGTACACGCACGCGGCCGAACCTGAACGCCAGCTGAACGGCGCGACGAAGACCGAGGACGATTACGCCTACTTCCGCA CCGAACCGCGAGTTTCGCGAACTTCACGCTGGCCGAGCTGCCGCACTACGGCCCGCTCGCCGGCACCAGCGCACGCCGACAAGGATTAC GCGGTACAGATCGTGCGCAATTTCTCTACGCGACGCTGATGCTGCACGTATGGAGCGCGCTCGAAACGTCGACCGACGCGCAGCT CGCCGCGATCGCCGCGAAGTCGGTGAAGGAAACGCGTTATCACGTGCAGCACGCGCGGAATGGCTCGTGCGCTTCGGCGACGGCA CCGACGAATCGCATCGCCGCGCGCAGGCCGCCCTCGACTACCTGATGCCGTACACGCGTGAATTCAACACAGCATTGCATCGGACC GGCTCGCGCCGCGCGCGCAAAGCCGGTCCACAGGAGAGAAAGATGAACAAGGAATGGCCGATCTGGGAAGTGTTCTGTCGCGACGAA GCAGGGCCTCGATCACAAGCACTGCGGCAGCCTGCACGCGGCCGACGCGACGATGGCGCTGCGCATGGCGCGCAGCTCTACACGC
Seq B	AGACCGGGCCGTGACCGCACCCTCGGCGTTGCGCTGACCGAGGATCAGCGCGTTGTCCGCGAGGCGCAGCACGTAGGAAAGGTGT TCGGGCGTGATCGTCATGGCGCGCGTTACATGTGGTTGACTTCGTTCGGGACGCGTGTAGAACGTCGGATGGCGATAGATCTTGTCTG CCGGCCCGTTTCGAACATTTTCGGCCTTCTCGTTTCGGATCCGATGCGGTGATCGCCGACGACGGCACCACCCAGATGCTCACGCCTTC CTGGCGGCGCGTGTAGACGTCGCGCGCCATGCGCAGCGCCATCGTCGCGTCGGCCGCGTGCAGGCTGCCGAGTGCTTGTGATCGA GGCCTTGCTTGTGTCGCGACGAACACTTCCAGATCGGCCATTCTTGTTCATCTTTCTCTCTCTGTGGACCGGCTTTGCGCGCGCGG CGCGAGCCCGTCCGATGCAATGCTGTGTTGAATTACGCGGTGTACGGCATCAGGTAGTCGAGGGCGGCCCTGCGCGCGCGGATGCGA TTCGTGCGTGCCGTGCGCGAAGCGCACGAGCCATTGCGCGCGGTGCTGCACGTGATAACGCGTTTCTTCCAGACTTCGCGGCGA TCGCGGCGAGCTGCGCGTTCGGTCGACGTTTCGAGCGCGCTCCATACGTGCAGCATCAGCGTCGCGTAGAGGAAATTGCGCACGATC GTGACCGCGTAATCCTTGTGCGCGTGCAGCGTGCAGGCGAGCGGCCGTAGTGCAGCGAGCTCGGCCAGCGTGAAGTTTCGCGAACTC GCGTTTCGGTGCGGGAGGTAGGCGTAATCGTCCCTCGGTCTTCGTGCGCGCGTCAGCTGGCGTTCCGAGTTTCGGCCGCGTGCGTG TACAGCATGCGCGCCTGGCCGATCAGGTT
Seq C	TTCTTTCTGTTACCGTCGACATGCATGGCGCGCCGGCGATCGCGGCCGGCCTAGGCGGCCAGATCTGATCAAGAGACAGCGGCC GGTCTCTCGAGGAAGACATCGCGCTCACCAACATGAGCCTCGACCTGATCGGCCAGGCGCGCATGCTGTACACGCACGCGGCCGAAC TCGAACGCCAGCTGAACGGCGCGACGAAGACCGAGGACGATTACGCCTACTTCCGACCCGAACGCGAGTTTCGCGAACTTCACGCTG GCCGAGCTGCCGCACTACGGCCCGCTCGCCGGCACCAGCGCACGCCGACAAGGATTACGCGGTACGATCGTGCGCAATTTCTCTA CGCGACGCTGATGCTGCACGTATGGAGCGCGCTCGAAACGTCGACCGACGCGCAGCTCGCCGCGATCGCCGCGAAGTCGGTGAAGG AAACGCGTTATCACGTGCAGCACGCGCGGAATGGCTCGTGCGCTTCGGCGACGGCACCAGCAATCGCATCGCCGCGCGCAGGCC GCCCTCGACTACCTGATGCCGTACACGCGTGAATTCAACACAGCATTGCATCGGACCGGCTCGCGCCGCGCGCGCAAAGCCGGTCC ACAGGAGAGAAAGATGAACAAGGAATGGCCGATCTGGGAAGTGTTTCGTGCGCAGCAAGCAGGGCCTCGATCACAAGCACTGCGGCA GCCTGCACGCGGCCGACGCGACGATGGCGCTGCGCATGGCGCGCGACGTCTACACGCGCCGCCAGGAAGGCGTGAGCATCTGGGTG GTGCGGTGCTCGGCGATCACCGCATCGGATCCGAACGAGAGGCCGAAATGTTTGAACCGGCCGCGACAAGATCTATCGCCATCCG ACGTTCTACACGCTGCCCCGACGAAGTCAACCACATGTAACGCGCGCCATGACGATCACGCCCGAACACCTTCTCTACGTGCTGCGC CTCGCGGACAACGCGCTGATCCTCGGTGACGCGAACG
Seq D	CCGGGCCGTGACCGCACCCTCGGCGTTGCGCTGACCGAGGATCAGCGCGTTGTCCGCGAGGCGCAGCACGTAGGAAAGGTGTTTCG GGCGTGATCGTCATGGCGCGCGTTACATGTGGTTGACTTCGTTCGGGACGCGTGTAGAACGTCGGATGGCGATAGATCTTGTGCGCG GCCGTTTCGAACATTTTCGGCCTTCTCGTTTCGGATCCGATGCGGTGATCGCCGACGACGGCACCACCCAGATGCTCACGCCTTCTTG GCGGCGCGTGTAGACGTGCGCGCCATGCGCAGCGCCATCGTCGCGTCGGCCGCGTGCAGGCTGCCGAGTGCTTGTGATCGAGGC CCTGCTTGTGTCGCGACGAACACTTCCAGATCGGCCATTCTTGTTCATCTTTCTCTCTCTGTGGACCGGCTTTGCGCGCGCGCGC GAGCCGGTCCGATGCAATGCTGTGTTGAATTCACGCGTGTACGGCATCAGGTAGTCGAGGGCGGCCCTGCGCGCGGCGATGCGATTTC GTCGGTGCCGTGCGCGAAGCGCACGAGCCATTGCGCGCGGTGCTGCACGTGATAACGCGTTTCTTCCAGACTTCGCGGCGATCG CGCGAGCTGCGCGTTCGGTCGACGTTTCGAGCGCGCTCCATACGTGCAGCATCAGCGTCGCGTAGAGGAAATTGCGCAC

Table S7 - Plasposon flanking sequences obtained from the plasmids recovered from the F27 mutant. Sequence A was obtained by primer oriR and sequence B with primer kmR.

F27 mutant	
Seq A	TTTTTTGTAGGAGCTTTGATATGTTCTTTCTGGTACGTCGACATGCATGGCGCGCCGGCGATCGCGGCCGGCTAGGCGGCCAGATCTGATCAAGAGACAGATCTGCACCAGGCCAACGTGCATCCGCTCGGCGCGCTGACCGTCGGGCTGAAGGGCGAAGTGATCACCGAGATGGTCGCGCTGACCGAGTCCGGCTGCGTCGGCTTCACGCATGCGAACGTGCCGCTGCGCGACACGCAAGTTCTGCTGCGCGCACTGCAGTACGCGAGCACCTACGGCTACACCACCTGGCTGCGCCCCGCTCGACGCGTTTCATCGGCAAGGGCGGCGTTCGCGGCGAGCGGGCCGCTGCGCTGCGACTCGGGCTGTCCGGCGTGCCGGTTCGCGGCCGAGACGATCGCGCTGCATACGATTTTCGAAGTGTATGCGCGTGACCGGCGCGCGGTGCACCTCGCGCGGCTGTCGTCGGCGGCCGGCTTCGCGCTCGTGCGCGGCGGAAGGCCGAAGGGCTGCCGGTCACGTGCGACGTGCGGCGTGAATCACCCTGCACCTGATCGACGTGACATCGGCTATTTTCGATTTCGCAGTTCGGGCTCGATCCGCCGCTGCGCGAGCGAGCGGATCGCGAGGCGATCCGTGCGGCGCTCGCGGACGGCACCATCGACGCGATCTGCTCCGATCACACGCCGGTTCGACGACGACGAGAAGCTGCTGCCGTTTCGGCGAAGCGACGCCGGTTCGACCGGCCCTCGAACTGCTGCTGCTGCTGCTGACCGTGAAGTGGCCGACGAGACGCGCACGCCGCTCGCGCAGGCGCTGCGCCGCATCACGTGCGGCGCTCGGGACGTGTGAACCTGCCGCCGGCCGCTGTGACCGAAGGCAGTTCGCGCCGATCTCTGCGTGTTTCGACCCGCGCGCGCACTGGCGTGTCGAGCCGCGCGGCGCTGAAGAGCCAGGGCCACAACCTCGCCGTTTCTTCGGATACGAGCTGCCCGCATGCGTGCGTGCGACGCTCGTCGCGGGGCGAGGTCGCGGTTTCGAGCGCCACTGAAACCCACGCCGGGCTTTTCGTCATGAAACGGCTTATCCCGCAAAGCTGGCGCGCTTCGTTTACACCTGGTTGGCGCGGCAATGGGCGAAATCGGTCGC
Seq B	GGCTACGTTGGGCTTTCCCCCCCCCGAGCTCTTAATTAATTTAAATCTAGACTAGTGCGGCCGCACTTGTGTATAAGAGTCAGGTGTCAGATTGCGCGCGCGGAACCTTCAGCATCTCGACGAGGCCCGGCTCGTCGAGCACGGGATCGGTGTCCGGCGGGCACACGAGCGTCGTACAGCCGCCGGCGACGCCGCCGATCTCGGACGCGAGCGTCGCCCTGTGTGCTCGTAGCCGGGCTCGCGCAGCCGCGCGCACAGGTCGACGAGGCCGGGCGCGACGATCAGGCCCGTCGCGTCGATCGTCTTGTGCGCCGCGAAGCCGGCCGGCGCGCGGCCGGCTTCGGGATCGCGTCGATCTTGCCGCCCGAGATGAATACGTCGGCTTGCCGCTCGCTGCCGGCGACCGGATCGATCAGCGTGCCGCCCTTGATATGAATCTTCATGCGCTGTCTGTGAATGCGTTGAATGCGTTGAATGCCTGGATAAGGAGGCGCGAAGCAGCTCAGTCGTTGTGCGCGGCGACGATGCCCCATCACGGCCATCCGCACGGCAATGCCGAACGTGACCTGATTGAGGATCACCGATTGCGGGCCGTCGCGCACCTGCGAGTCGATCTCGACGCCGCGGTTTCATCGGGCCCCGGGTGCATCACGATCGCGTCGGGTGCGGCGAGCGCGAGGCGCTCGGGCGTGAGCCCCACGTCCTTGAATACTCCTGCGCGGACGGCAGCAGCGCGCCGCTCATCCGCTCGTTCTGCAGGCGCAGCATGATGATGATGACGTCGACGCCCTTCAGCCCTTCGTCGAGGTTGTGGAACACCTTTCACGCCCATCTGCTCGAGGCCGCCGGCAACAGCGTGCGCGGGCGATCGCGCGCACTTTCGGGACGCGCGAGCGTGCTGTCAGCGCGTGATGTTCTTAAATACTA

Table S8 - Plasposon flanking sequences obtained from the plasmids recovered from the D19 mutant. Sequence A was obtained by primer oriR and sequence B with primer kmR.

D19 mutant	
Seq A	CAAATGTAGTTTGCTAGGTTACGTCACCTAGTCATACGATTGAATGGAGCGCCGGCTATCGCGGCCGGCCTAGGCGGTTTAAATCTGATCAGAGACAGATGCGTCGCCGCGTGCGTTCCACTACGACAAGCTGACCGAAGGCGTCGCGACGATTGCTGCGGCGTTCTATCCGAAATCCCGTGATCGTGCGTCTGCCCTACTTCAAGTCGAACAAGTTCAAGAAGCTGATCTTTGGTTTGCGCTACGAGCCGGACGAGGAAAACCCGATGCTGGGTTTCCGCGGCGCGTCTCGCTACATCGCCTACGATTTTCGCGCAGGCCCTTCGAGATGTAGTGCTCGCGCTCAAGCGCGTGCGCGACGAGATGGGCTTGTCTAACGTCGAGATCTTGTTGCCGTTTCGTGCGCACCGTGAATCAGGCGGAGCGCGTTGTGCGCCTGCTCGAGTAGTTTCGGCTGAAACGCGCCGAGAACGGGCTGCGCCTCGTGTTGATGTTTCGAGTTGCCGACTAACGCTATTCTGCTAAAGAGTTCTGTAATACTTCTACGGGTTCTCTATCGG
SeqB	GAAGGTTGGGGCTTTTCTCTCCCCGCGAGCTCTTAATTAATTTAAATCTAGACTAGTGCGGCCGCACTTGTGTATAAGAGTCAGGCGACGATGACCGCGCGGACGCTCTCGACGGCCTTCTTCAGATCCTGATCGACGTTTCGATACTCGAGGATCGCCTTCGGGTGACACGCCGATGTTGTTGTTGATGATGAACCTCGAGACGCGCGAGGCCGACGCCGGCGTTTCGGCAGCTGCGAGAAGTCGAATGCGAGCTGCGGGTTGCCGACGTTTCATCATGATCTTCACCGGAATTTCCGGCAGTTTCGCCGCGTGCCTTCGGTGACTTCGGTCTCGAGCAGCCGTCGTAGATCTTGCCCTTCGTCGCTTCCGCGCACGACACGGTGACGAGCGCGCCGCTCCTTCAGCACGTCGGTCGCGTCGCCGACGCCACCACGGCCGCGAGCTCACGCGGATGATCGCCGCGTGGCAGGTGCGCCCCGCCACGGTTCGTGACGATCGCCGACGCGCGCTTCATTACCGGCTCCAGTTTCGGGTCGGTCATGTGCGCGATGAGCACGTCGCCCCGCTGCACGCGTTCCATTTCGGACGGATCCTGGATCTCGCGACGCGGCCGACCGATCTTCTGGCCGATCGTACGGCCGGTCGCGAGCACTTCGCACTGGTCTTCATCTTGAAAGCTTTGCTCGGCCCTTGTTGCTCGTCTGCTCTTCTCCGTCTCCGGGCGCGCCTGCAGGATGAAGATTCTTGCCGCTCTCGGCTGTCTTGCTCCCTATCATGTCTCCGACGCTCGCAATTGCTTCTCTGATGATGATCCTCTACTTGCTATTTT

Table S9 - Plaspodon flanking sequences obtained from the plasmids recovered from the D3 mutant. Sequences A, B and C were obtained by primer oriR and sequence D with primer kmR.

D3 mutant	
Seq A	CGTGCCCTTTTTTCTTGTGCGCTTACTGAGTCCGTGCACTGCATGGCGCGCCGGCGATCGCGGCCGGCCTAGGCGGCCAGATCTG ATCAAGAGACAGCTTTTCGGCTCGTGCCTTCGGGCGGCCGGTTCGCGACGTATCAGGACAGCCTGCTGCAGCGGATGGTGTGCGCCA CGCTGTGCGCGCAGCAGTCTGTCGCTGCGCTTGTGCGGTGAGCGGCCGCGTCCCCGAGCTGCTCGAGAAGTCCCGGCTCGCGAAACGC TACGGCGCGACGCTGATTGCGATCACGGCGCCCGCTGCGCGCTCGCGAAGCTGGCCGACCACCTGATTCCGGTCTGTCGCTTCGA GACCGATTTCATTACAAGCCGTCGACGTGCGCTACGGCGATGATGATGGCGATCGACGTGCTGTCGACGGGGGTCGCGCTGCGGC TCGGCGATGCGGGCCGGGAATCGCTGCGCGTATCAAGCATGCGCTCGACGCGCATCGCGCGCGCGGACCGTCAACCGGTAGGA GACTGACCATGCATTGCGATCCCGAAGCCGCCGATACGCTGATCGTTCGGCGCGCAACTGTACGACGGGACCGGCGCGCCGCCGTC ACGCGCGACGTGCGGATCCGCAACGGCATGATCGGCGGCGATCGGCAACCTGTGAACTGGCTTGCCGAAACCGTTTCGTCGATGCG AACGGCCGCGCGCTCGCGCCGGGCTTCGTACGTTACACGCACGACGACACGACGTCGATCCGCGCGCGGAGATGCTGCCGAAA GATTTTCGACAGGGCGTGACGACCGTATCGTTCGGCACTTCGCGGAATCAGCGCGTTCGCCGGGTGACGCCCT
Seq B	AAAGCCCTTTCTTTGATAATGCATCGTTCCTGCTCCGTCGACTTGCATGGCGCGCCGGCGATCGCGGCCGGCCTACGCGGCCAGA TCTGATCAAGAGACAGCTTTTCGGCTCGTGCCTTCGGGCGGCCGGTTCGCGACGTATCAGGACAGCCTGCTGCATCGGATGGTGTGCG GCCACGCTGTGCGCGCAGCAGTCTGTCGCTGCGCTTGTGCGGTGAGCGGCCGCGTCCCCGAGCTGCTCGAGAAGTCCCGGCTCGCGAA ACGCTACGGCGCGACGCTGATTGCGATCACGGCGCCCGCTGCGCGCTCGCGAAGCTGGCCGACCACCTGATTCCGGTCTGTCGCT TCGAGACCGATTTCATTTACAAGCCGTCGACGTGCGCTACGCGATGATGATGGCGATCGACGTGCTGTCGACGGGGGTCGCGCTG CGGCTCGGCGATGCGGGCCGGGAATCGCTGCGCCGATCAAGCATGCGCTCGACGCGCATCGCGCGCGCGGACCGTCAACCGGT AGGAGACTGACCATGCATTGCGATCCCGAAGCCGCCGATACGCTGATCGTTCGGCGCGCAACTGTACGACGGGACCGGCGCGCCGCC CGTCACGCGCGACGTGCGGATCCGCAACGGCATGATCGGCGGATCGGCAACCTGTGAACTGGCTTGCCGAAACCGTTCGTCGATGC GAACGGCCGCGCGCTCGCGCCGGGCTTCGTGCGACGTTACACGCACGACGACGACGACGTCGATCCGCGCGCGCGGAGATGCTGCCG AAGATTTTCGACAGGGCGTGACGACCGTATCGTTCGGCAACTGCGGGATCAGCGCGGTTCGCGGTGACGCTCGCGAGCGACCCCGCTC GATCCGATGAAACCTGCTCGGCGATCCGACGCGTTCGCTATCCACCTTCGCGGACTATGTCGCGGTCCGTCAACGAT
Seq C	GCCTTTAACGATTGGGCTTTCCCCCCCCCCCCGAGCTCTTAATTAATTTAAATCTAGACTAGTGCGGCCGCACTTGTGTATAAGA GTCAGAGCCGAAAGCGCAGCTCGTTCGGCCAGCGCGGTTCGAGCCGCCACCTGCCCCGTACACGTAGATCATCTTCGCGCCGACGAGC CGGTTCGGCCGCCGCGTCAACGACGCGTTGCGCAACAGCTGATGGTTGTGCGCGAGCGCGACGCGGATCTCGTCTGACGACCGGT CGCCGGGTTTTCGCTCTTCTTCGGCAGGCACCTGCTCGGCGGGCACGAGAAAGCGCCGGCCGACGGCCGCCGCTGCGCGACGAGCA GCTTCAGTTTCGCGCACGTGCGGACAGCCGACCGCTTCGCGAAGCGCGTGACCGTTCGCGACGCTACGCGCGGTGTCGCGCGCAAGC GCGCCGATGCTTGCATGCGCGGCGCGCGGAGATCGGCGAGGATGAATTTCGGCGACCTTTCGCTCGGCATCGCGCGAGCTCGGGCGC GCATTTCGGCGATGCGCGCGACGATGTCGAGGACGGGTGCGCGACCGACGCGGATTCGCGCGTGGCCGCGCGGACGCGGAGCGGA CGGCGCGCGTATTTCATCTGCGGAAACGGGGATAAGGGTTCATGTTACTAAATAACATCACCCTGCCGATGCTACTTTCTGTACCAT CTGACTGTCAACTTCAGTGAATGCATAGTGATGATGGAGCCGGATGACATGAAAGTTACAAAATATCAGGAACCGACGATCGAT CCTTTTCGGCAAGGGCCTCGGCAACCTGCCGGGCGCGAGCGTGCCGCTCGACGAGGCCGGGCCGCTCGAATGGAATCTGCTCGCGG AAAGACATCAGCCTGCCGGCGGCGGTGCTGTACGAGGAGCGCATCGAGCACAACCTGAACTGGGATGCAGCCATTTCGTCCAGCAA GTATGGCGTGCAGTTTCGCGCCGACGCGGACGACCGATGGCGCCGCAACTGTTCCGCCGCCAGCTCGCGCGGGGCGCATGGGGC ATCACGCTCGCGACCGCGCACAGTACGACAGGCCGCTATCACGGCGCGGTGCGCGCGGTGCTGGCTCGCTAACAGCTGGGTTCGG GCCGGCAGAACATGAACATCATCGGGGCGCTTGTGTCCGAACCCGACTTCGAATTCCTCTGCTGTGCTCGAT
Seq D	TACGTTCCGTTAAGGATTTACCTCTTTTACAAGCTCTTTTCCGATAGGGTCTGTACTGTTGCGGCCGACCTTGTACCATGAGTCA GAGCCGACTATGTAGCTCGCCGGGCTCGCCGGCCCTTTCCGCCACCTGCCCATCTCGAAGATCATCTTCGACTTCCCCGAGACGGT CGGCCGCCGCGCTCTCGACGCTTTCGCGAACAGCTGATGGTTGTGCGCGAGCGCGACGCGGATCTCGTCTGACGACCGCTCGCCG GGTTTTCGCTCTTCTTCGGCAGGCACCTGCTCGGCGGGCACGAGAAAGCGCCGGCCGACGGCCACCGCTGCGCGACGACGAGATT AGTTTCGCGCACGTGCGGACGCGACCGCTTCGCGAAGAGCGTGACCGTTCGCGACGCTACGCGCGGTGTCGCGCGCAAGCGCGCC GATGCTTGCCTGCCCGGCGCCCGGAGATCGGCGAGGATGAATTTCGGCGACCTTTCGCTCGGCATCGCGCTTCTCGGGCGCGCAT CGGCGATGCCCCGCGACGTTGTCGAGGACGGGCTGTGCGACC